

UNIVERSITY OF OKLAHOMA

GRADUATE COLLEGE

CATALYTIC HYDRODEOXYGENATION OF PHENOLIC COMPOUNDS OF
IMPORTANCE IN BIO-OIL UPGRADING

A DISSERTATION

SUBMITTED TO THE GRADUATE FACULTY

in partial fulfillment of the requirements for the

Degree of

DOCTOR OF PHILOSOPHY

By

LEI NIE
Norman, Oklahoma
2014

CATALYTIC HYDRODEOXYGENATION OF PHENOLIC COMPOUNDS OF
IMPORTANCE IN BIO-OIL UPGRADING

A DISSERTATION APPROVED FOR THE
SCHOOL OF CHEMICAL, BIOLOGICAL AND MATERIALS ENGINEERING

BY

Dr. Daniel E. Resasco, Chair

Dr. Richard G. Mallinson

Dr. Lance L. Lobban

Dr. Steven P. Crossley

Dr. Kenneth M. Nicholas

© Copyright by LEI NIE 2014
All Rights Reserved.

Acknowledgements

Firstly, I would like to express my great gratitude and respect to my Ph.D. research advisor, Dr. Daniel Resasco, for his guidance in my research, encouragement when I were facing challenges, patience when I did something not perfect and providing us a free environment to conduct research work in our own ways. Because of his guidance and advice, in the past five years, I grew up from a freshman who only knew the difference between Lewis acid and Brønsted acid to an independent research fellow. Moreover his profound knowledge not only in catalysis, but also his philosophy on how to get along with people well, never give up and just do your own best would benefit me greatly in my future. It is a great pleasure and luck working in his group. It will always be my best memory and treasure.

I would like to thank Dr. Richard Mallinson, Dr. Lance Lobban and Dr. Steven Crossley for their support all the time. The numerous group meetings we had as well as great suggestions from them and discussions with them provided me more knowledge and also broaden my view.

I would like to thank Dr. Kenneth Nicholas for being my dissertation committee member and teaching me in his great and famous Advance Organic Chemistry class.

I would like to thank Dr. Tawan Sooknoi at the King Mongkut's Institute of Technology Ladkrabang for his great discussion and suggestions in both chemistry knowledge and technical issues. I always make great progress with his ideas.

I would like to thank our previous group members Dr. Trung Pham, Dr. Surapas Sitthisa and Dr Xinli Zhu for handing over their knowledge and reactor systems.

Finally I would like to thank all the staffs in OU Chemical Engineering Department, all of faculty and my fellow students and post-docs. All of them help to create a friendly and supportive research environment. I want to thank Anh, Tu, Dr. Dachuan Shi and Dr. Shaolong Wan for their warm support and friendship.

Table of Contents

Acknowledgements	iv
List of Tables	ix
List of Figures.....	xi
Abstract.....	xvi
Chapter I. Introduction and Background	1
1.1 Introduction	1
1.2 Biomass conversion to fuel	3
1.3 Hydrodeoxygenation (HDO) vs. hydrodesulfurization (HDS) and Hydrodenitrogenation (HDN)	8
1.3.1 Hydrodesulfurization (HDS)	8
1.3.2 Hydrodenitrogenation (HDN)	10
1.3.3 Hydrodeoxygenation (HDO)	12
1.4 Concept process for bio-oil refinery and upgrading.....	15
References	18
Chapter II. Hydrodeoxygenation of m-Cresol to Toluene over SiO ₂ supported Bimetallic Ni-Fe Catalysts	21
2.1 Introduction	21
2.2 Experimental.....	23
2.2.1 Catalyst synthesis and characterization	23
2.2.2 Catalytic activity measurements.....	25
2.2.3 Computational Method.....	25
2.3 Results and discussion.....	26

2.3.1	Catalyst characterization	26
2.3.2	Catalytic activity and product distribution at varying m-cresol conversion	29
2.3.3	Using 3-methylcyclohexanone and 3-methylcyclohexanol as feeds	34
2.3.4	Mechanistic implications of the observed product distributions	37
2.3.5	DFT Calculation	40
2.4	Conclusion	41
	Reference	42
 Chapter III. Kinetics and Reaction Mechanism of m-Cresol Hydrodeoxygenation over supported Pt catalysts		
		46
3.1	Introduction	46
3.2.	Experimental.....	49
3.2.1	Catalyst preparation and characterization	49
3.2.2	Reaction Kinetics.....	50
3.3	Results and Discussion for Pt/SiO ₂	54
3.3.1.	Experimental Measurements in Integral Reactor Mode	54
3.3.2	Kinetic Model	57
3.3.3.	Experimental Measurements in Differential Reactor Mode.....	61
3.3.4.	Goodness of the Fitting from the Integral Reactor	65
3.3.5.	Analysis of the Toluene/Methylcyclohexane Product Ratio	67
3.3.6.	Possible Direct Deoxygenation Pathways	69
3.4	Support Effect.....	73
3.5	Conclusions	74

Chapter IV. Improving Carbon Retention in Biomass Conversion by Alkylation of Phenolics with Small Oxygenates	80
4.1 Introduction	80
4.2. Experimental.....	81
4.2.1 Catalyst Preparation.....	81
4.2.2 Catalyst Characterization.....	82
4.2.3 Catalytic Activity Testing.....	83
4.3. Results and discussion.....	84
4.3.1 Alkylation of meta-Cresol with 2-Propanol	84
4.3.2 Alkylation of meta-Cresol with different Alkylating Agents.....	86
4.3.3 Catalyst Deactivation.....	89
4.3.4 Hydrogenation of Propanal and Acetone	93
4.3.5. Combination of Hydrogenation and Alkylation	96
4.4. Conclusions	99
Reference.....	101

List of Tables

Table 1.II.	Characterization of SiO ₂ supported catalysts.	28
Table 2.II.	Conversion and product yield from the reaction of m-cresol over different catalysts at W/F= 0.46 h and 300°C. H ₂ /Feed molar ratio =60. Pressure = 1atm.	30
Table 3.II.	Product distribution from different feed at 300°C. C ₇ Products: 3-methyl-cyclohexanone (ONE) ; 3-methylcyclohexanol (OL); Toluene (TOL); methylcyclohexane (ENE).....	35
Table 4.III.	Characteristics of the Pt/SiO ₂ catalyst.	50
Table 5.III.	Product distribution, rate and rate constant for 3-methyl-1-cyclohexene over Pt/SiO ₂ and 3-methyl-cyclohexanol over SiO ₂ at 300°C. Pressure = 1atm. MCH: methyl-cyclohexane; TOL: toluene; OL: 3-methyl-cyclohexanol; 3-Me-CYHE: 3-methyl-1-cyclohexene; Me-CYHE: methyl-cyclohexene.....	56
Table 6.III.	Adsorption constants calculated from data in Figure 19. m-Cr: m-cresol; ONE: 3-methyl-cyclohexanone; OL: 3-methyl-cyclohexanol; TOL: toluene; MCH: methyl-cyclohexane; ENE: 3-methyl-1-cyclohexene. ..	63
Table 7.III.	Rate constant for different reaction steps. m-Cr: m-cresol; ONE: 3-methyl-cyclohexanone; OL: 3-methyl-cyclohexanol; TOL: toluene; MCH: methyl-cyclohexane; ENE: 3-methyl-1-cyclohexene.	65
Table 8.III.	Bond dissociation energy [Ref:39].	70
Table 9.III	Product selectivity for m-cresol conversion over different support Pt catalysts at 300°C. Pressure = 1atm. MCH: methyl-cyclohexane; TOL:	

toluene; m-Cr: m-cresol; ONE: 3-methyl-cyclohexanone; OL: 3-methyl-cyclohexanol.....	73
Table 10.IV. Yield of hydrogenation products of different metal catalysts. W/F = 0.5 h. Carrier gas H ₂ 60 ml/min. 200 °C . TOS = 30min.	93
Table 11.IV. Products distribution for different feed and different catalysts.	96
Table 12.IV. Products distribution for different feed and different catalysts. Carrier gas H ₂ 60 ml/min. 200 °C. TOS =15min. Feed Rate 0.2ml/h.	98

List of Figures

Figure 1.I.	World primary energy consumption from 1980 to 2010 by region.....	2
Figure 2.I.	Current strategies for production of liquid fuels from biomass	2
Figure 3.I.	Candidate process for conversion of biomass to biofuels	3
Figure 4.I.	Catalytic cascade connected to a multi-stage pyrolysis.	16
Figure 5.II.	XRD patterns of monometallic Ni, Fe and bimetallic Ni-Fe catalysts pre-reduced ex-situ in hydrogen at 450°C for 1h.....	27
Figure 6.II.	DRIFT spectra of the pyridine chemisorption experiments at 100 °C and atmospheric pressure after pyridine chemisorption for (a) pure SiO ₂ , (b) Ni/SiO ₂ , (c) (1:2)Ni-Fe/SiO ₂ , (d) Fe/SiO ₂	28
Figure 7.II.	Product distribution of m-cresol over 5 wt.% Ni/SiO ₂ at 300°C as a function of W/F. H ₂ /Feed molar ratio =60. Pressure = 1atm.....	30
Figure 8.II.	Yield of products of m-cresol over Ni-Fe bimetallic catalysts as a function of Fe loading at 300°C. H ₂ /Feed ration =60. Pressure = 1atm. W/F= 0.46h. (a) C ₇ Products: 3-methyl-cyclohexanone (ONE); 3-methylcyclohexanol (OL); Toluene (TOL); (b) Transalkylation and hydrogenolysis products.	32
Figure 9.II.	Product distribution of m-cresol over (1:2)Ni-Fe/SiO ₂ at 300°C as a function of W/F. H ₂ /Feed ration =60. Pressure = 1atm. (a) C ₇ Products: 3-methyl-cyclohexanone(ONE); 3-methylcyclohexanol(OL); Toluene(TOL); (b) Transalkylation and hydrogenolysis products.....	33

Figure 10.II.	C ₇ Product selectivity as a function of conversion of m-cresol at 300°C. a. Ni/SiO ₂ ; b. (1:2) Ni-Fe/SiO ₂ . H ₂ /Feed molar ratio =60. Pressure = 1atm. C ₇ Products: 3-methyl-cyclohexanone (ONE) ; 3- methylcyclohexanol (OL); Toluene (TOL).....	33
Figure 11.II.	Effect of time on stream on of conversion of m-cresol and product distribution (major products) over (1:2)Ni-Fe/SiO ₂ at 300°C. H ₂ /Feed ration =60. Pressure = 1atm. 3-methyl-cyclohexanone (ONE) ; Toluene (TOL).....	34
Figure 12.II.	Tautomerization reaction pathways over Ni, Fe, and Ni-Fe catalysts....	37
Figure 13.II	Optimized adsorption structures of m-cresol on (a)Ni (111), (b) ... perfect NiFe(111), (c) patched NiFe(111) and (d) Fe(110) surface. (e) gas phase. C-OH bond lengths are labeled in each molecule.	40
Figure 14.III.	HRTEM of 1wt% Pt/SiO ₂ after calcination at 400°C in air, reduction at 300°C and passivation at room temperature.....	51
Figure 15.III.	Conversion and yield of products of different feeds over Pt/SiO ₂ as a function of W/F at 300°C. Carrier gas: H ₂ . Pressure = 1atm. (a) m- cresol; (b) 3-methyl-cyclohexanone; (c) 3-methyl-cyclohexanol. MCH: methyl-cyclohexane; TOL: toluene; m-Cr: m-cresol; ONE: 3-methyl- cyclohexanone; OL: 3-methyl-cyclohexanol. The points are experimental data and the lines are calculated from the Langmuir-Hinshelwood kinetics model.....	53
Figure 16.III.	Reaction pathway over Pt/SiO ₂ with rate constant. (Denotation) k _{CK} : rate constant for m-cresol to 3-methyl-cyclohexanone. (Subscript) C : m-	

cresol; K : 3-methyl-cyclohexanone; O : 3-methyl -cyclohexanol; E: 3-methyl-1-cyclohexene; T: toluene; M : methyl-cyclohexane; DOH : dehydroxylation; DW : dehydration..... 55

Figure 17.III. Effect of co-feeding water on the product distribution for m-cresol conversion over Pt/SiO₂ as a function of partial pressure ratio between water and m-cresol. Temperature = 300°C. Pressure = 1atm. P_{m-Cr} = 1486 Pa. MCH: methyl-cyclohexane; TOL: toluene; m-Cr: m-cresol; ONE: 3-methyl-cyclohexanone; OL: 3-methyl-cyclohexanol. 58

Figure 18.III. Sequence of elementary steps for m-cresol conversion over Pt/SiO₂. ... 61

Figure 19.III. 1/r vs. 1/P plot for different reactants in differential reactor over Pt/SiO₂. Temperature = 300°C. Pressure = 1atm. P_{m-Cr} = 1486 Pa. MCH: methyl-cyclohexane; TOL: toluene; m-Cr: m-cresol; ONE: 3-methyl-cyclohexanone; OL: 3-methyl-cyclohexanol; ENE: 3-methyl-1-cyclohexene. 63

Figure 20.III. Product distribution from reaction of methyl-cyclohexane and toluene over Pt/SiO₂. (a) methyl-cyclohexane, (b) toluene. Temperature = 300°C. Pressure = 1atm. P_{MCH} (P_{TOL}) = 1486 Pa. MCH: methyl-cyclohexane; TOL: toluene. The points are experimental data and the lines are calculated from the kinetics model. 64

Figure 21.III. Product distribution from reaction of mixture of m-cresol and 3-methyl-cyclohexanol (1:1 molar ratio) over Pt/SiO₂. Temperature = 300°C. Pressure = 1atm. MCH: methyl-cyclohexane; TOL: toluene; m-Cr: m-cresol; ONE: 3-methyl-cyclohexanone; OL: 3-methyl-cyclohexanol. The

points are experimental data and the lines are calculated from the Langmuir-Hinshelwood kinetics model.	66
Figure 22.III. Product toluene to methyl-cyclohexane ratio as a function of conversion of different feeds over Pt/SiO ₂ at 300°C. Pressure = 1atm. MCH: methyl-cyclohexane; TOL: toluene; m-Cr: m-cresol; ONE: 3-methyl-cyclohexanone; OL: 3-methyl-cyclohexanol.	68
Figure 23.III. Deoxygenation reaction pathway: a. hydrogenolysis; b. partial hydrogenation with sequential dehydration; c. tautomerization route. ..	69
Figure 24. IV. Left: Conversion of m-Cresol; Right: Alkylate products selectivity as a function of W/F. Reaction conditions: 2-Propanol : m-Cresol = 2:1 (mole). Carrier gas H ₂ 60 ml/min. TOS = 15min. 200 °C. 2I5MP: 2-isopropyl-5-methylphenol; 3I5MP: 3-isopropyl-5-methylphenol; 4I3MP: 4-isopropyl-3-methylphenol.	84
Figure 25.IV. Products Distribution as a function of TOS at 200 °C. W/F = 0.1hr. 2-Propanol : m-Cresol = 2:1 (mole). Carrier gas H ₂ 60 ml/min.....	86
Figure 26.IV. Conversion of m-Cresol with different alkylating agent as a function of W/F. Alkylating agent : m-Cresol = 2:1 (mole). Carrier gas H ₂ 60 ml/min. 200 °C. C ₃ [≡] : propylene; 2-POL: 2-propanol; 1-POL: 1-propanol.	87
Figure 27.IV. Products Distribution as a function of W/F at 200 °C. 1-Propanol : m-Cresol = 2:1 (mole). TOS = 15min. Carrier gas H ₂ 60 ml/min. C ₃ [≡] : propylene; m-C: m-cresol; DPE: dipropyl ether; ALK: alkylated products ; 1-POL: 1-propanol.	88

Figure 28.IV.	a. Conversion of m-Cresol with different agents as a function of TOS;	
	b. (ortho+para)/meta substitution ratio. Carrier gas H ₂ 60 ml/min. 200 °C. W/F = 0.15hr.	89
Figure 29.IV.	Conversion of m-Cresol as a function of TOS. Propylene : m-Cresol = ...	
	2:1 (mole). Carrier gas H ₂ 60 ml/min. W/F = 1hr. 200°C . (a):	
	continuous feed.	90
Figure 30.IV.	Conversion of m-cresol over H-Beta at two temperatures as a function	
	of W/F . 2-Propanol : m-Cresol = 2:1 (mole). Carrier gas H ₂ 60 ml/min.	
	TOS = 15min.	91
Figure 31. IV.	Conversion of m-cresol as a function of temperature. 2-Propanol : m-	
	Cresol = 2:1 (mole). TOS = 15min. Carrier gas H ₂ 60 ml/min. W/F =	
	0.3h.	92
Figure 32.IV.	Hydrogenation activity of metal/SiO ₂ as a function of Iron loading .	
	Acetone : m-Cresol = 4:1 (mole). TOS = 15min. Carrier gas H ₂ 60	
	ml/min. W/F = 0.5hr. 200°C	94
Figure 33.IV.	Conversion as a function of W/F over 1%Pt-0.4%Fe/SiO ₂ . Acetone :	
	m-Cresol = 4:1 (mole). TOS = 15 min. Carrier gas H ₂ 60 ml/min. 200	
	°C	95
Figure 34.IV.	Conversion of m-cresol with and without cofeeding acetone. W/F = 0.3	
	h. Carrier gas H ₂ 60 ml/min.	98

Abstract

Economic and environmental concerns including the increasing energy consumption and demand, ensuring energy security, reducing green-house gas emission and producing cleaner energy have caused tremendous interest in research and development on use of renewable energy resources such as biomass. Fast pyrolysis has proven to be a cost efficient method to convert biomass to liquid bio-oil which could be further upgraded to blend with conventional transportation fuels. Since the high oxygen content in fast pyrolysis bio-oil has brought bad properties such as instability during storage and transportation and low heating value. Hydrodeoxygenation (Hydrotreating), a refinery hydroprocessing technology, is cited to be an efficient technology to remove the excess oxygen in bio-oil. Moreover, during the process, the retention carbon in the bio-oil liquid as well as reduction of the hydrogen consumption is other important issue to investigate. Thus in the scope of this dissertation, a detailed study of the reaction kinetics and the mechanism of hydrodeoxygenation of phenolic compounds in fast pyrolysis bio-oil is presented. Also the understanding of the fundamental catalytic chemistry will be applied to tailor catalyst formulations to convert the model phenolics in bio-oil to higher value hydrocarbon products.

In this dissertation, a tautomerization reaction pathway for the hydrodeoxygenation of m-cresol (a model phenolic compound in bio-oil) is proven, which has not been previously proposed in any previous literature. The tautomerization path starts with the tautomerization of m-cresol to an unstable ketone intermediate (3-methyl-3,5-cyclohexadienone). The fate of this intermediate is determined by the ability of the catalyst to either hydrogenate the carbonyl group or the ring. The former

would be preferred over catalysts with oxophilic sites (Ni-Fe/SiO₂, Pt/TiO₂), while the latter would mostly occur over catalysts with a pure metallic function (Pt/SiO₂, Ni/SiO₂).

Hydrogenation of the carbonyl group produces a very reactive unsaturated alcohol (3-methyl-3,5-cyclohexadienol), which can be easily dehydrated to toluene. This dehydration step is driven by the formation of aromaticity. Thus, strong acid site is not required. By contrast, hydrogenation of the ring would result in 3-methylcyclohexanone, which can be further hydrogenated to 3-methylcyclohexanol. On supports that contain strong acid sites, which are active for dehydration of the corresponding alcohol, the formation of toluene would occur via dehydration of the alcohol and subsequent dehydrogenation. On the catalysts and conditions investigated in this dissertation, dehydration of the corresponding alcohol does not occur due to low acidity of the supports (SiO₂, TiO₂ etc.), so the only path to toluene is via hydrogenation of the carbonyl of the unstable ketone intermediate.

Catalysts formulation can be tailored by introducing oxophilic sites either by incorporating bimetallic catalysts or the metal support interaction. Oxophilic sites help improve the chemoselective hydrogenation of the carbonyl group of the unstable ketone intermediate thus dramatically increase the selectivity of hydrodeoxygenation. At the same time the hydrodeoxygenation reaction rate is increased.

Chapter I. Introduction and Background

1.1 Introduction

Due to fast growing global economy, the global energy consumption is expected to rise by 41% from 2012 to 2035. Especially in emerging economies, the demand of energy is increasing very fast [1], shown in Figure 1.I. Thus to enhance the energy security, reduce the dependence on fossil fuels, and minimize greenhouse gas emissions, much effort in research and development of alternative greener energy has been taken over the past several decades. New sources such as shale gas, tight oil, oil sands, nuclear energy and biofuels can help to supply sufficient energy for the global economic growth. Among all, biomass derived biofuels is very attractive, not only because of the rising oil prices but also the net greenhouse gas emission is greatly reduced for biofuels. Another important advantage of biofuel is the negligible amount of SO₂ and NO_x residing in the fuels which make it safer and cleaner. Generally the biomass can be converted to conventional energy containing substance in three major technologies including thermal conversion, chemical conversion and biochemical conversion. For most biomass feedstocks, it is necessary to use a combination of two or three of the technologies. For example a combination of thermal conversion and chemical conversion was proven to be an efficient method to produce fungible biofuels [2].

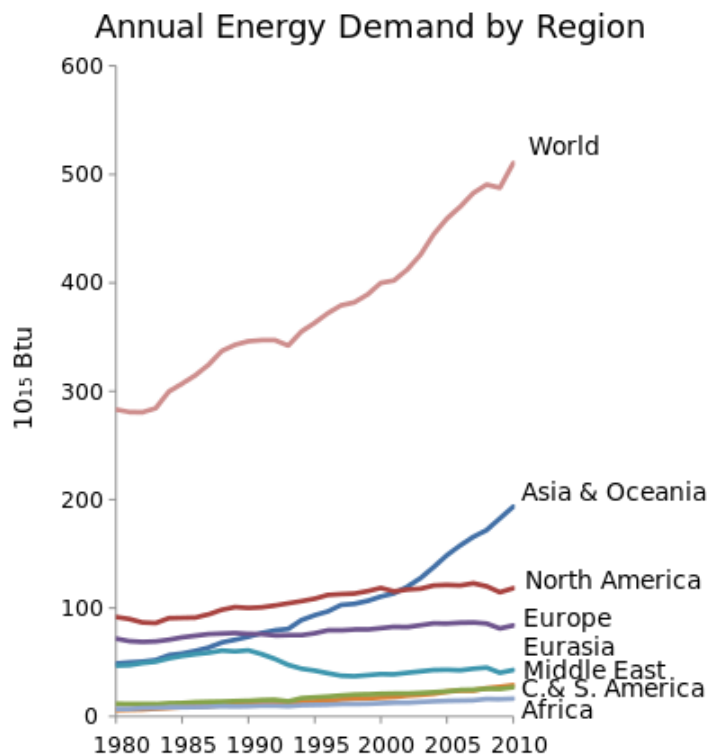


Figure 1.I. World primary energy consumption from 1980 to 2010 by region [3].

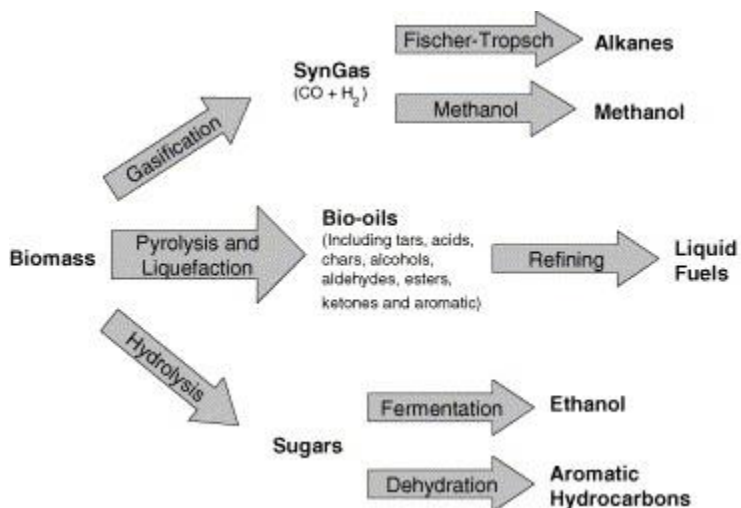


Figure 2.I. Current strategies for production of liquid fuels from biomass [4].

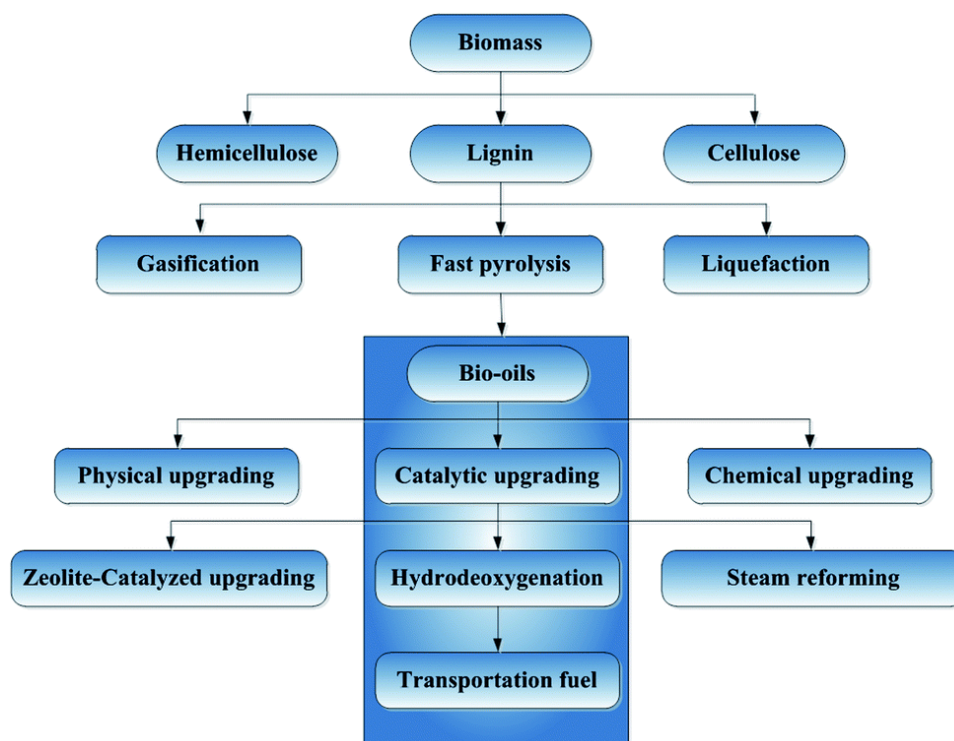


Figure 3.I. Candidate process for conversion of biomass to biofuels [5].

1.2 Biomass conversion to fuel

Three main processes for production of liquid fuels from biomass are shown in Figure 2.I and Figure 3.I. The processes include gasification of biomass to syn-gas followed by Fischer-Tropsch synthesis or methanol synthesis; thermochemical liquefaction and/or pyrolysis for bio-oil production followed by catalytic upgrading into hydrocarbon products; acid hydrolysis for sugar production followed by fermentation to ethanol or catalytic upgrading to aromatic hydrocarbons [4,6].

At the present time, bioethanol by fermentation from carbohydrates produced in sugar or starch is the primary technology as the first generation of liquid fuels from renewable biomass resources. In this technology, sugarcane or sweet sorghum can be used as the feedstock as well as non-food sources such as trees and grasses. Ethanol can be used directly as fuels but it is more common to mix it with gasoline up to 15% and gives a higher octane rating [7]. Another common technology is transesterification process, which is mixing feedstock such as vegetable oil with methanol and sodium hydroxide. The chemical reaction process produces the final product called biodiesel. This technology is mostly used in European countries.

Moreover, hydrocracking process of biological oil feedstocks such as vegetable oils and animal fats can be used to produce biodiesel. Under evaluated temperature and pressure, with the help of a catalyst, the larger molecules in the oil can be broken down into shorter hydrocarbon chains which fit in the diesel range. During the process the excess oxygen in the feedstock can be removed by hydrodeoxygenation (HDO) under hydrocracking conditions. This biodiesel has the same chemical properties as the conventional petro-based diesel however with a much higher price [8].

Currently, much attention focuses on research and development of second-generation (advanced) biofuels. Generally the second generation biofuels are based on lignocellulosic biomass such as switchgrass, woody crops, agricultural residues or waste. For these kinds of biomass it is harder to extract the required fuel. However pyrolysis is cited as an effective method to convert the solid biomass to a complicated liquid mixture called bio-oil. Slow pyrolysis bio-oil was recovered in lower mass yields but with lower oxygen and water content and better thermal stability. Fast pyrolysis,

due to its cost efficiency and short residence time has attracted significant attention [2,9].

Fast pyrolysis (Flash pyrolysis) is a pyrolysis process taking place in less than two seconds with a temperature between 300°C to 550°C in presence of an inert gas. The resulting product is a complicated mixture of light gases, char, tar and a dark viscous liquid called bio-oil. The yields and properties of the resulting products depend on a large number of variables such as the properties of the biomass feedstock, heating rate, residence time, and temperature etc. In most case, pyrolysis is a thermal process, however catalytic pyrolysis as well as pyrolysis followed by catalytic upgrading was also proposed [10,11]. The advantages of fast pyrolysis include: yields of bio-oil can exceed 70%, operates at atmospheric pressure and modest temperatures 450°C, can be applied to most biomass feedstock and low in total cost. And the disadvantages includes: phase-separation and polymerization of the liquids and corrosion of containers make storage of these liquids difficult, high oxygen and water content of pyrolysis liquids makes them need further upgrading to be fungible with conventional hydrocarbon fuels.

Since the fast pyrolysis bio-oil has high viscosity, high acid content, high water content and high oxygen content, it needs further upgrading before using as conventional gasoline or diesel. Catalytic upgrading processes using zeolites and oxides and hydrotreating processes have been applied [12,13]. Catalytic upgrading of several fractions of bio-oil have been carried out using zeolites such as HZSM-5, HY and metal oxides such as $Ce_xZr_{1-x}O_2$. Some studies have focused on reactions involving the light fraction components of bio-oil, such as ketonization and aldol

condensation reactions of propanal over $Ce_xZr_{1-x}O_2$. It was shown that gasoline range molecules could be obtained from short chain aldehydes present in bio-oil as a result of these condensation reactions [14,15]. The goal of such studies was not primarily to remove oxygen but to increase the carbon chain length of the molecules in bio-oil by catalytic upgrading. Zeolites have also been studied for the upgrading of the phenolic fraction of bio-oil. For instance, the reaction of anisole over HZSM-5 was studied and it was found that transalkylation reactions which kept the methyl group on the aromatic ring were significant. Products such as phenol, cresols, methylanisoles and xylenols were observed. The deactivation of zeolites in the presence of phenolics is a major challenge due to acid catalyzed polymerization, oligomerization and coke deposition over the catalysts. It has been shown that the presence of compounds such as guaiacol lead to a significant deactivation over zeolites such as HZSM-5 and HY [16].

Hydrodeoxygenation (Hydrotreating) is one of the most important catalytic processes in bio-oil upgrading, since it can dramatically reduce the oxygen content of the bio-oil liquid. Hydrodeoxygenation (HDO) increases the energy density and stability but reduces the viscosity of fuels. To minimize hydrogen consumption, hydrodeoxygenation (HDO) is better to applied without saturation of the aromatic rings in the feedstock. This will also help to maintain a higher octane number.

Over the past 30 years, a wide range of studies on fundamental and practical assessments of hydrotreating bio-oils and their oxygen-containing model compounds have been done over a variety of catalysts. Based on the information and results from literature, the reactivity of oxygenated groups over sulfided catalysts are listed. At low

temperatures (150-200°C), olefins, aldehydes and ketones are readily reduced by hydrogen. These reactions help stabilize bio-oil since olefins can lead to polymerization at hydrotreating conditions. At 250 – 300°C the alcohols are reacted by catalytic hydrogenation or thermal dehydration to olefins. At 300°C and above, phenolic ethers, phenols, di-phenyl ether and dibenzofuran can be deoxygenated at different reaction conditions [17].

Several groups have investigated the use of conventional hydrotreating sulfided catalysts (e.g., CoMo, NiMo) for the deoxygenation of biomass-derived feedstocks. These catalysts require the addition of H₂S to remain stable and active; however, sulfidation is not required in the HDO of biomass-derived feedstocks since hydrodesulfurization is not a necessary requirement. If sulfur does not represent a critical issue, noble metal catalysts (Pt, Pd, and Ru) can become attractive since they are significantly more active for HDO than other catalysts. For example, bifunctional Pt/Al₂O₃ and Pt/H-Beta zeolite have been found to be active for the deoxygenation of oxygenated aromatics. However, the high cost of noble metals may be an impediment for practical applications. The search for alternative catalysts based on non-noble metals (e.g. Ni, Fe, Co, Ga) is also an important issue. Also the use of bimetallic catalysts and different support add another interesting aspect to HDO topics [18-22].

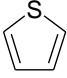
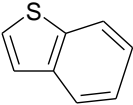
In this dissertation, the hydrodeoxygenation (HDO) reaction pathway and mechanism will be intensively discussed. Preliminary results on HDO of model phenolic compounds (meta-cresol) over monometallic, bimetallic catalysts and support effect will be presented and investigated.

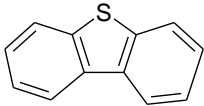
1.3 *Hydrodeoxygenation (HDO) vs. hydrodesulfurization (HDS) and Hydrodenitrogenation (HDN)*

The most important hydrotreating reactions include: hydrodesulfurization (HDS), hydrodenitrogenation (HDN), hydrodechlorination (HDCI) and hydrodeoxygenation (HDO). There's similarity between HDS, HDN and HDO such as catalyst used and high hydrogen pressure needed for deep removal. For example, sulfided CoMo/ γ -Al₂O₃ can be used in all of HDO, HDS and HDN [23-25]. Novel metal catalysts can also be used. According to what has been reported, Pt/ γ -Al₂O₃ is effective in HDS of 4,6-dimethyldibenzothiophene [26] and HDO of m-cresol [27]. The similarity of HDO with HDS and HDN allows us to look into the reaction mechanism of HDS and HDN which already been discussed over decades before going to HDO.

1.3.1 *Hydrodesulfurization (HDS)*

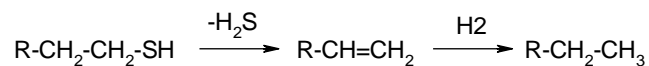
The organosulfur compounds present in petroleum feed are: thiols (R-SH),

sulfides (R-S-R), disulfides (RSSR), thiophene , benzothiophene  and

dibenzothiophene  [28]. The HDS reactivity of organosulfur

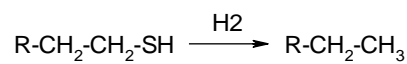
compounds depends on their structure. The low boiling point fraction thiols, thioethers and disulfides undergo desulfurization more readily. The thiophenes, benzothiophenes and their alkylated derivatives, which are the higher boiling fractions require strenuous conditions in hydrotreating.

Thiols, coming from ring opening of cyclic sulfur compounds, do not occur in oil because of their high reactivity. Aliphatic thiols may react through elimination and hydrogenation [29]:



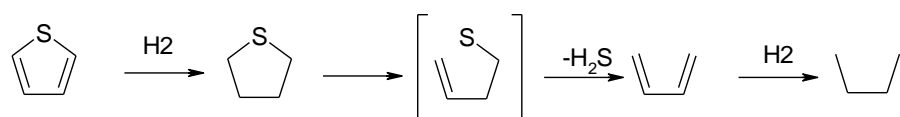
This is a Hofmann-type β -hydrogen elimination reaction.

Also hydrogenation and hydrogenolysis could take place via C-S and H-H bond scissions and C-H and S-H bond formation [30].



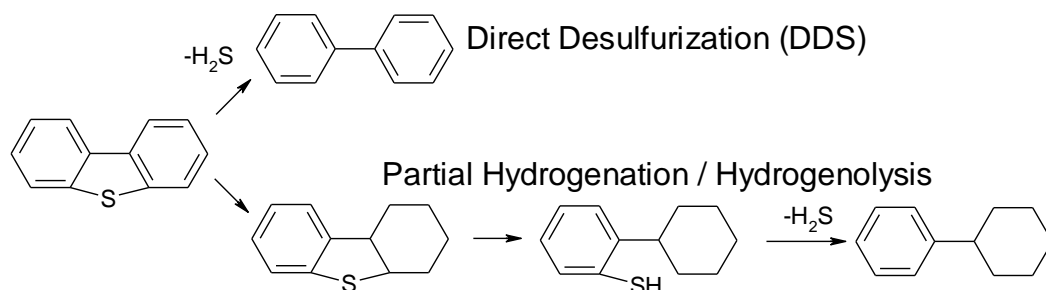
Aliphatic thiols with a β -H atom undergo elimination faster than hydrogenolysis. Those without β -H atom must undergo HDS through hydrogenolysis. Benzene is a major product obtained from thiophenol, which may also occur by hydrogenolysis.

Under high hydrogen pressure, the major reaction path for the HDS of thiophene is via hydrogenation of thiophene to tetrahydrothiophene, which undergoes two successive β -H eliminations to butene.



Since under high hydrogen pressure butadiene and 4-mercaptobutene-1 could quickly be hydrogenated, they would not be observed as a reaction intermediate in the gas phase. At atmospheric pressure, the reaction pathway is still under debate. Some argued it is essentially the same as in high hydrogen pressure, while others believe direct hydrogenolysis is the main route.

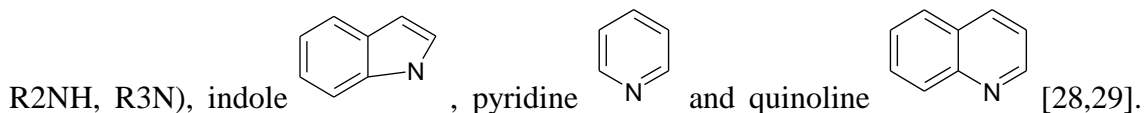
For dibenzothiophene and dialkyldibenzothiophene (such as dimethylbenzothiophene), again basically two pathways exist, hydrogenolysis which is also called direct desulfurization (DDS) and partial hydrogenation/hydrogenolysis.



For dibenzothiophene, DDS accounts for more than 80%. However the alkyl groups in 4,6-dimethyldibenzothiophene sterically hinder the perpendicular adsorption of the molecular onto the catalyst surface, thus the DDS route is strongly suppressed. The partial hydrogenation/ hydrogenolysis route is about equally fast for dibenzothiophene and 4,6-dimethyldibenzothiophene.

1.3.2 Hydrodenitrogenation (HDN)

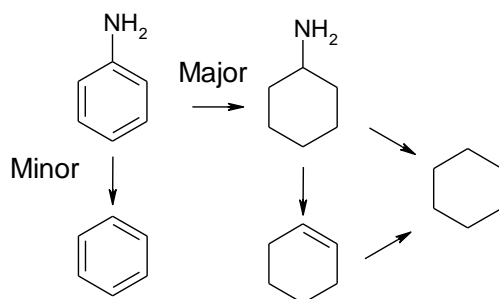
The organonitrogen compounds in oil product mainly include amines (RNH₂,



The nitrogen atom of alkyl amines can be easily removed under mild condition. However, because of greater aromaticity, much higher hydrogen pressure is required for HDN of aromatic nitrogen compounds than HDS. N-containing ring of unsaturated heterocycles need to be saturated before removal of N atom. The hydrogenation of the unsaturated N-containing ring usually determines overall HDN rate for the N-

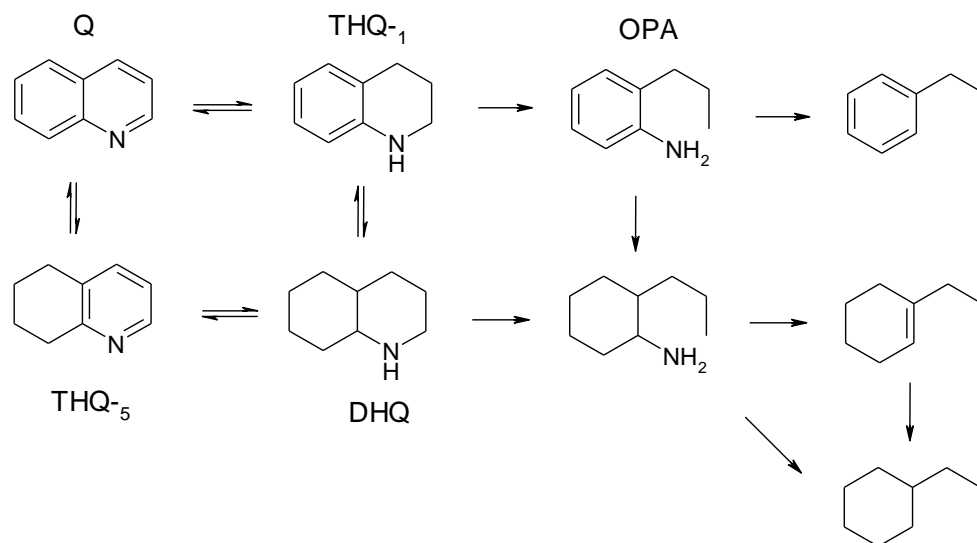
heteroaromatic compounds. The activity decrease in the following order: quinoline > pyridine > indole > pyrrole.

Hydrogenation of the aromatic ring is a prerequisite not only for heterocycles such as pyridine, but also for aniline. The HDN of aniline takes place partly by hydrogenolysis (direct denitrogenation, DDN) and mainly by hydrogenation to cyclohexylamine, followed by quickly reacts to cyclohexene and cyclohexane, shown in



the following scheme:

When it comes to HDN of quinoline, it is a little more complicated. In principle there are two ways to remove N atom, shown in the scheme below:



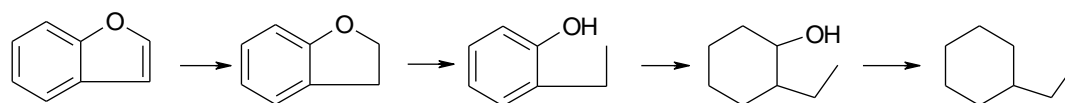
One pathway goes through o-propylaniline (OPA) while the other one goes via decahydroquinoline (DHQ). Under most of the cases, hydrogenation of quinoline takes place, leading to equilibrium established between 1,2,3,4-tetrahydroquinoline (THQ-1),

5,6,7,8-tetrahydroquinoline (THQ-5) and decahydroquinoline (DHQ). Here the OPA pathway is similar to HDN of aniline, mainly via saturation of the aromatic ring followed by removal of N atom. However the rate of this OPA path is strongly suppressed by strong adsorption of other species including DHQ (around 20 times stronger adsorption), Q and THQ-1. Thus the other DHQ pathway is dominant. In this pathway, DHQ undergoes N-removal via a ring opening and then reacts quickly to propylcyclohexane and 1-propylcyclohexene.

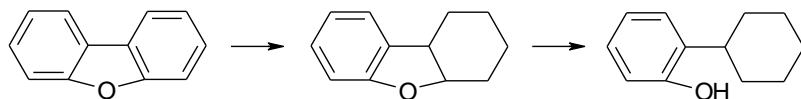
1.3.3 Hydrodeoxygenation (HDO)

Over decades ago, HDO does not attract too much attention, since the content oxygen is less than 2wt% in conventional crude oil, and it is only applied to treat coal derived liquid. However the rising interest in synthetic oil from biomass-derived feed makes HDO becoming more and more important.

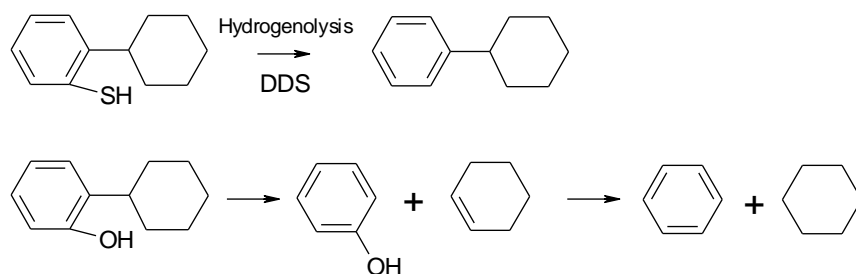
HDO of benzofurans occurs similarly to HDS of benzothiophene and HDN of indole. Saturation of the ring followed by a ring opening is needed before O-removal via elimination of H₂O, as shown below [31]:



However when it comes to HDO of dibenzofuran, the reaction path is very different. Double ring products (biphenyl and cyclohexylbenzene) are main products in HDS, while cyclohexane, cyclohexene and benzene are obtained in HDO of dibenzofuran. The first step is the same that is partial hydrogenation of one of the phenyl rings:



In the following steps the intermediate o-cyclohexylphenol and o-cyclohexylthiophenol reacts differently. The o-cyclohexylthiophenol undergoes direct desulfurization (DDS) via hydrogenolysis. For o-cyclohexylphenol, it first loses the cyclohexyl group followed by deoxygenation of phenol. This reaction is a reverse of acid-catalyzed alkylation reaction between cyclohexene and phenol.



Based on above content, simply making conclusion for HDO from extrapolate from HDS and HDN results is not enough. Thanks to growing interest on upgrading biomass-derived liquids, there are numerous studies on HDO involving model O-compounds now [18]. In this contribution, the mechanism of HDO will be focused in more detail, not only from literatures but also from my own study.

Also, HDO of furanic compounds including furan, methylfuran, dimethylfuran, benzofuran and dibenzofuran have been studied over Mo-based sulfide catalysts [32]. Over $\text{CoMo}/\text{Al}_2\text{O}_3$ at 400°C , the products of furan conversion include hydrocracking products ethylene, propane and propene, with CO formation. Butane and butenes are obtained from hydrogenation of butadiene, which is a HDO product. Under typical hydroprocessing condition, furan can be fully hydrogenated to tetrahydrofuran (THF) which is an important intermediate before O-removal. The HDO of THF is about three

times faster than furan, which supports the above statement [33]. Conversion of furan over Pt supported on TiO₂, SiO₂ and Al₂O₃ shows significant support effect [34]. On Pt/TiO₂, the main product was butane, while on the other two, decarbonylation took place. The butoxy species was proposed to be the key intermediate. The CO formed during decarbonylation caused self-poisoning of Pt surface.

HDO of methyl-furan gives pentenes, pentane and a small amount of pentadiene, while HDO of 2,5-dimethylfuran yields 1-hexene and 1,5-hexadiene as major products [18]. HDO of benzofuran and dimethyl-benzofuran have been briefly discussed in the previous text.

Furfural, as an aromatic compounds derived from dehydration of sugars, is another important component in bio-oil. Sitthisa et al. had done beautiful research work on HDO of furfural over SiO₂ supported monometallic Pd, Cu, Ni and bimetallic Pd-Cu, Ni-Fe catalysts [19-21]. Over Cu/SiO₂ the major product is furfuryl alcohol coming from hydrogenation; for Pd/SiO₂, furan and tetrahydrofuran from decarbonylation are main products while hydrogenation was in low amount; over Ni/SiO₂, hydrogenation and decarbonylation were both obtained, and also ring opening to C₄ compounds (butanal, 1-butanol and butane) was also found. Bimetallic catalysts dramatically changed the product selectivity. The addition of Fe onto Pd/SiO₂ helped suppress the decarbonylation and hydrogenation while methyl-furan was more selectively produced. Over Pd-Fe/Al₂O₃ where the alloy was worse formed than Pd-Fe/SiO₂, the bimetallic effect decreased. On Ni-Fe/SiO₂ similar conclusions were made. This reduction in decarbonylation can be attributed to an increase of the stability of $\eta^2(\text{C},\text{O})$ -surface species. The increase in the interaction of the carbonyl O with surfaces through Fe-O

interaction hinders the formation of acly species, which is responsible for decarbonylation. In addition, the C-O hydrogenolysis of the adsorbed furfuryl alcohol is improved by this interaction.

HDO of furfural has been studied by Zhao et al. in water phase using Ni/HZSM-5 catalyst at 523 K and 5 MPa of H₂ in a batch reactor. Two parallel reactions took place: intermolecular dehydration of furfural to tetrahydropyran and deoxygenation to pentane, competed to ultimately produce 64% pentane and 36% tetrahydropyran. It has been claimed that the HDO of furfural occurred by hydrogenation of the furan ring, followed by hydrolysis of the C5 ring, and subsequent alcohol dehydration/hydrogenation to form the straight-chain alkane [32,35].

Phenolic compounds (phenols, guaiacol, anisole ...), one of the most important group components in fast pyrolysis bio-oil, would be discussed in every detail in the following texts.

1.4 Concept process for bio-oil refinery and upgrading

In the previous text, we have already discussed that fast pyrolysis bio-oil is a complicated mixture with properties depending on a large number of variables such as the properties of the biomass feedstock, heating rate, residence time, and temperature et al. Directly upgrading the whole fraction of bio-oil using hydrotreatment or zeolite upgrading will cause severe loss of carbon, fast deactivation of catalysts and acid contamination et al [36-38]. For example, direct hydrodeoxygenation of the small oxygenates, which constitute a large carbon fraction of the whole bio-oil, results in production of light gases with significant losses in liquid yield. Thus fractionation of

fast pyrolysis before upgrading is an effective alternative method and necessary to solve these challenges [12].

However the full bio-oil cannot be fractionated by conventional distillation since re-heating would result in undesirable side reactions such as oligomerization and condensation. One alternative way is to conduct thermochemical conversion of biomass in different temperature stages, as shown in Fig 4.I. Sequential heating treatment at increasing temperature stages can be applied for fractionation. Initial torrefaction temperature is below 300°C, small oxygenates (mainly acetic acid and acetol) and water decomposed from hemicellulose is extracted as the products. The second stage of torrefaction holds at around 400°C, where the cellulose derived sugar compounds such as levoglucosan and hydroxymethyl furfural (HMF) are produced. The final stage, fast-pyrolysis at around 550°C, gives lignin derived compounds mostly phenolic compounds [12].

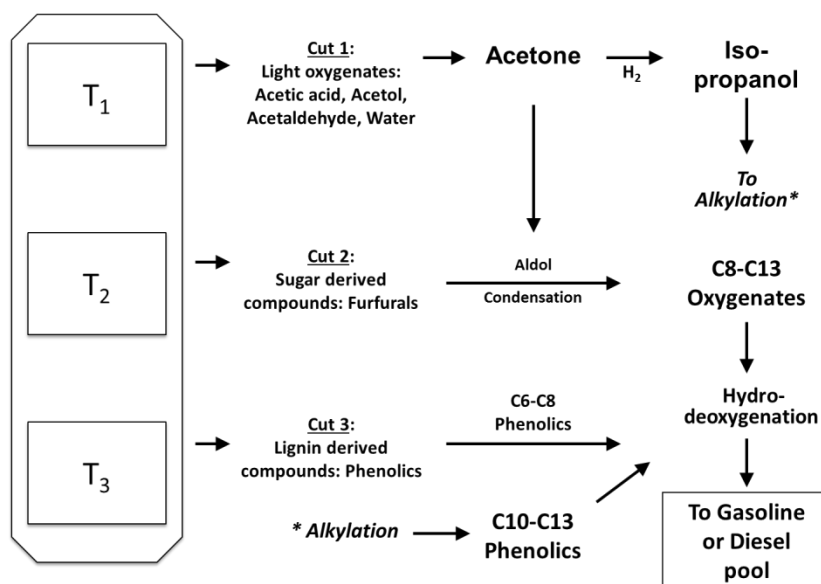


Figure 4.I. Catalytic cascade connected to a multi-stage pyrolysis.

Based on the above fractionation, to retain the carbon of the small oxygenates in the liquid is necessary to carry out C-C bond formation reactions to bring them to the fuel range before carrying out the hydrodeoxygenation. An attractive approach is to take advantage of the high reactivity of the oxygen functionalities before eliminating them. One method to achieve this is explore alkylation as an alternative path to incorporate C2-C3 oxygenates in phenolic compounds and form C8-C13 phenolics, which subsequently can be deoxygenated to obtain drop-in fuel components, or stabilized feedstocks that can be further upgraded in a refinery. For example, since small aldehydes and ketones cannot be used directly to alkylate phenolic compounds, as a first step we propose to hydrogenate the aldehydes or ketones to alcohols, which are known to be an effective alkylating agents. Metal catalysts such as Ni, Ru, Pd, and Cu can be used to catalyze the hydrogenation of the short oxygenates, while acidic zeolites are highly effective for the alkylation step. Acidic catalysts such as H-Beta, HY, H-mordenite, HZSM-5 and MCM-41 have been previously used for alkylating phenol and cresol with small alcohols and/or with olefins [39].

Pre-fractionation before hydrotreating/hydrodeoxygenation helps: a) reduce the complexity of treating the whole bio-oil; b) couple C-C bonds to build up the carbon chain into gasoline or diesel range; c) minimizes the liquid yield loss. Then, which might be more important, is the direct hydrotreating for the lignin derived phenolic group compounds, which is the main focus of this contribution.

References

- [1] BP Energy Outlook 2035.
- [2] S. Wan, T. Pham, X. Zhang, L.L. Lobban, D.E. Resasco, R.G. Mallinson, *AIChE Journal* 59(7) (2013) 2275-2285.
- [3] <http://www.eia.gov/countries/data.cfm>.
- [4] G.W. Huber, J.A. Dumesic, *Catal Today* 111(1-2) 2006 119-132.
- [5] M. Saidi, F. Samimi, B.C. Gates, M.R. Rahimpour, *Energy Environ. Sci.* 7 (2014) 103-129.
- [6] G.W. Huber, S. Iborra, A. Corma, *Chem. Rev.* 106 (2006) 4044-4098.
- [7] Towards Sustainable Production and Use of Resources: Assessing Biofuels, United Nations Environment Program. 16 October 2009.
- [8] G. Knothe, *Progress in Energy and Combustion Science* 36 (2010) 364–373.
- [9] D.C. Elliott, *Energy & Fuels* 21 (2007) 1792-1815.
- [10] A. Demirbas, *Fuel Proc. Technol.* 88 (2007) 591.
- [11] M.G. Perez, J. Shen, X.S. Wang, C.Z Li, *Fuel Proc. Technol.* 91 (2010) 296.
- [12] T.N. Pham, D. Shi, D.E. Resasco, *J. Catal* 145 (2014) 10-23.
- [13] T. Prasomsri, A.T. To, S. Crossley, W.E. Alvarez, D.E. Resasco, *Appl. Catal. B* 106(1-2) (2011) 204-211.
- [14] T.N. Pham, D. Shi, T. Sooknoi, D.E. Resasco, *J. Catal.* 295 (2012) 169-178.
- [15] A. Gangadharan, M. Shen, T. Sooknoi, D. E. Resasco, R. G. Mallinson, *Appl. Catal. A: General* 385 (2010) 80–91.
- [16] X.L. Zhu, R.G. Mallinson, D.E. Resasco, *Appl. Catal. A* 279 (2010) 181.
- [17] E. Furlmsky, *Ind. Eng. Chem. Prod. Res. Dev.* 22 (1983) 31-34.

-
- [18] E. Furimsky, *Appl. Catal. A* 199 (2000) 147-190.
- [19] S. Sitthisa, W. An, D.E. Resasco, *J. Catal.* 284 (2011) 90–101.
- [20] S. Sitthisa, D.E. Resasco, etc, *J. Catal.* 280 (2011) 17–27.
- [21] S. Sitthisa, D.E. Resasco, *Catal. Lett.* 141(6) (2011) 784-791.
- [22] A.J. Foster, P.T.M. Do, *Top Catal* 55 (2012) 118-128.
- [23] E.O. Odebunmi, D.F. Ollis, *J. Catal* 80 (1983) 56-64.
- [24] E.O. Odebunmi, D.F. Ollis, *J. Catal* 80 (1983) 65-75.
- [25] E.O. Odebunmi, D.F. Ollis, *J. Catal* 80 (1983) 76-89.
- [26] H. Guo, Y. Sun, R. Prins, *Catal Today* 130 (2008) 249-253.
- [27] A.J. Foster, P.T.M. Do, *Top Catal* 55 (2012) 118–128.
- [28] R.J. Angelici, *Polyhedron* Vol. 16, No. 18, pp. 3073-3088.
- [29] R. Prins, *Handbook of Heterogenous Catalysis*, pp 2696-2718.
- [30] T.Todorova, R. Prins, *J. Catal* 236 (2005) 190-204.
- [31] L.D. Rollmann, *J. Catal* 46 (1997) 243-252.
- [32] H. Wang, J. Male, Y. Wang, *ACS Catal.* 3 (2013) 1047–1070.
- [33] E. Furlmsky, *Ind. Eng. Chem. Prod. Res. Dev.* 22 (1983) 31-34.
- [34] M. Bartok, G. Szollosi, J. Apjok, *Reaet.Kinet.Catal.Lett.* 64 (1998) 21-28.
- [35] C. Zhao, J.A. Lercher, *J Catal.* 296 (2012) 12–23.
- [36] C.A. Fisk, T. Morgan, Y. Ji, M. Crocker, C. Crofcheck, S.A. Lewis, *Appl. Catal. A* 358 (2009) 150–156.
- [37] X. Yang, S. Chatterjee, Z. Zhang, X. Zhu, C. U. Pittman Jr, *Ind. Eng. Chem. Res.* 49 (2010) 2003–2013.

-
- [38] T.Q. Hoang, X. Zhu, T. Sooknoi, D.E. Resasco, R.G. Mallinson, *J. Catal.* 271 (2010) 201-208.
- [39] L. Nie, D.E. Resasco, *Appl. Catal. A: General* 447-448 (2012) 14-21.

Chapter II. Hydrodeoxygenation of m-Cresol to Toluene over SiO₂ supported Bimetallic Ni-Fe Catalysts

2.1 Introduction

Phenolics are abundant components of the liquid product (bio-oil) obtained from the fast pyrolysis of biomass. They derive from both pyrolytic decomposition of lignin and from condensation/aromatization of small oxygenates. They can represent an important building block for potential production of fuels and chemicals from biomass. However, following the primary conversion step, an effective catalytic upgrading step is needed in the production of more useful products [1-6]. As we have previously pointed out [7], the upgrading process should not only minimize the oxygen content in the product, but also maximize carbon retention. As a result, conventional hydrotreating, the most common and effective method that has been tested for hydrodeoxygenation may not be the optimum path for upgrading of bio-oil with maximum carbon efficiency [8,9]. We have recently investigated different paths, including ketonization, aldol condensation, aromatization and alkylation to accomplish the formation of C-C bonds before deoxygenation, which maximizes the liquid fuel yield and carbon efficiency [10-12].

Several groups have investigated the use of sulfided catalysts (e.g., CoMo, NiMo) typically used in conventional hydrotreating for the deoxygenation of biomass-derived feedstocks [13]. These catalysts require addition of H₂S to remain stable and active; however, sulfidation is not required in the HDO of biomass-derived feedstocks since hydrodesulfurization is not a necessary requirement.

Thus noble metal catalysts (Pt, Pd, and Ru) can become attractive since they are significantly more active for HDO than other catalysts. For example, bifunctional Pt/Al₂O₃ [14,15] and Pt/H-beta zeolite [16] have been found to be active for the deoxygenation of

oxygenated aromatics. However, the high cost of noble metals may be an impediment for practical applications. The search for alternative catalysts based on non-noble metals (e.g. Ni, Fe, Co, Ga) has been the focus of several recent studies [17-22]. A combinations of metal sites (active for hydrogenation) with acid sites provided by the support or added promoters (active for transalkylation and dehydration) can optimize the catalyst resulting in improved deoxygenation and carbon efficiency.

The use of bimetallic catalysts adds another interesting aspect since changes in electronic structure and/or surface ensemble size due to the presence of adjacent atoms may greatly modify the resulting selectivity [17,19]. In three recent studies, Ni and Ni-Cu catalysts have been evaluated for the HDO of guaiacol [23-25]. The studies agree that the addition of Cu improves the catalyst performance for HDO. Similarly, in a recent investigation of our own group, Ni-Fe bimetallic catalysts were evaluated for the hydrogenation and deoxygenation of furfural as a model compound of sugar dehydration products. We found that the reaction pathways on Ni-Fe bimetallics were dramatically different from those on pure Ni or pure Fe catalysts. While pure Fe was inactive at the reaction conditions investigated, it greatly altered the behavior of Ni when added in 1:1 molar ratio. The high decarbonylation activity typically observed on pure Ni was suppressed on the bimetallic catalyst, while the C=O hydrogenation (at low temperatures) and C-O hydrogenolysis (at high temperatures) were drastically enhanced [26].

A mechanism for the deoxygenation of phenolic compounds that has been widely proposed in the literature [9,14,15,27] is the two-step pathway, which involves an initial hydrogenation of the aromatic ring followed by C(sp³)-O bond cleavage via dehydration. This HDO pathway normally requires a bi-functional catalyst, with a metal function that catalyzes hydrogenation/dehydrogenation of the ring and an acid function that catalyzes dehydration. An alternative mechanism that has been suggested in several studies [27,28]

does not involve the C(sp²)-to-C(sp³) conversion. In analogy to the direct desulfurization (DDS) path typically proposed in HDS catalysts, a direct cleavage of the C(sp²)-O bond has been claimed in several reports and referred to as direct deoxygenation (DDO) [27]. Since such cleavage would require a very high activation energy, one may expect that this path might only be possible at high temperatures. In the present contribution, the comparison of the different product distributions obtained on Ni and Ni-Fe catalyst has allowed us to infer a novel reaction pathway that includes some important conceptual differences from those previously considered and may be operative at relatively moderate conditions, i.e. T ~ 300 °C.

2.2 Experimental

2.2.1 Catalyst synthesis and characterization

Monometallic catalysts Ni/SiO₂ and Fe/SiO₂ (5 wt % metal loading) were prepared by incipient wetness impregnation of the support (SiO₂, HiSil 233) with an aqueous solution of the respective metal precursor: Ni(NO₃)₂·6H₂O (98%, Alfa Aesar) and Fe(NO₃)₃·9H₂O (98% Sigma–Aldrich). As described in our previous work [26], the bimetallic Ni-Fe/SiO₂ catalysts were prepared by incipient wetness co-impregnation. In this case, the Ni loading was kept constant at 5.0 wt.% on all samples, while the Fe loading was varied from 2.0, 5.0 to 10 wt.%. As summarized in Table 1.II, they are indicated with the corresponding mass ratios as (2.5:1) Ni-Fe, (1:1) Ni-Fe, and (1:2) Ni-Fe/SiO₂, respectively.

XRD analysis was conducted on samples pre-reduced ex-situ under pure H₂ (100 ml/min) at 450 °C for 1 h and passivated by slow exposure to low O₂ concentrations at room temperature, before exposure to the atmosphere. The measurements were carried out with a D8 Series II X-Ray Diffractometer (BRUKER AXS) operated at 40 kV and 35 mA,

using Cu K α monochromatic radiation ($\lambda= 0.154178$ nm) in the 30 to 60° diffraction angle range.

The reducibility of the calcined samples was determined by temperature programmed reduction (TPR). In these measurements, 20 mg of a sample was placed in a quartz reactor and heated at 30 °C/min up to 500 °C under a He flow of 20 ml/min, and held at this temperature for 1 h. The reactor was then cooled down to 30 °C and the sample exposed to a stream of 5% H₂/Ar at a flow rate of 20 ml/min. Subsequently, the sample was heated to 800°C at a heating rate of 5°C/min. The variation in hydrogen uptake was monitored on a TCD detector as a function of temperature. The molar H₂ uptake per gram of sample was quantified from the peak area in the TPR profiles and calibrated with a CuO standard. Morphology and size of the Ni-Fe clusters were characterized by transmission electron microscopy (TEM, JEOL model JEM-2100 LaB6). Before TEM analysis, the samples were reduced ex situ in pure H₂ (100 ml/min) at 450°C for 1 h. The reduced samples were then mixed with 2-propanol, sonicated, deposited onto the TEM (Cu) grids, and dried. Average particle sizes for all the samples, as determined by TEM, are summarized in Table 1.II. The BET surface area (S_g) was measured by conventional N₂ physisorption on a Micromeritics ASAP 2010 unit, after evacuation at 350°C for 3 h.

The surface chemistry of the catalysts was investigated by Diffuse Reflectance Infrared Fourier Transform Spectroscopy (DRIFTS) of adsorbed pyridine. For these measurements, the catalyst powder was loaded in the sample cup, reduced in situ at 400 °C for 1 h under a flow of H₂ (30 ml/min) and cooled down to 100 °C. Then, pyridine vapor was passed through the cell for approximately 30 min. To eliminate the weakly bound pyridine, the sample was purged under H₂ flow for 20 min at 100 °C. Background and absorption spectra were recorded at a resolution of 4 cm⁻¹, accumulating 256 scans.

2.2.2 Catalytic activity measurements

The vapor-phase conversion of m-cresol in H₂ over the Ni, Ni-Fe and Fe catalysts was evaluated in a tubular quartz reactor at atmospheric pressure. The flow reaction system is equipped with a mass flow controller and a syringe pump for the continuous injection of m-cresol. All lines were heated to avoid condensation of the compounds. Pelletized catalyst (40-60 mesh) was packed in the reactor between two layers of quartz wool and a preheating layer of glass beads on top to improve the temperature uniformity. The catalyst was reduced in situ under a down-flow of 60 mL / min of H₂ at 450 °C for 1 h, and then the temperature was reduced to the reaction temperature 300 °C. The H₂/m-cresol molar ratio was kept at 60:1 for all runs. The products were quantified by gas chromatography (GC 6890, Agilent), using an Innowax capillary column and a flame ionized detector (FID). The catalyst was evaluated under different W/F (0.058 – 0.464 h) varying the amount of catalyst (30 – 120 mg). The W/F is defined as the ratio of the catalyst mass (g) to organic feed flow rate (g/h)². The product yield and selectivity for each product were calculated as follows:

$$Yield (\%) = \frac{\text{mol of product produced}}{\text{mol of m - cresol fed}} \times 100$$

$$Selectivity (\%) = \frac{\text{mol of product produced}}{\text{mol of m - cresol consumed}} \times 100$$

2.2.3 Computational Method

DFT calculations were performed in the Vienna ab initio simulation package (VASP) [29,30]. A spin-polarized GGA PBE functional [31], all-electron plane-wave basis sets with an energy cutoff of 400 eV, and a projector augmented wave (PAW) method [32,33] were adopted. The Ni (111), Fe(110) and NiFe(111) alloy surface were

modeled by a three-layer p(4×4) slab with the bottom two layers fixed at their optimized bulk positions. The calculated lattice constants are 3.522 Å for fcc Ni, 2.831 Å for bcc Fe, and a=c= 3.553 Å b=3.582 Å for fcc Ni₂Fe₂. The two successive slabs were separated by a 18 Å vacuum region. Considering that the surface composition may differ from that of the bulk alloy and surface segregation may occur in a NiFe alloy [34], we also considered a model that contains “disordered” NiFe alloy surface, which has the same Ni:Fe molar ratio of 1:1 as the perfect surface, but is re-arranged to create “islands” of Ni and Fe. Such a “disordered” surface is energetically unfavorable compared to the perfect one, i.e., having energy penalty of 0.39kcal/mol per surface atom. The previous Mössbauer investigation [35] suggested that certain phase separation could accompany particle growth in NiFe alloy catalysts using the similar synthesis process as in this work. The 3×3×1 k-points using the Monkhorst–Pack scheme was used in the calculations. First-order Methfessel–Paxton smearing of 0.2 eV was employed in the integration to speed up the convergence. The conjugate gradient algorithm was used in the optimization. The convergence threshold was set 10⁻⁴ eV in total energy and 10⁻² eV/Å in force on each atom. The adsorption energy (E_{ads}) is defined as E_{ads} = E(cresol/slab) – E_{slab} – E(cresol), where E(cresol/slab), E_{slab}, and E(cresol) are the total energy of cresol/slab, clean surface, and gas-phase m-cresol in one supercell.

2.3 *Results and discussion*

2.3.1 *Catalyst characterization*

Figure 5.II displays the XRD patterns of the catalyst samples after H₂ reduction. The monometallic Ni catalyst showed one peak at 2θ = 44.41 °, which is ascribed to the Ni (111) reflection. The bimetallic catalysts exhibited a single peak around this region, but shifted to lower angles with increasing Fe content. In agreement with previous studies

[19,26,36], these XRD data indicate the formation of a Ni-Fe solid solution, rich in Ni. The shift to lower angles with Fe content indicates an increase in the Fe concentration in the solid solution. In addition to the peak corresponding to the Ni-Fe solid solution, the sample with the highest Fe concentration (1:2) Ni-Fe/SiO₂, exhibited a shoulder at 2 θ =44.64°, which is ascribed to the α -Fe (110) reflection resulting from a fraction of unalloyed Fe. The same result has been observed in previous XRD studies conducted on a sample of Fe/Ni=2 ratio, and the authors assigned this double peak to unalloyed α -Fe or Fe-rich alloys with a bcc structure [36]. The TPR profiles [26] also support the formation of bimetallic clusters in the Fe-Ni catalysts. The characterization results of the catalysts are summarized in Table 1.II; further details about these catalysts can be found in our previous publication, elsewhere [26].

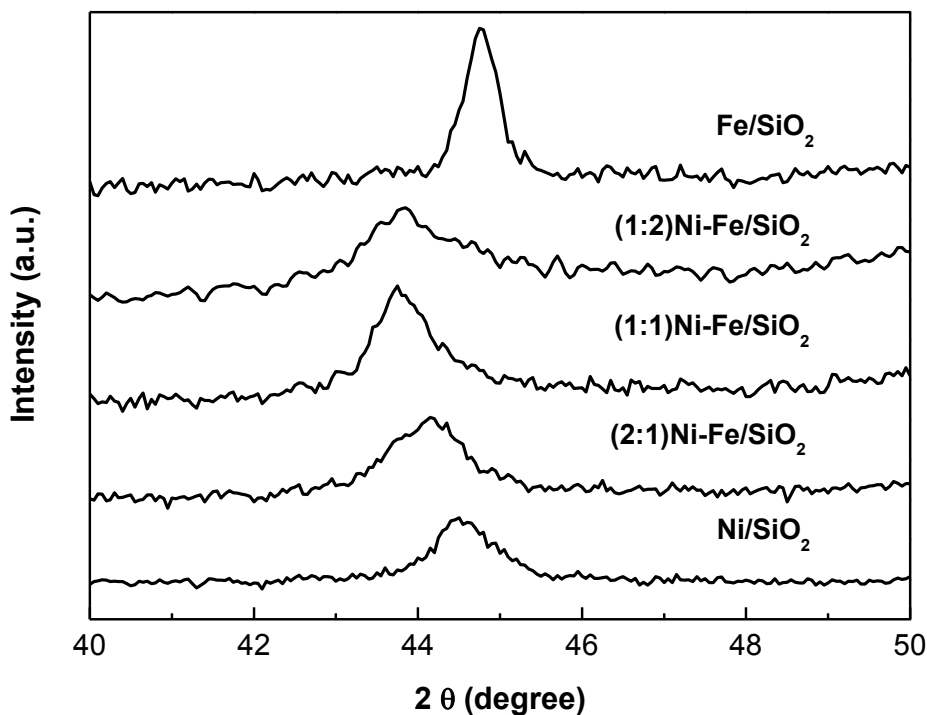


Figure 5.II. XRD patterns of monometallic Ni, Fe and bimetallic Ni-Fe catalysts pre-reduced ex-situ in hydrogen at 450°C for 1h.

Catalysts	Wt%Ni	Wt%Fe	BET (m ² /g)	H ₂ consumption from TPR (mmol/gcat)	Diameter (nm)	Lattice constant (Å)		
						XRD	DFT	Std.
Ni	5	0	126	1.01	11.2	3.53	3.52	3.52
(2:1)Ni-Fe	5	2	130	1.48	10.0	3.57	-	-
(1:1)Ni-Fe	5	5	115	2.20	10.0	3.58	3.55 ^a	3.58 ^a
(1:2)Ni-Fe	5	10	124	-	9.6	3.58	-	-
Fe	0	5	128	-	19.1	2.87	-	2.87

Table 1.II. Characterization of SiO₂ supported catalysts.

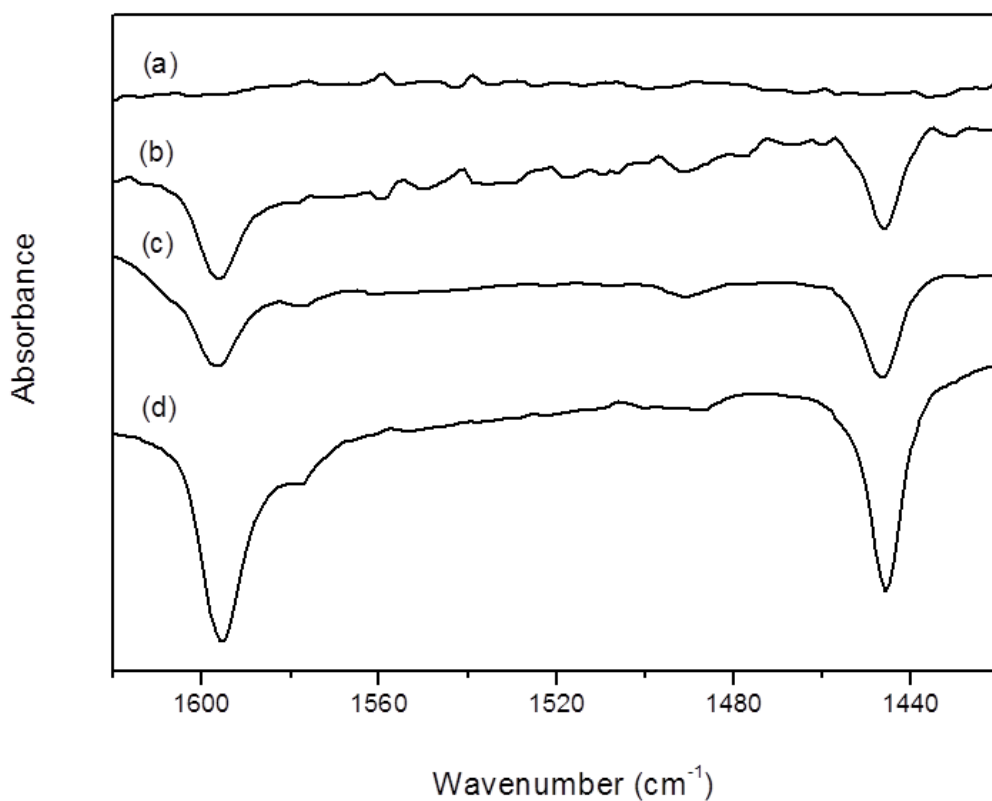


Figure 6.II. DRIFT spectra of the pyridine chemisorption experiments at 100 °C and atmospheric pressure after pyridine chemisorption for (a) pure SiO₂, (b) Ni/SiO₂, (c) (1:2)Ni-Fe/SiO₂, (d) Fe/SiO₂.

DRIFTS of adsorbed pyridine was conducted on the different catalysts to compare their surface properties. The DRIFT spectra obtained on the Ni, (1:2) Ni-Fe, and Fe/SiO₂ catalysts after exposure to pyridine at atmospheric pressure and 100 °C are reported in Figure 6.II, along with the spectrum obtained on pure SiO₂ exposed to pyridine. An intense band at 3,741 cm⁻¹ (not shown) corresponding to the silanol O-H stretching mode was observed for all samples [37]. No absorption band was observed for the SiO₂ support in the frequency region corresponding to adsorbed pyridine (1,620-1,420 cm⁻¹). Therefore, it can be concluded that any contribution to the spectra of pyridine interacting with hydrogen-bonded or free silanols [38] are negligible under the conditions of the measurements (i.e., purged at 100 °C). By contrast, the catalysts do display pronounced absorption bands at 1,445, 1,577 and 1,596 cm⁻¹, which are characteristic of the vibrational modes 19b and 8a of pyridine species interacting with coordinatively unsaturated cations [39,40]. According to the relative band intensity for comparable amounts of catalyst and surface areas, we can estimate that the density of coordinatively unsaturated cations increases in the order Ni/SiO₂ < (1:2) Ni-Fe/SiO₂ < Fe/SiO₂. The presence of unreduced cations remaining on the surface of silica even after high temperature reduction treatments has been demonstrated for Fe/SiO₂ [40] as well as for Ni/SiO₂ [41].

2.3.2 Catalytic activity and product distribution at varying m-cresol conversion

The product distribution from the m-cresol conversion over Ni/SiO₂ at 300 °C is shown in Figure 7.II as a function of W/F. Three C₇ compounds are obtained, 3-methylcyclohexanone that is the main product, 3-methylcyclohexanol, and toluene (TOL). In addition to the three C₇ compounds, methane, phenol, and xylenol are also obtained as products. They may arise from hydrogenolysis and transalkylation side reactions. Metallic Ni is a well-known hydrogenolysis catalyst, but transalkylation (disproportionation) is typically catalyzed by acid sites. While the silica support provides no significant acidity, a

fraction of Ni may not be fully reduced, as described above. The presence of coordinatively unsaturated cations may act as Lewis acid sites [40], which might catalyze the transalkylation that produces phenol and xylenols. On the other hand, methane may arise from metal-catalyzed hydrogenolysis or acid-catalyzed demethylation.

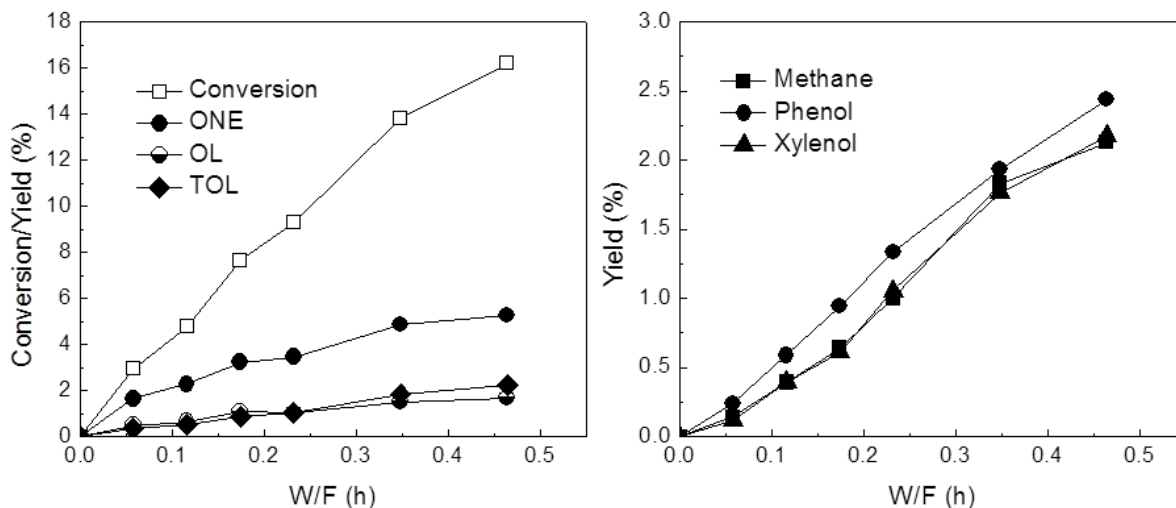


Figure 7.II. Product distribution of m-cresol over 5 wt.% Ni/SiO₂ at 300°C as a function of W/F. H₂/Feed molar ratio =60. Pressure = 1atm.

	5% Ni/SiO ₂	5% Fe/SiO ₂	5% Ni/SiO ₂ + 5% Fe/SiO ₂ (physical mixture)	5% Ni-5% Fe/SiO ₂
Conversion %	16.2	8.8	12.6	13.7
Selectivity %				
Toluene	14.2	60.2	18.5	52.6
3-methylcyclohexanone	33.3	0.0	33.1	0.0
3-methylcyclohexanol	11.1	0.0	13.7	0.0
Methane	13.0	0.0	10.5	2.2
Transalkylation Products	28.4	39.8	24.2	45.3

Table 2.II. Conversion and product yield from the reaction of m-cresol over different catalysts at W/F= 0.46 h and 300°C. H₂/Feed molar ratio =60. Pressure = 1atm.

A remarkable difference in product distribution relative to that obtained on Ni/SiO₂ is observed on the iron-containing Fe and Ni-Fe/SiO₂ catalysts when compared under

identical reaction conditions. As summarized in Table 2.II, when the three different catalysts are compared at 300 °C and W/F= 0.46 h a drastic change in product selectivity is observed. While, as mentioned above, 3-methylcyclohexanone is the dominant C₇ compound over Ni/SiO₂ it is not formed either on Fe or Ni-Fe/SiO₂ catalysts. By contrast, on these catalysts the largely dominant product is toluene (TOL). Interestingly, the physical mixture of Fe/SiO₂ and Ni/SiO₂ catalysts behaves very similarly to the Ni/SiO₂ catalyst alone. That is, ring hydrogenation products were formed and 3-methylcyclohexanone was the main one. Small amounts of toluene and xylenols were observed on this mixture, while they were the main products over the bimetallic catalysts, which may be due to the rather low activity of Fe/SiO₂ compared to Ni/SiO₂. Thus, these results demonstrate that the typical behavior of unalloyed Ni is not observed on the Ni-Fe bimetallic surface. As discussed below, the observed difference in behavior may be due to surface enrichment of Fe, or at least, the formation of Fe islands on the surface, as suggested by the DFT results discussed in section 2.3.5 below.

The Fe-containing catalysts also produce xylenols, xylene, phenol, and methane. In this case, again, the transalkylation reaction responsible for the production of C₈ products might be catalyzed by the Lewis acid sites created by the presence of coordinatively unsaturated cations of unreduced Fe and/or Ni.

Figure 8.II shows the effect of Fe in the catalyst on the product distributions obtained at 300 °C at a fixed W/F (0.46 h). It is interesting to note that the yield of toluene increases with increasing Fe loading. This clearly shows that the addition of Fe improves the deoxygenation activity. However, the pure Fe catalyst exhibits a lower yield to toluene, i.e. about 5 % for the same conditions (see Table 2.II). The second interesting trend is that the yields of 3-methylcyclohexanone and 3-methylcyclohexanol decrease with increasing Fe loading. Only a small fraction of 3-methylcyclohexanone is observed over

(2.5:1) Ni-Fe/SiO₂, but essentially zero on the other catalysts. This result indicates that the addition of Fe inhibited the hydrogenation of the ring.

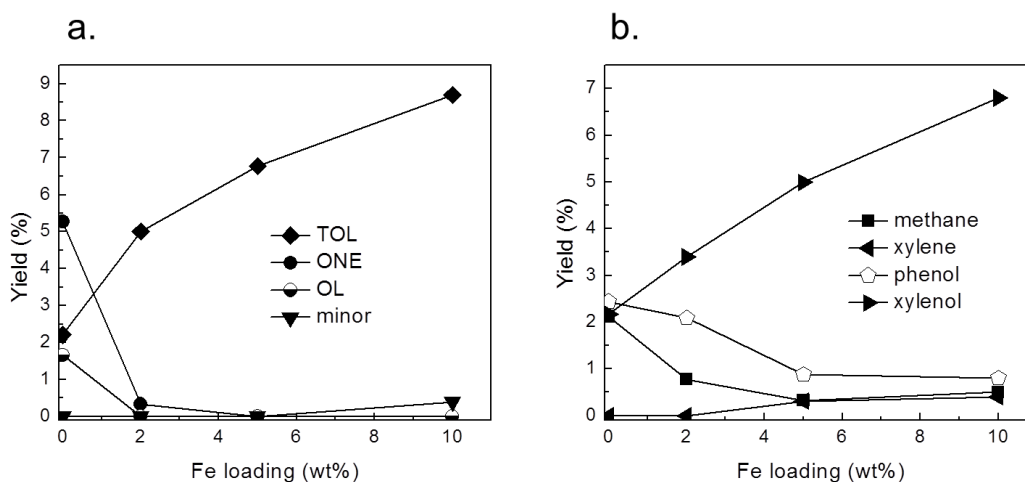


Figure 8.II. Yield of products of m-cresol over Ni-Fe bimetallic catalysts as a function of Fe loading at 300°C. H₂/Feed ratio =60. Pressure = 1atm. W/F= 0.46h. (a) C₇ Products: 3-methyl-cyclohexanone (ONE); 3-methylcyclohexanol (OL); Toluene (TOL); (b) Transalkylation and

Finally, as shown in Figure 8.II. b, the yields of xylenols (transalkylation product) increase appreciably with increasing Fe loading. This may be related to the increasing amount of Lewis acidity created by un-reduced Fe, as discussed in Figure 6.II. In line with these findings, a recent study [23] on Ni and Ni-Cu catalysts used for the HDO of guaiacol indicated that the selectivity for methyl-substitution compounds increased with addition of Cu due to improvement of the acidic properties on the catalyst surface.

Figure 9.II shows the product distributions for m-cresol conversion on the (1:2) Ni-Fe/SiO₂ as a function at W/F. The yields of toluene and xylenol are the two major products and their yields increase with W/F. By contrast, the hydrogenation products 3-methylcyclohexanone and 3-methylcyclohexanol are negligible at all W/F.

Figure 10.II shows the C₇ product selectivities as a function of m-cresol conversion. Over Ni/SiO₂, the selectivity to 3-methylcyclohexanone is the highest, around 60%, while the selectivities to 3-methylcyclohexanol and toluene are both around 20%. Over (1:2)Ni-

Fe/SiO₂, toluene is the only dominant one, whose selectivity is almost 100% along all conversion. This again shows that addition of Fe to Ni/SiO₂ helps enhance the deoxygenation activity dramatically.

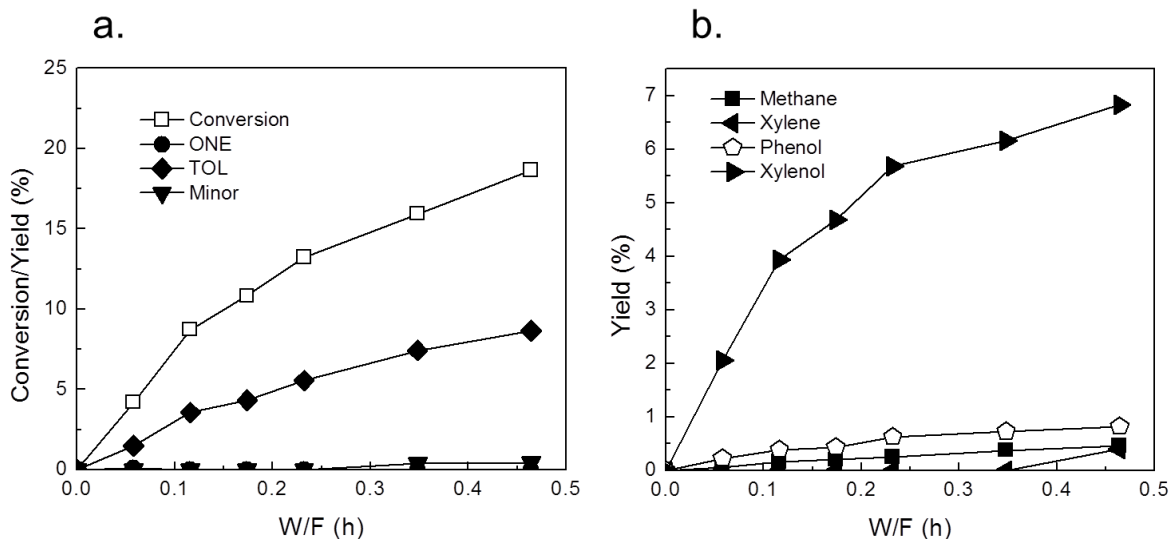


Figure 9.II. Product distribution of m-cresol over (1:2)Ni-Fe/SiO₂ at 300°C as a function of W/F. H₂/Feed ratio =60. Pressure = 1atm. (a) C₇ Products: 3-methyl-cyclohexanone(ONE); 3-methylcyclohexanol(OL); Toluene(TOL); (b) Transalkylation and hydrogenolysis products.

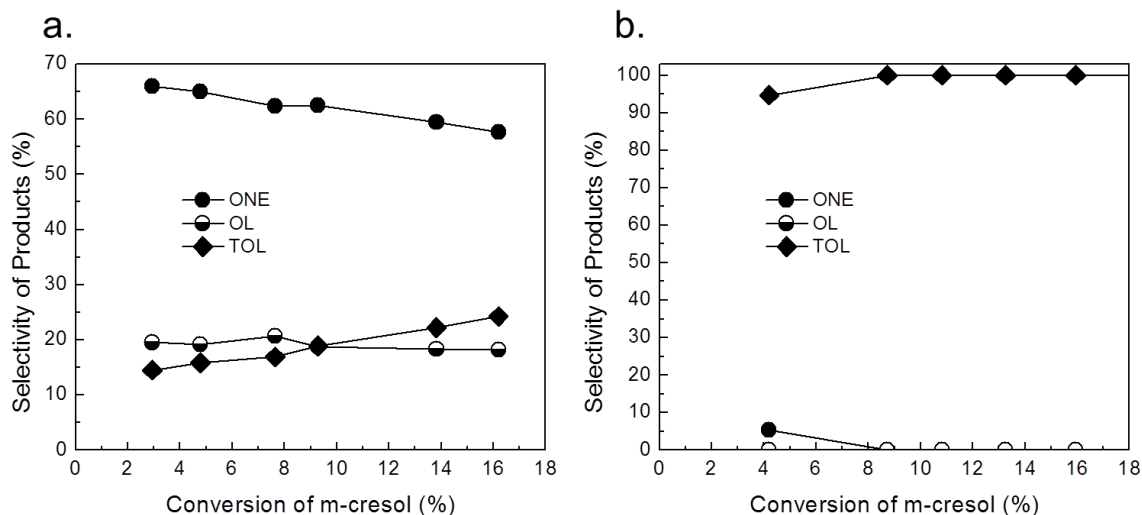


Figure 10.II. C₇ Product selectivity as a function of conversion of m-cresol at 300°C. a. Ni/SiO₂; b. (1:2) Ni-Fe/SiO₂. H₂/Feed molar ratio =60. Pressure = 1atm. C₇ Products: 3-methyl-cyclohexanone (ONE) ; 3-methylcyclohexanol (OL); Toluene (TOL)

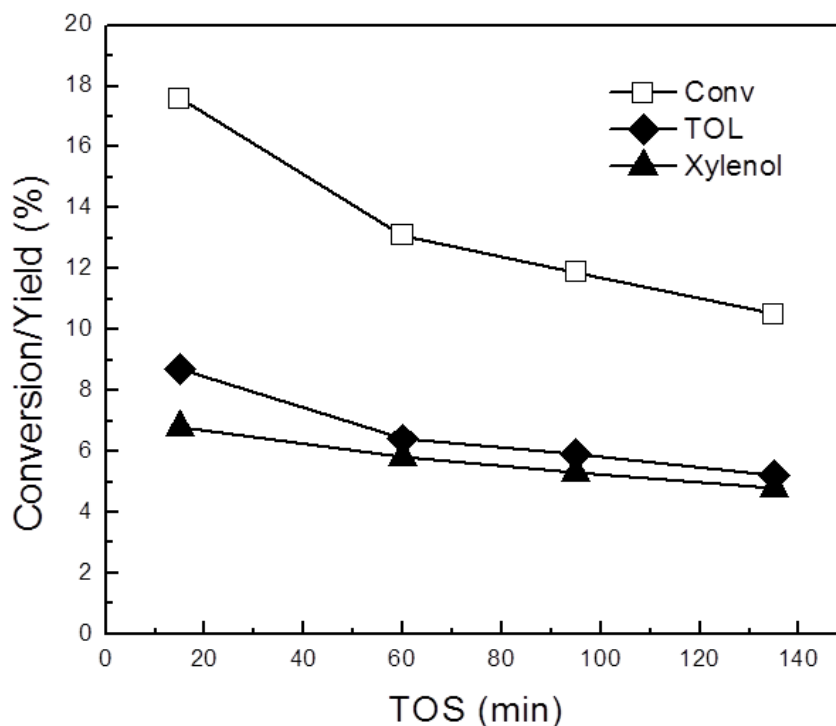


Figure 11.II. Effect of time on stream on of conversion of m-cresol and product distribution (major products) over (1:2)Ni-Fe/SiO₂ at 300°C. H₂/Feed ratio =60. Pressure = 1atm. 3-methyl-cyclohexanone (ONE) ; Toluene (TOL).

Figure 11.II shows the m-cresol conversion and yield of toluene and 3-methylhexanone over (1:2) Ni--Fe/SiO₂ as a function of time on stream, up to 135min. The yields of other products such as methane, xylene, phenol etc... are very low (sum of they is around 1%), thus they are not shown in the figure. The conversion of m-cresol drops from initial 18% to 11%, while the yield of toluene drops from 9% to 5%. This indicates the initial deactivation of the catalyst is not negligible.

2.3.3 Using 3-methylcyclohexanone and 3-methylcyclohexanol as feeds

Table 3.II compares the product distributions obtained by feeding 3-methylcyclohexanol (OL), 3-methylcyclohexanone (ONE), or m-cresol over the

monometallic and bimetallic catalysts. When 3-methylcyclohexanol was fed over the Ni/SiO₂ catalyst, it was quickly converted to 3-methylcyclohexanone. Similarly, when 3-methylcyclohexanone was the feed, the corresponding alcohol was obtained at high yield. These results indicate that this is a fast and reversible reaction. In both cases, m-cresol was also observed as a product, but toluene was not obtained. To get the same level of conversion with m-cresol the W/F had to be raised by almost 20 times since the rate of interconversion between 3-methylcyclohexanol and 3-methylcyclohexanone is much faster than the conversion of m-cresol to either of these compounds, which would suggest that during the HDO of m-cresol the saturated alcohol and ketone are pseudo-equilibrated.

Catalyst	Feed	OL	ONE	m-Cresol
Ni/SiO ₂	W/F (h)	0.02	0.02	0.36
	Conversion(%)	13.8	16.6	13.8
	Yield (%)			
	ONE	11.5	-	4.9
	OL	-	8.3	1.5
	m-Cresol	2.3	8.3	-
	TOL	0	0	1.8
	ENE	0	0	0
	Transalkylation	0	0	5.6
(1:2)Ni-Fe/SiO ₂	W/F (h)	0.02	0.02	0.12
	Conversion (%)	8.7	7.6	8.7
	Yield (%)			
	ONE	8.2	-	0
	OL	-	7.1	0
	m-Cresol	0.3	0.3	-
	TOL	0	0	3.6
	ENE	0.5	0.2	0
	Transalkylation	0	0	5.1
SiO ₂	W/F	0.46		
	Conversion (%)	0.3		

Table 3.II. Product distribution from different feed at 300°C. H₂/Feed molar ratio =60. Pressure = 1atm. C₇ Products: 3-methyl-cyclohexanone (ONE) ; 3-methylcyclohexanol (OL); Toluene (TOL); methylcyclohexane (ENE).

Interestingly, the absence of toluene as a product when 3-methylcyclohexanol was the feed indicates that dehydration does not occur to any significant extent at the low W/F used (i.e., 0.02 h). To further investigate the role of dehydration on the support, 3-methylcyclohexanol was fed at the same W/F used with m-cresol (i.e., W/F = 0.36 h) over pure SiO₂. As shown in Table 3.II, no conversion was observed.

In addition, a significant fraction of the products from m-cresol over Ni/SiO₂ are due to transalkylation (xylenols, xylene, phenol). However, this reaction did not occur when 3-methylcyclohexanol or 3-methylcyclohexanone was used as a feed at W/F = 0.02 h.

One of the most interesting differences observed over the bimetallic Ni-Fe/SiO₂ catalyst was the appearance of the alcohol dehydration product methylcyclohexene (ENE). This product was particularly abundant when 3-methylcyclohexanol was used as feed. The Lewis acid sites present on the bimetallic catalyst might be responsible for the observed dehydration. However, even in this case, no toluene was formed. This further proves that the dehydration of 3-methylcyclohexanol cannot give toluene under this reaction conditions. Again, 3-methylcyclohexanone and m-cresol were seen as products from 3-methylcyclohexanol.

When feeding 3-methylcyclohexanone over the bimetallic catalyst, the hydrogenation product 3-methylcyclohexanol and dehydrogenation product m-cresol are detected. As in the previous case, methylcyclohexene is also formed from the dehydration of methylcyclohexanol, but no toluene is detected. An interesting question arises when comparing these trends. If m-cresol is readily formed when feeding either 3-methylcyclohexanol or 3-methylcyclohexanone, why is toluene not formed by ring dehydrogenation from methylcyclohexene? If m-cresol were produced by ring dehydrogenation of 3-methylcyclohexanol the dehydrogenation of methylcyclohexene to

toluene would be much easier. As discussed below, the reason for this discrepancy is that m-cresol is not directly produced from 3-methylcyclohexanol, but rather from 3-methylcyclohexanone.

2.3.4 Mechanistic implications of the observed product distributions

The significant differences observed between the m-cresol conversion over Ni or over Fe-containing catalysts may be explained in terms of a reaction pathway that we summarize in Figure 12.II, which can account for all the results and product trends reported above.

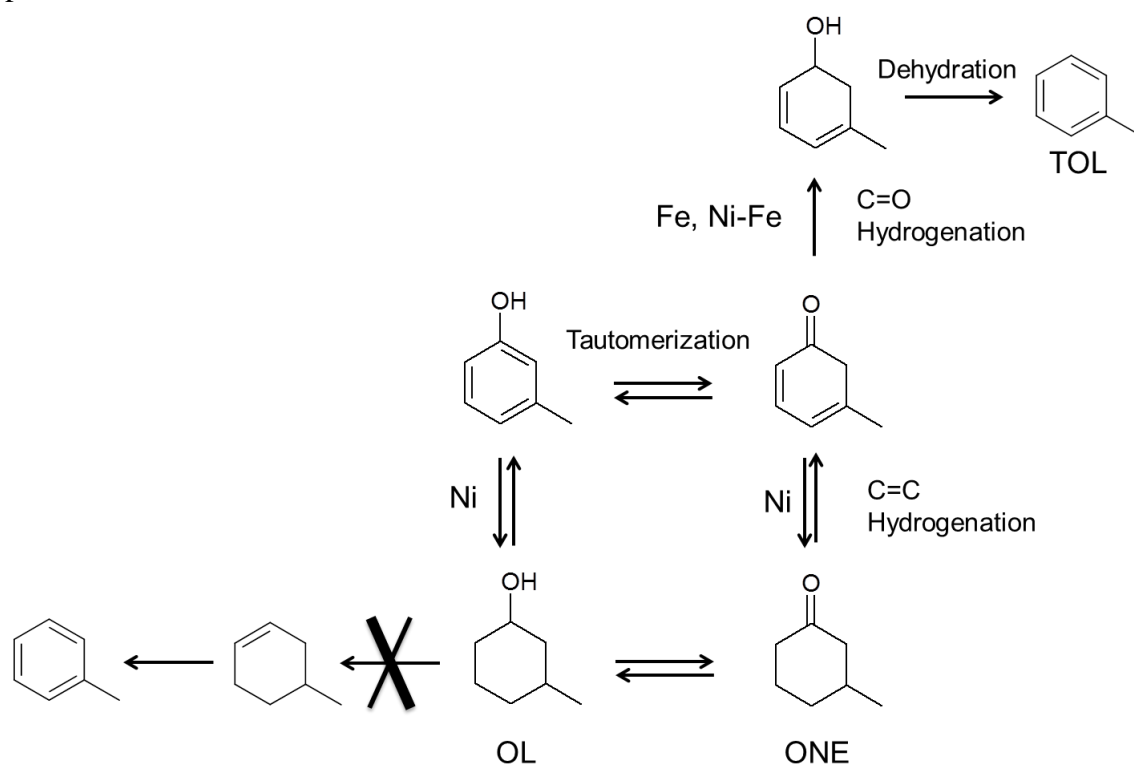


Figure 12.II. Tautomerization reaction pathways over Ni, Fe, and Ni-Fe catalysts.

First, we propose that over Ni/SiO₂ at least two parallel pathways may exist. One is the direct hydrogenation of the aromatic ring to 3-methylcyclohexanol, which could be dehydrated and then dehydrogenated to toluene. However, a second (indirect) path can also exist and this might be crucial for the highly selective production of toluene. It is known

that m-cresol can tautomerize to a highly unstable methyl cyclohexadienone. While this intermediate cannot be detected under reaction conditions, we may anticipate that depending on the catalyst, it could result in:

- a) methyl cyclohexanone, when the double bonds in the ring are hydrogenated, or
- b) methyl cyclohexadienol, when the C=O group is hydrogenated.

The preference in hydrogenating the ring or the carbonyl group strongly depends on the catalyst used. For example, Group VIII metal catalysts such as Ni, Pt, or Pd have a strong affinity for the aromatic ring and/or C=C. On these metals aromatics and/or olefins adsorb parallel to the surface and they are highly active for ring and/or C=C saturation [42-47]. When Group VIII metals are alloyed with oxophilic metals such as Sn, Re, or Fe we may anticipate that the interaction with the ring will be decreased while the interaction with the carbonyl group will be enhanced. This is in fact the case for α,β -unsaturated aldehydes, for which Group VIII metals result in saturation of the C=C double bond, but bimetallics such as Pt-Sn or Pt-Fe that contain oxophilic elements produce unsaturated alcohols [48-52].

We may expect that this chemoselective hydrogenation of the carbonyl group may occur in our case for the conversion of m-cresol over Fe-containing catalysts.

Therefore, in case (a), which is typical of Ni, 3-methylcyclohexanone becomes dominant [Table 3.II]. This product can be further hydrogenated to 3-methylcyclohexanol. As mentioned above, if the support contains enough acidity to catalyze the dehydration of the saturated alcohol 3-methylcyclohexanol, which is not the case of silica, toluene could be obtained after dehydration/dehydrogenation, as previously proposed for the conversion of phenol over Ni/SiO₂ [53] and cresol over Pt catalysts [22]. As reported previously [9,14,22], over a bi-functional catalyst containing acid and metal functions, the deoxygenation of phenolic compounds proceeds via hydrogenation of the aromatic ring to the corresponding alcohols followed by dehydration to the olefin then dehydrogenated

back to aromatic. However, over our Ni/SiO₂ catalyst under the reaction conditions investigated, dehydration does not occur to a significant extent. As shown in Table 3.II, when we fed 3-methylcyclohexanol over Ni/SiO₂, we did not observe any formation of toluene or methylcyclohexene. Only dehydrogenation of 3-methylcyclohexanol to 3-methylcyclohexanone and cresol was seen. This indicates that toluene does not derive from the dehydration / dehydrogenation of the 3-methylcyclohexanol.

In case (b), since hydrogenation of the aromatic ring is suppressed on the Fe-containing catalysts, the deoxygenation of m-cresol requires the participation of its keto tautomer methylcyclohexadienone intermediate. Once the carbonyl group of such species is hydrogenated, the resulting methylcyclohexadienol can be readily dehydrated to toluene, which is driven by aromatic stabilization. The electrophilic character of unreduced metal (either Fe or Ni) might help stabilize the tautomer intermediate, thus enhancing the deoxygenation activity [54]. Due to its oxophilicity, Fe is more efficient in linking to the O of the carbonyl than Ni, which in turn has a higher affinity for the aromatic ring. Hence, case (b) is largely promoted over Fe containing catalyst resulting enhanced deoxygenation activity. It must be emphasized that although the products from this pathway would appear to result from from a direct C(sp²)-O cleavage, i.e. DDO, this is not the case. This is a pathway that requires a relatively low activation energy and is more likely to occur under the reaction conditions investigated (300°C, atmospheric H₂).

As reported in our previous study on furfural and benzaldehyde [26], the addition of Fe to the monometallic Ni catalyst, suppresses the hydrogenation of the ring. The reason for this activity drop may be that Fe causes repulsion to the π electron system of the ring. As shown in the DFT calculations below, this repulsion is particularly pronounced when the Ni-Fe particles show a non-uniform distribution, forming Fe patches on the surface. Thus, it is then expected that Ni-Fe and Fe catalysts will have a poor aromatic ring

hydrogenation activity compared to Ni catalysts [3,18,55]. By contrast, the presence of Fe promotes the hydrogenation of the C=O group.

2.3.5 DFT Calculation

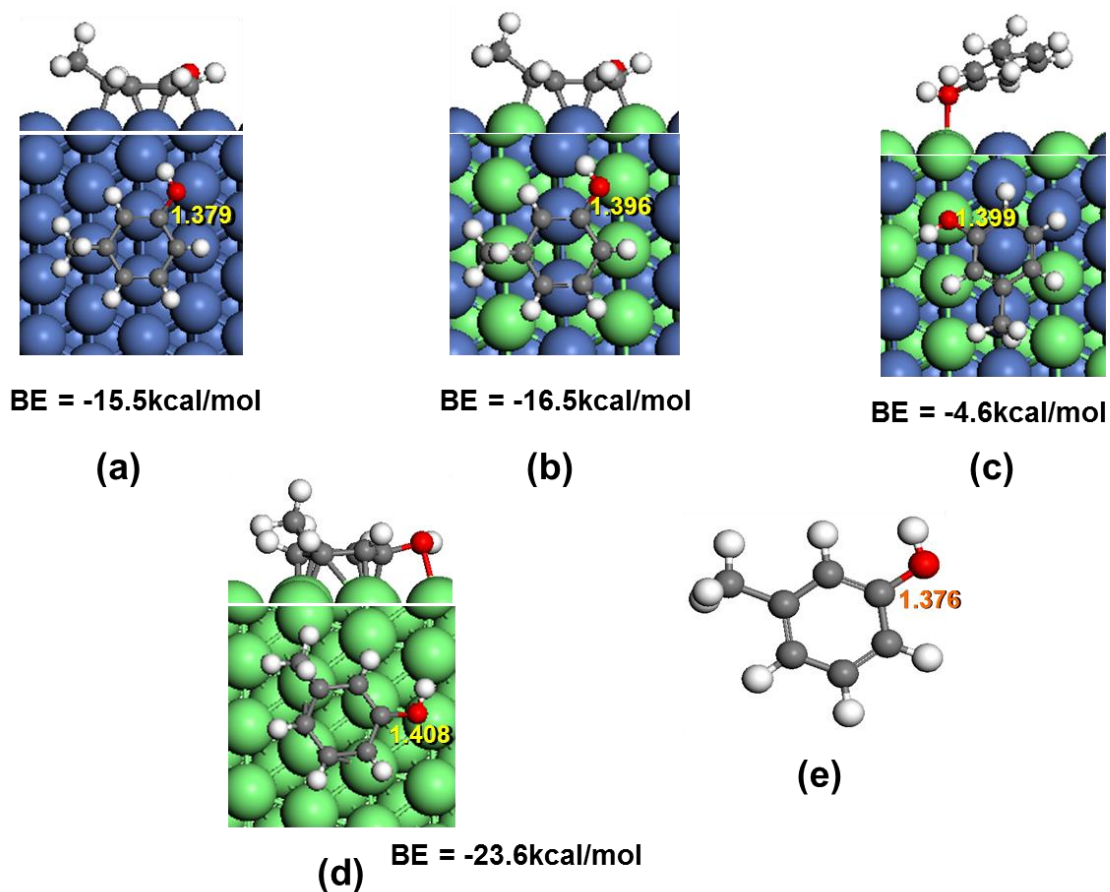


Figure 13.II Optimized adsorption structures of m-cresol on (a)Ni (111) surface, (b) perfect NiFe(111) surface, (c) patched NiFe(111) surface and (d) Fe(110) surface. (e) gas phase. C-OH bond lengths are labeled in each molecule.

We have calculated the energetics of the adsorption of m-cresol on Ni (111), Fe(110) and NiFe(111) alloy surface, which can provide information on how m-cresol molecules interact with the metal surfaces. As shown in Figure 13.II, the m-cresol prefers a flat adsorption configuration on Ni (111) surface, Fe(110) surface and bulk-terminated NiFe(111) alloy surface, but a slanted configuration on a patchy NiFe(111) alloy surface

due to repulsion of the phenyl ring. The reason for the major difference is in line what was proposed above from the analysis of the reaction products. That is, the interaction with the O of the C-O is strongest on the Fe(110) surface, followed by the NiFe(111) alloy surface, and negligible or rather repulsive on the Ni (111) surface. If the C-O bond elongation is used as an indicator for the M-O affinity a clear trend is observed, i.e., $1.408\text{\AA} > 1.399$ (1.396) $> 1.379 > 1.376$ for the Fe, Ni-Fe, Ni, and gas-phase, respectively.

Note that the calculated binding energy of m-cresol on Fe (110) (-23.6kcal/mol) is even higher than that on Ni (111) (-15.5kcal/mol) or the bulk-terminated alloy NiFe (111) surface (-16.5kcal/mol). However, in the case of Fe (110) the enhanced adsorption energy is due to a strong interaction with the oxygenated group rather than the ring.

2.4 Conclusion

A novel type of cresol deoxygenation catalyst has been identified. It is demonstrated that when the catalyst contains an oxophilic metal, such as Fe, the chemoselective hydrogenation of a keto tautomer intermediate can be greatly enhanced, resulting in a cyclohexene alcohol that is readily dehydrated to the aromatic hydrocarbon, favored by the stabilization provided by the aromaticity. This mechanism does not involve the partial hydrogenation of the ring nor a direct $\text{C}(\text{sp}^2)\text{-O}$ cleavage, as has been previously proposed. By contrast, when Fe is not present, the Ni-containing catalyst promotes hydrogenation of the ring producing 3-methyl-cyclohexanone and 3-methylcyclohexanol, which on the catalysts investigated, are not able to produce toluene via dehydration/dehydrogenation. In addition to these C_7 products, some transalkylation products are also observed. It is proposed that they arise from Lewis acids associated with the incomplete reduction of Fe and/or Ni cations.

Reference

- [1] P. M. Mortensen, J.-D. Grunwaldt, P. A. Jensen, K. G. Knudsen, A. D. Jensen, *Appl. Catal. A: General* 407 (2011) 1–19.
- [2] G.W. Huber, S. Iborra, A. Corma, *Chem. Rev.* 106 (2006) 4044-4098.
- [3] R. Olcese, M.M. Bettahar, B. Malaman, J. Ghanbaja, L. Tibavizco, D. Petitjean, A. Dufour, *Appl. Catal. B* 129 (2013) 528– 538.
- [4] D.M. Alonso, S.G. Wettstein, J.A. Dumesic, *Chem. Soc. Rev.* 41 (2012) 8075–8098.
- [5] P.M. Mortensen, J.D. Grunwaldt, P.A. Jensen, K.G. Knudsen, A.D. Jensen, *Appl. Catal. B* 407 (2011) 1-19.
- [6] S. Echeandia, P.L. Arias, V.L. Barrio, B. Pawelec, J.L.G. Fierro, *Appl. Catal. B* 101 (2010) 1-12.
- [7] D. E. Resasco, *J. Phys. Chem. Lett.*, 2 (2011) 2294-2295.
- [8] A. Ausavasukhi, Y. Huang, A.T. To, T. Sooknoi, D.E. Resasco, *J. Catal.* 290 (2012) 90-100.
- [9] E. Furimsky, *Appl. Catal. A* 199 (2000) 147–190.
- [10] P. A. Zapata, J. Faria, M. P. Ruiz, D. E. Resasco, *Topics in Catalysis*, 55 (2012) 38-52.
- [11] L. Nie, D.E. Resasco, *Appl. Catal. A* 447–448 (2012) 14-21.
- [12] T.N. Pham, D. Shi, T. Sooknoi, D.E. Resasco, *J. Catal.* 295 (2012) 169-178.
- [13] D. C. Elliott, *Energy Fuels* 21 (2007) 1792–1815.
- [14] A.J. Foster, P.T.M. Do, R. F. Lobo, *Top Catal* (2012) 55 118-128.
- [15] Zhao, C.; Kou, Y.; Lemonidou, A.A.; Li, X.B.; Lercher, J.A.; *Chem. Commun.* 46 (2010) 412-414.
- [16] X. Zhu, L. L. Lobban, R. G. Mallinson, D. E. Resasco, *J. Catal.* 281 (2011) 21–29.

-
- [17] V.A. Yakovlev, S.A. Khromova, O.V. Sherstyuk, V.O. Dundich, D.Yu Ermakov, V.M. Novopashina, M.Y. Lebedev, O. Bulavchenko, V.N. Parmon, *Catal. Today* 144 (2009) 362–366.
- [18] R. Olcese, M.M. Bettahar, D. Petijean, B. Malaman, F. Giovanella, A. Dufour, *Appl. Catal. B* 115-116 (2012) 63-73.
- [19] A. Ausavasukhi, T. Sooknoi, D. E. Resasco, *J. Catal.* 268 (2009) 68–78.
- [20] A. Ausavasukhi, Y. Huang, A. T. To, T. Sooknoi, D. E. Resasco, *J. Catal.* 290 (2012) 90–100
- [21] A. Cho, J. Shin, A. Takagaki, R. Kikuchi, T. S. Oyama, *Top Catal* (2012) 55:969–980.
- [22] C. Zhao, S. Kasakov, J. He, J.A. Lercher, *J. Catal.* 296 (2012) 12–23.
- [23] X. Zhang, T. Wang, L. Ma, Q. Zhang, Y. Yu, Q. Liu, *Catal. Commun.* 33 (2013) 15–19.
- [24] M.V. Bykova, D.Y. Ermakov, V.V. Kaichev, O.A. Bulavchenko, A.A. Saraev, M.Y. Lebedev, V.A. Yakovlev, *Appl. Catal. B* 113–114 (2012) 296–307.
- [25] V.A. Yakovlev, S.A. Khromova, O.V. Sherstyuk, V.O. Dundich, D.Y. Ermakov, V.M. Novopashina, *Catal. Today* 144 (2009) 362–366.
- [26] S. Sitthisa, W. An, D. E. Resasco, *J. Catal.* 284 (2011) 90–101.
- [27] M. Badawi, J.-F. Paul, E. Payen, Y. Romero, F. Richard, S. Brunet, A. Popov, E. Kondratieva, J.-P. Gilson, L. Mariey, A. Travert, F. Maugé *Oil Gas Sci. Technol.* (2013) DOI: 10.2516/ogst/2012041.
- [28] E.O. Odebunmi, D.F. Ollis, *J. Catal.* 80 (1983) 56-64.
- [29] G. Kresse, J. Hafner, *Phys. Rev. B* 48(17) (1993) 13115-13118.
- [30] G. Kresse, J. Furthmuller, *Phys. Rev. B* 54(16) (1996) 11169-11186.
- [31] J. P. Perdew, K. Burke, *Phys. Rev. Lett.* 77(18) (1996) 3865-3868.

-
- [32] P. E. Blochl, *Phys. Rev. B* 50(24) (1994) 17953-17979.
- [33] G. Kresse, D. Joubert, *Phys. Rev. B* 59(3) (1999) 1758-1775.
- [34] A.V. Ruban, H.L. Skriver, J.K. Norskov, *Phys. Rev. B* 59(24) (1999) 15990-16000.
- [35] G.B. Raupp, W.N. Delgass, *Journal of Catalysis*, 58(3) 1979 337-347.
- [36] L. Wang, D. Li, M. Koik, S. Koso, Y. Nakagawa, Y. Xu, K. Tomishige, *Appl. Catal. A* 392 (2011) 248–255.
- [37] A.P. Legrand, H. Hommel, A. Tuel, A. Vidal, H. Balard, E. Papirer, P. Levitz, M. Czernichowski, R. Erre, H. Van Damme, J.P. Gallas, J.F. Hemidy, J.C. Lavalley, O. Barres, A. Burneau, Y. Grillet, *Adv. Coll. Interface Sci.* 33 (1990) 91.
- [38] H.E. Bergna, W.O. Roberts, *Surfactant science series*, v.131 (2006).
- [39] L. Oliviero, A. Vimont, J-C Lavalley, F.R. Sarria, M. Gaillard, F. Mauge, *Phys. Chem. Chem. Phys.* 7 (2005) 1861–1869.
- [40] G. Connell, A. Dumesic, *J. Catal.* 105 (1987) 285-298.
- [41] K. Hadjiivanov, M. Mihaylov, D. Klissurski, P. Stefanov, N. Abadjieva, E. Vassileva, L. Mintchevz, *J. Catal.* 185 (1999) 314–323.
- [42] Rylander, P. N. *Catalytic Hydrogenation over Platinum Metals*; Academic Press: New York, 1967; p 309.
- [43] G. C. Bond, *Platinum Metals Rev.*, 12, 3 (1968), 100-105.
- [44] M. L. Honkela, J. Bjork, M. Persson; *Phys. Chem. Chem. Phys.*, 14 (2012) 5849–5854.
- [45] L. Delle Site, A. Alavi, C. F. Abrams, *Phys. Rev. B* 67 (2003) 193406.
- [46] M.L. Honkela, J. Bjork, M. Perssonbd, *Phys. Chem. Chem. Phys.* 14 (2012) 5849–5854.
- [47] S.D. Lin, M.A Vannice, *J. Catal.* 143 (1993) 554-562.

-
- [48] Beccat, J.; Bertolini, J. C.; Gauthier, Y.; Massardier, J.; Ruiz, P. J. *Catal.* 126 (1990) 451.
- [49] Birchem, T.; Pradier, C. M.; Berthier, Y.; Cordier, G. J. *Catal.* 161 (1996) 68.
- [50] Borgna, A.; Anderson, B. G.; Saib, A. M.; Bluhm, H.; Havecker, M.; Knop-Gericke, A.; Kuiper, A. E. T.; Tamminga, Y.; Niemantsverdriet, J. W. J. *Phys. Chem. B* 108 (2004) 17905.
- [51] Marinelli, T. B. L. W.; Naubuurs, S.; Ponec, V. J. *Catal.* 151 (1995) 431.
- [52] Marinelli, T. B. L. W.; Ponec, V. J. *Catal.* 1995, 156, 51
- [53] E. Shin, M.A. Keane, *Ind. Eng. Chem. Res.* 39 (2000) 883-892.
- [54] G.V. Smith, F. Notheisz, in "Heterogeneous Catalysis in Organic Chemistry." Academic Press (1999).
- [55] K. J. Yoon, M. A. Vannice, *J. Catal.* 82 (1983) 457-468.

Chapter III. Kinetics and Reaction Mechanism of m-Cresol Hydrodeoxygenation over supported Pt catalysts

3.1 Introduction

The liquid product from the fast pyrolysis of biomass (i.e., bio-oil) requires a significant degree of chemical transformation to produce transportation fuels. Oxygen removal is one of the most important upgrading reactions since the high oxygen content is responsible for most of the undesirable properties of bio-oil, including corrosivity, low thermal stability, low volatility, and low energy content [1-4]. Over the past few decades, extensive research and development efforts have focused on the hydroprocessing of bio-oil [5-12]. Among the hundreds of compounds present in bio-oil, the lignin-derived phenolics (phenols, anisoles, guaiacols, and syringols) represent an important fraction [13,14]. The two main oxygenated groups that appear in these compounds attached to the aromatic ring are the hydroxy (Ar-OH) and the methoxy (Ar-O-CH₃) groups. In order to gain a detailed understanding of the fundamental chemistry beyond the upgrading of phenolics, researchers have conducted extensive studies using model phenolic compounds such as phenol, cresols, anisole, and guaiacol [15-18].

Elucidating the detailed reaction mechanism of the hydrodeoxygenation (HDO) of phenolics has been the goal of a number of recent studies [16-24]. Yet, as discussed in this contribution, there are aspects of the mechanism that remain unsettled and require further analysis. Most of the proposed deoxygenation mechanisms reported in the literature can be grouped into two major pathways, (a)

hydrogenation/deoxygenation (HDO) route [16,17,25-28], and (b) direct deoxygenation (DDO) route via C-O hydrogenolysis [23,24,29,30]. The HDO route typically starts with hydrogenation of the aromatic ring of phenolic compounds to their corresponding alcohols. Subsequently, oxygen removal could occur via C-OH hydrogenolysis or dehydration [16,19]. Usually, the HDO route has been proposed to occur over bifunctional catalysts with a metal function that hydrogenates the aromatic ring and an acid function that catalyzes the removal of the O atom by dehydration [21]. For example, in a recent study [17] the hydrodeoxygenation of phenol was investigated over a bifunctional Ni/HZSM-5 catalyst in a batch reactor at 5MPa H₂ and 200°C. It was proposed that a partial hydrogenation of the aromatic ring took place over the Ni metallic function to form cyclohexanone (via tautomerization) and cyclohexanol, followed by dehydration over the acid sites provided by HZSM-5 of cyclohexanol to cyclohexene. Finally cyclohexene was hydrogenated to cyclohexane, which was the major hydrocarbon observed at this temperature [15,17].

The direct deoxygenation (DDO), i.e., the direct cleavage of the C_{sp2}-O bond via hydrogenolysis, has been proposed as a hydrodeoxygenation pathway for phenolic compounds on CoMo sulfide catalysts. For example, Massoth et al. [20,31] have proposed that the DDO route dominates over the HDO route when converting phenol and cresol over sulfides at high temperatures. Based on the observation that benzene (and toluene) appeared as primary products, it was concluded that DDO C_{sp2}-O hydrogenolysis mainly took place at vacancy sites that expose Mo (or Co), while the adjacent HDO sites were S or SH saturated sites. As will be discussed below, due to the

excessive strength of the C_{sp^2} -O bond, hydrogenolysis could only take place at very high temperatures due to the high energy barriers required by the cleavage of this strong bond.

In a recent study conducted at mild temperatures over a bimetallic catalyst on a non-acidic support [32], we proposed that a fast enol-keto tautomerization of m-cresol step precedes the ring hydrogenation. In that case, an unstable ketone intermediate (3-methyl-3,5-cyclohexadienone) would form over the catalyst surface, which could be hydrogenated via two possible paths.

(a) When the carbonyl group of this intermediate gets hydrogenated instead of the ring, a very reactive unsaturated alcohol (3-methyl-3,5-cyclohexadienol) is formed and it can be readily dehydrated to toluene. This easy dehydration step is driven by the aromaticity of the product. As a result, this dehydration step might even occur thermally and would not require any catalyst acidity.

(b) When the hydrogenation occurs at the C=C bonds of the unstable intermediate 3-methyl-3,5-cyclohexadienone, the typically observed 3-methylcyclohexanone is formed and is further hydrogenated to 3-methylcyclohexanol. Over supports that contain acid sites strong enough to dehydrate this alcohol, methylcyclohexene could be formed and a sub-sequent dehydrogenation would produce toluene. However, on most of the metal catalysts on inert supports dehydration of saturated alcohols does not occur to a great extent.

This mechanism can explain several important experimental results that none of the previously proposed mechanisms can. For example, it explains how toluene can be

obtained at mild temperatures and in the absence of strong acid sites. It also explains why toluene is formed as a primary product, before methylcyclohexane, and why methylcyclohexene is not observed on this catalyst, even at low conversions.

In this part of the dissertation, we have selected a Pt/SiO₂ catalyst, in which the support is inert enough that minimizes the dehydration path. Therefore, only the metal function is investigated. Furthermore, we have selected a moderate reaction temperature, at which the toluene / methylcyclohexane equilibrium ratio is low enough that has allowed us to follow the evolution of these two crucial hydrocarbon products as a function of conversion towards equilibrium, giving us further insight into the mechanism. In addition, the measurements of the m-cresol conversion rate were combined with direct measurement of the conversion rates of each individual intermediate product, which provides further validation to the kinetic side reaction constants, and the thermodynamic adsorption constants. These consistent kinetics data have been analyzed by using a Langmuir-Hinshelwood model, which results in meaningful thermodynamic and kinetics parameters that can be used to obtain a more detailed picture of the HDO mechanism than those previously proposed.

3.2. *Experimental*

3.2.1 *Catalyst preparation and characterization*

As summarized in Table 4.III, the catalyst used in this study was a 1 wt % Pt/SiO₂ prepared by incipient wetness impregnation of the SiO₂ support (HiSil 210, PPG, S_{BET} = 135 m²/g) with an aqueous solution of H₂PtCl₆ .6H₂O (Aldrich), dried

overnight at room temperature and then at 110 °C for 12 h, followed by calcination at 400 °C for 4 h. To estimate the metal dispersion, the CO uptake was measured at room temperature in a dynamic pulse unit, giving a value of CO/Pt = 0.28. The catalyst was further characterized by high-resolution electron microscopy. Figure 14.III shows an HRTEM image of the catalyst after reduction at 300°C and passivation at room temperature. The average particle size calculated from counting 100 particles is 3.5nm. The pre-reduction of the catalyst was conducted in flowing H₂ at 300°C at atmospheric pressure, before each run or characterization analysis, as detailed in previous work [13].

	Pt Metal		Silica Support
Metal loading	1 %	Type	HiSil 210
CO/Pt	0.28	Manufacturer	PPG Industries
d _p (TEM)	3.5 nm	BET	135 m ² /g

Table 4.III. Characteristics of the Pt/SiO₂ catalyst.

3.2.2 Reaction Kinetics

The vapor-phase reaction of m-cresol over Pt/SiO₂ was investigated on an isothermal tubular reactor operating under H₂ flow at atmospheric pressure. The data were analyzed assuming an isothermal plug flow reactor (PFR) operating in two modes, differential (conversion < 10 %) and integral (entire W/F range). The pelletized catalyst (size range: 250–425 μm) was placed at the center of a vertical tubular quartz reactor

between two layers of glass beads and quartz wool. Following the criteria proposed by Madon and Boudart [33], calculations were done to ensure that external and internal mass transfer limitations were eliminated. The catalyst was pre-reduced in flow of H₂ (120 ml/min, Airgas, 99.99%) for 1 h at 300°C. After reduction, the reaction was conducted at the same H₂ flow rate and temperature. A 0.5 ml/h flow of liquid m-cresol (Aldrich, 99.5%) was fed continuously from a syringe pump (Cole Palmer) and vaporized into a gas stream of 120 ml/min H₂. The H₂/feed molar ratio was kept at 70-80:1 to minimize catalyst deactivation. The reaction products were analyzed online by gas chromatography (Agilent model 6890) using an HP-Innowax capillary column and a FID detector. The carbon balance was checked in every run, and it was found to be better than 95% in each case.

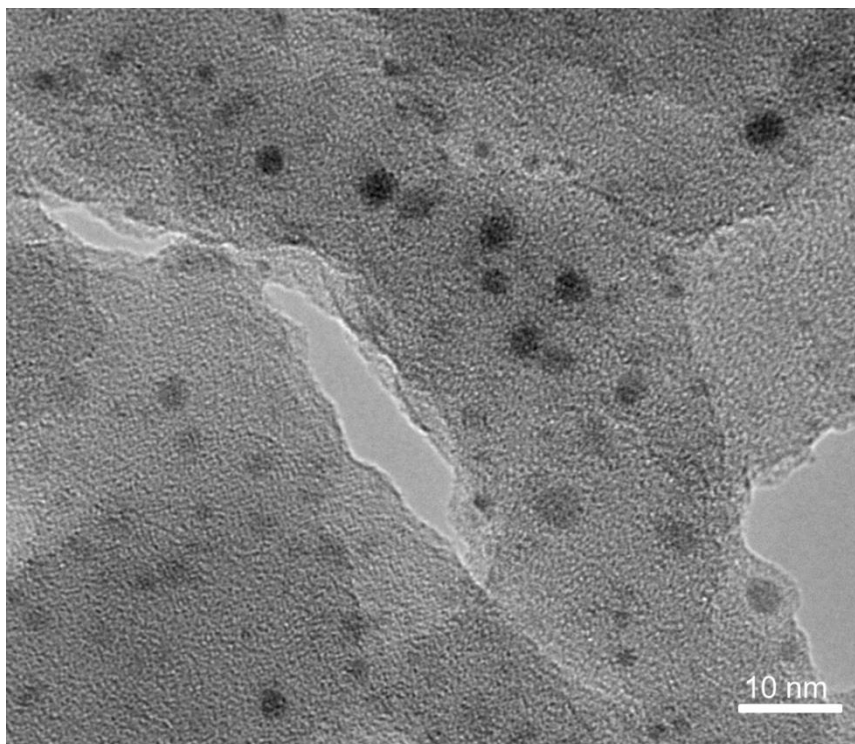


Figure 14.III. HRTEM of 1wt% Pt/SiO₂ after calcination at 400°C in air, reduction at 300°C and passivation at room temperature.

A rate expression based on the conventional Langmuir-Hinshelwood model that includes the partial pressures of m-cresol, 3-methyl-cyclohexanone, 3-methyl-cyclohexanol, toluene, methyl-cyclohexane, and 3-methyl-1-cyclohexene was used to fit the experimental results. Nonlinear least-square regression analysis of the differences between the experimental values and the kinetic model calculated values was used to fit simultaneously the experimental data for different reactant feeds. That is, the fitting of the rate expression was obtained by alternatively using as feed not only m-cresol, but also the intermediate compounds that participate in the reaction pathway (i.e., m-cresol, 3-methyl-cyclohexanone, 3-methyl-cyclohexanol, toluene, and methylcyclohexane) as a function of W/F. Several other constraints were used to ensure that the fitting resulted in the global minimum and values with reasonable physical meanings. For example, the values for the initial guesses in the fitting routine were obtained from the kinetics and thermodynamic parameters calculated from the differential reactor data for each compound, which eliminates the competition of the products. Also, as an external validation a mixture of m-cresol and 3-methyl-cyclohexanol was used as the reactant and the evolution of partial pressures with W/F was compared to that calculated using the rate expression with the parameters obtained with the pure feeds.

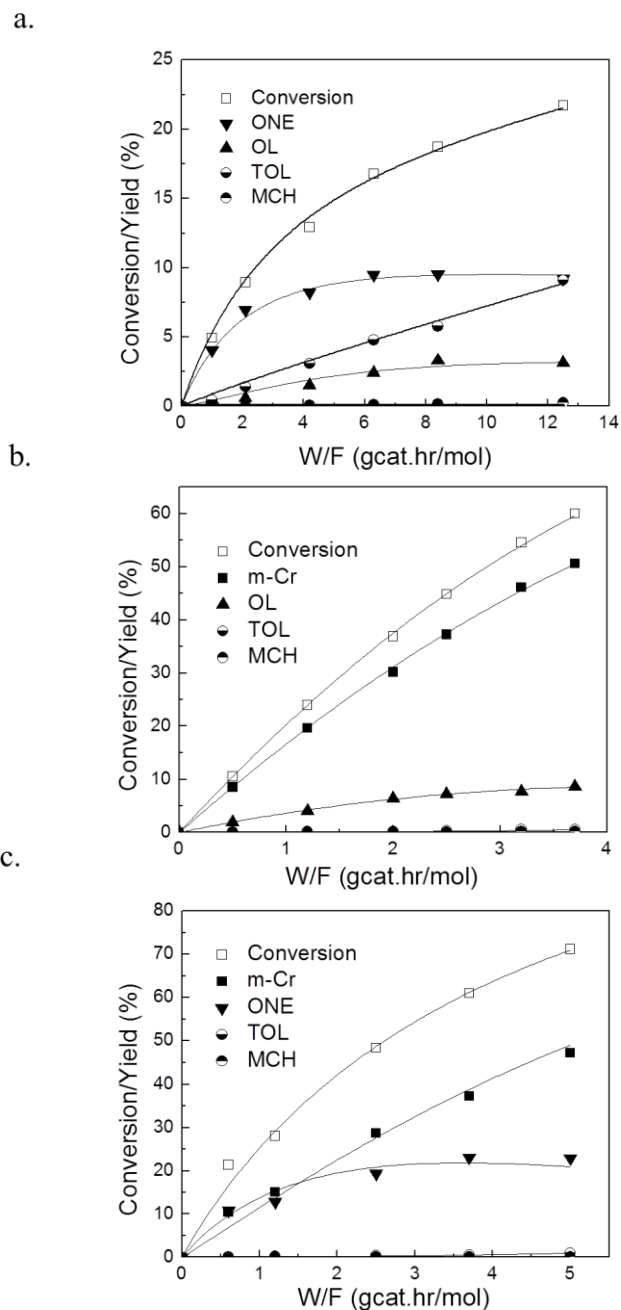


Figure 15.III. Conversion and yield of products of different feeds over Pt/SiO₂ as a function of W/F at 300°C. Carrier gas: H₂. Pressure = 1atm. (a) m-cresol; (b) 3-methyl-cyclohexanone; (c) 3-methyl-cyclohexanol. MCH: methyl-cyclohexane; TOL: toluene; m-Cr: m-cresol; ONE: 3-methyl-cyclohexanone; OL: 3-methyl-cyclohexanol. The points are experimental data and the lines are calculated from the Langmuir-Hinshelwood kinetics model.

3.3 *Results and Discussion for Pt/SiO₂*

3.3.1. *Experimental Measurements in Integral Reactor Mode*

Figure 15.III shows the evolution of products as a function of W/F when the feeds were (a) m-cresol, (b) 3-methyl-cyclohexanone, and (c) 3-methyl-cyclohexanol, respectively over Pt/SiO₂ at 300°C. The symbols represent the actual experimental data and the solid lines the calculated values from the Langmuir-Hinshelwood model, which will be discussed below in more detail. According to Figure 15.III. a, the major products from m-cresol are 3-methyl-cyclohexanone, 3-methyl-cyclohexanol and toluene. The yield of methyl-cyclohexane is less than 0.3% for all W/F values. A critical result that will be relevant in the discussion below is that the yield of toluene from m-cresol is significant, even at low conversions. In fact, the slope of the yield curve when W/F approaches 0 is not zero, which suggests that toluene may be a primary product. By contrast, as shown in both Figure 15.III. b and Figure 15.III. c, for the other two feeds the toluene yields were less than 1% in the entire W/F range. This clearly indicates that, on this non-acidic catalyst, neither 3-methyl-cyclohexanone nor 3-methyl-cyclohexanol is a major precursor for the formation of toluene.

Figure 15.III. b shows the product distribution for 3-methyl-cyclohexanone conversion over Pt/SiO₂ as a function of W/F. m-Cresol and 3-methyl-cyclohexanol are the two major products, while toluene and methyl-cyclohexane yields are both lower than 1%. Similarly, Figure 15.III. c shows the product distribution for 3-methyl-cyclohexanol conversion over Pt/SiO₂ as a function of W/F. In this case, again, toluene

and methyl-cyclohexane yields are both lower than 1%, while m-cresol and 3-methyl-cyclohexanone are the two major products.

Even from a qualitative observation of the data in Figure 15.III, it can be concluded that m-cresol, 3-methyl-cyclohexanone, and 3-methyl-cyclohexanol interconvert at faster rates than the hydrodeoxygenation to hydrocarbons. However, while the hydrogenation and de-hydrogenation rates between these three components are relatively high, they are still far from equilibrium at all W/F values investigated. The equilibrium composition at 300°C for m-cresol, 3-methyl-cyclohexanone and 3-methyl-cyclohexanol is 33:52:15 in molar percentage. Therefore, as illustrated in Figure 16.III, while m-cresol, 3-methyl-cyclohexanone, and 3-methyl-cyclohexanol interconvert relatively fast; toluene is only obtained as a primary product from m-cresol, which indicates the participation of a direct deoxygenation reaction pathway.

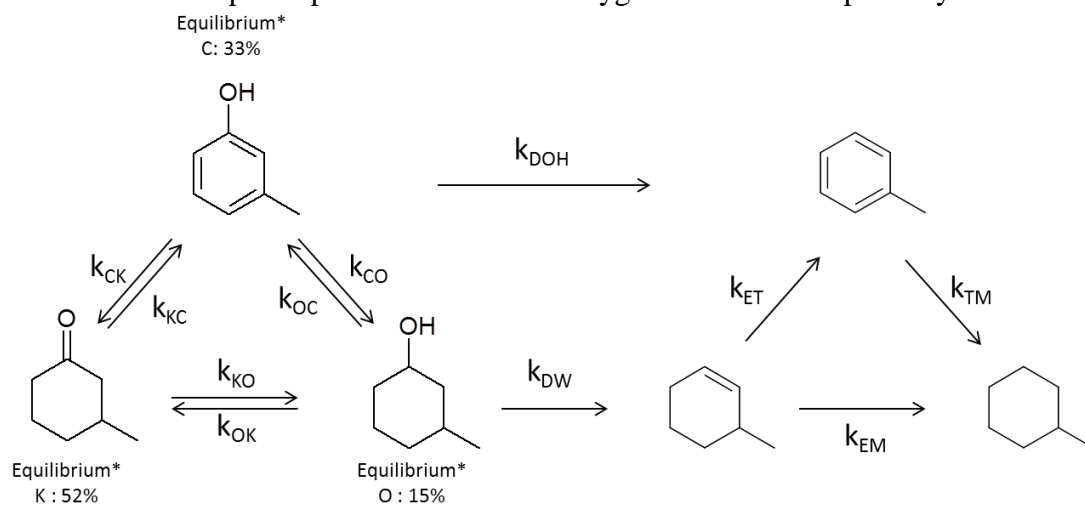


Figure 16.III. Reaction pathway over Pt/SiO₂ with rate constant. (Denotation) k_{CK} : rate constant for m-cresol to 3-methyl-cyclohexanone. (Subscript) C : m-cresol; K : 3-methyl-cyclohexanone; O : 3-methyl-cyclohexanol; E: 3-methyl-1-cyclohexene; T: toluene; M : methyl-cyclohexane; DOH : de-hydroxylation; DW : dehydration.
* : equilibrium molar % between m-cresol, 3-methyl-cyclohexanone and 3-methyl-cyclohexanol under this condition.

In a study of m-cresol conversion over Pt/ γ -Al₂O₃ at 260°C Foster et al. [21] proposed that, following hydrogenation of the aromatic ring, dehydration of 3-methyl-cyclohexanol produces methyl-cyclohexene as an intermediate, which can be sequentially hydrogenated or dehydrogenated to methyl-cyclohexane or toluene, which is the HDO route mentioned above. However, this cannot be a dominant path over the Pt/SiO₂ catalyst investigated here since, as shown Table 5.III, the dehydration activity of the SiO₂ support is very low. Furthermore, this in agreement with the low toluene yield obtained when 3-methyl-cyclohexanol was used as a feed on Pt/SiO₂, as shown in Figure 15.III. c.

Feed	Catalyst	W/F (gcat·h/mol)	Product Yield (%)			r_{DW}	r_{ET}	r_{EM}	k_{DW}	k_{ET}	k_{EM}
			TOL	MCH	Me-CYHE Isomers						
3-Me-1-CYHE	Pt/SiO ₂	0.06	1.7	1.9	9.0	-	0.28	0.32	-	1.7	2.0
		0.10	4.7	3.9	10.3						
OL	SiO ₂	12.5			1.4	0.002	-	-	0.005	-	-

Table 5.III. Product distribution, rate and rate constant for 3-methyl-1-cyclohexene over Pt/SiO₂ and 3-methyl-cyclohexanol over SiO₂ at 300°C. Pressure = 1atm. MCH: methyl-cyclohexane; TOL: toluene; OL: 3-methyl-cyclohexanol; 3-Me-CYHE: 3-methyl-1-cyclohexene; Me-CYHE: methyl-cyclohexene.

In fact, if dehydration occurred, the olefin thus produced would be rapidly converted. As also shown in Table 5.III, when 3-methyl-1-cyclohexene was fed over Pt/SiO₂ at 300°C the conversion was high, even at very low space times. For example, at W/F = 0.06 ~ 0.10 (gcat h)/mol, conversions of 12.6% and 18.9% were achieved, which show the very fast reaction rates for this molecule. This agrees well with the literature reports [16,17,19,21] indicating that when the HDO route is operative, the intermediate olefin is usually not detected in the products or at very low amount due to

its high activity. At the low W/F values measured here, in addition to toluene and methyl-cyclohexane, the isomerization products 1-methyl-1-cyclohexene and 4-methyl-1-cyclohexene were obtained from 3-methyl-1-cyclohexene.

Therefore, in addition to the reversible hydrogenation/dehydrogenation steps of the oxygenated compounds, Figure 16.III includes a direct hydrodeoxygenation pathway from m-cresol to toluene, with rate constant denoted as k_{DOH} . As mentioned above and further discussed below, this direct de-hydroxylation step does not involve a hydrogenolysis step, but rather a tautomerization path. The dehydration step of 3-methyl-cyclohexanol to 3-methyl-1-cyclohexene (minor in this case) is denoted as k_{DW} (dehydration). The dehydrogenation of methyl-cyclohexane to toluene step was neglected in the scheme due to the very low yields of methyl-cyclohexane observed in all cases. The Langmuir-Hinshelwood model that follows is based on this reaction scheme and proved to represent very well the experimental behavior.

3.3.2 Kinetic Model

Previous kinetic studies of the HDO of m-cresol over sulfided CoMo catalysts have used the Langmuir-Hinshelwood model [20,23, 34]. In those studies, H_2 was assumed to adsorb noncompetitively over sites different from those used by the phenolic reactant and intermediates. In all cases, the authors considered two parallel reaction pathways: (1) a direct dehydroxylation via hydrogenolysis of the Ar-OH bond (direct deoxygenation, DDO route) leading to toluene formation (which, should not occur under mild conditions) and (2) a pre-hydrogenation of the aromatic ring to the

corresponding alcohol followed by dehydration to cyclohexene and subsequent hydrogenation to cyclohexane (HDO route).

In this contribution, since the reaction temperature is mild, deoxygenation through dehydroxylation is considered negligible. This will be further discussed in the discussion part. However a direct deoxygenation pathway is still included in the reaction scheme. In the discussion part of this contribution it will be shown that instead of direct hydrogenolysis of the Ar-OH bond, this direct de-hydroxylation occurs via a tautomerization pathway.

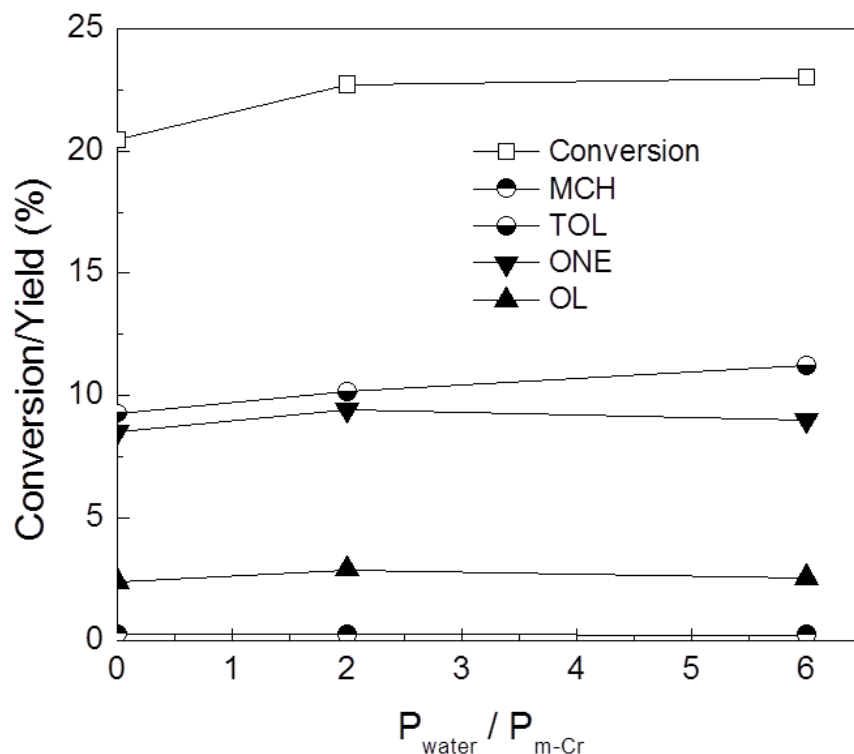


Figure 17.III. Effect of co-feeding water on the product distribution for m-cresol conversion over Pt/SiO₂ as a function of partial pressure ratio between water and m-cresol. Temperature = 300°C. Pressure = 1atm. $P_{\text{m-Cr}}$ = 1486 Pa. MCH: methyl-cyclohexane; TOL: toluene; m-Cr: m-cresol; ONE: 3-methyl-cyclohexanone; OL: 3-methyl-cyclohexanol.

The effect of co-feeding water with the reactant is shown in Figure 17.III. It is observed that, the conversion of m-cresol as well as the product distribution is not remarkably affected by the presence of water, even when the partial pressure of the water was six times higher than that of m-cresol. This result supports the assumption that the adsorption of water has little impact on the reaction rate and that dehydration does not play a significant role, but rather the activity of the metal dominates the kinetics.

Based on this semiquantitative analysis, a rate expression was derived based on the conventional Langmuir-Hinshelwood model, with the following assumptions:

- (i) Competitive molecular adsorption of m-cresol, 3-methyl-cyclohexanone, 3-methyl-cyclohexanol, toluene, methyl-cyclohexane, and 3-methyl-1-cyclohexene occurs over the same metal sites on the catalyst.
- (ii) Rate inhibition by water adsorption is neglected.
- (iii) Hydrogen adsorbs dissociatively on the metal [35], but it does not compete for the same sites with the phenolic molecules. It is well known that the small H atom preferentially adsorbs on high-coordination 3-fold and 4-fold hollow sites on a metal surface [36,37]. Therefore, in hydrogenation / dehydrogenation reactions of organic compounds, the larger molecules occupy one or more top sites without being inhibited by an adsorbed H atom at a lower hollow site. As a result, the co-adsorption of H can be considered as an independent adsorption on different sites (S_1 and S_2) as summarized in the sequence of elementary steps included in Fig. 4 [38].
- (iv) Surface reaction is rate-determining step.

From these assumptions, the rate expression for the deoxygenation of m-cresol to toluene can be written as follows:

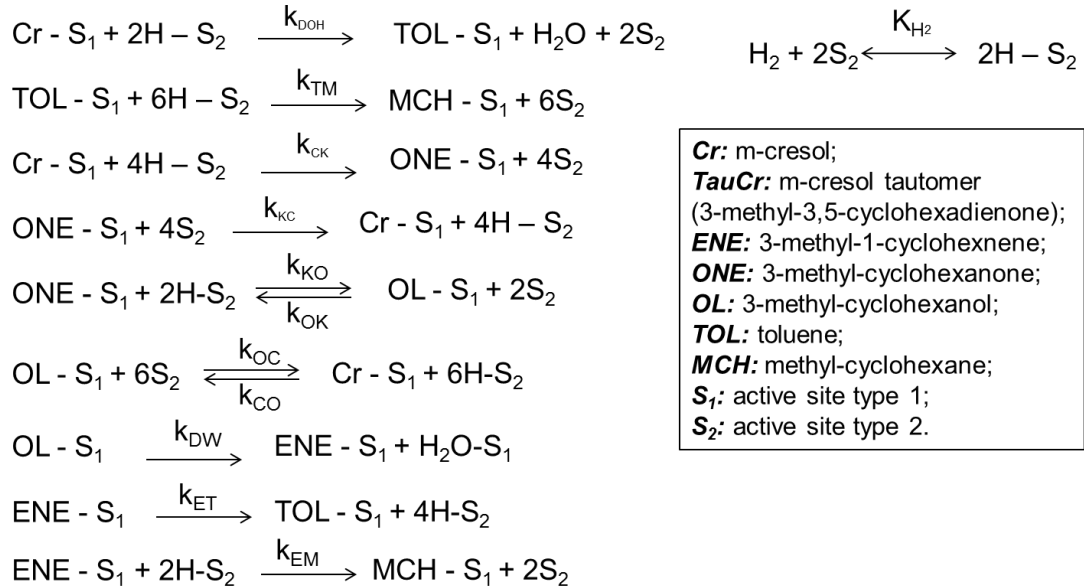
$$r_{DOH} = \left(\frac{k'_{DOH} \cdot K_C \cdot P_C}{1 + K_C \cdot P_C + K_{ONE} \cdot P_{ONE} + K_{OL} \cdot P_{OL} + K_{TOL} \cdot P_{TOL} + K_{MCH} \cdot P_{MCH} + K_{ENE} \cdot P_{ENE}} \right) \cdot \left(\frac{\sqrt{K_{H_2} \cdot P_{H_2}}}{1 + \sqrt{K_{H_2} \cdot P_{H_2}}} \right) \quad (1)$$

Since the partial pressure of hydrogen is in excess of the amount consumed and remains practically constant across the reactor, the last term in equation (1) is a constant that can be lumped into the k'_{HDO} constant, giving:

$$r_{DOH} = \frac{k_{DOH} \cdot K_C \cdot P_C}{1 + K_C \cdot P_C + K_{ONE} \cdot P_{ONE} + K_{OL} \cdot P_{OL} + K_{TOL} \cdot P_{TOL} + K_{MCH} \cdot P_{MCH} + K_{ENE} \cdot P_{ENE}} \quad (2)$$

where,

$$k_{DOH} = k'_{DOH} \cdot \left(\frac{\sqrt{K_{H_2} \cdot P_{H_2}}}{1 + \sqrt{K_{H_2} \cdot P_{H_2}}} \right) \quad (2.1)$$



<p>Cr: m-cresol; TauCr: m-cresol tautomer (3-methyl-3,5-cyclohexadienone); ENE: 3-methyl-1-cyclohexene; ONE: 3-methyl-cyclohexanone; OL: 3-methyl-cyclohexanol; TOL: toluene; MCH: methyl-cyclohexane; S₁: active site type 1; S₂: active site type 2.</p>

Figure 18.III. Sequence of elementary steps for m-cresol conversion over Pt/SiO₂.

3.3.3. Experimental Measurements in Differential Reactor Mode

To obtain meaningful fitting parameters, we have made independent measurements in the differential reactor, which allows us to simplify the rate expression by ignoring the terms of the products and obtaining the reactant parameters. Thus, under differential conditions for any reactant j

$$r_j = \frac{k_j \cdot K_j \cdot P_j}{1 + K_j \cdot P_j} \quad (5)$$

which can be rearranged as the following linear expression,

$$\frac{1}{r_j} = \left(\frac{1}{k_j \cdot K_j}\right) \cdot \frac{1}{P_j} + \frac{1}{k_j} \quad (5.1)$$

By plotting $1/r_j$ vs $1/P_j$, the adsorption constant K_j of any given reactant can be obtained from the ratio of the intercept ($\frac{1}{k_j}$) to the slope ($\frac{1}{k_j \cdot K_j}$) [38]. Here, again, the H_2 term is lumped into the rate constant k and does not affect the calculation of K_j .

Independent measurements at varying reactant partial pressures were made under differential conditions for m-cresol, 3-methyl-cyclohexanone (ONE), 3-methyl-cyclohexanol (OL), toluene (TOL), methyl-cyclohexane (MCH) and 3-methyl-1-cyclohexene (ENE). Each of them was run independently as a reactant over the Pt/SiO₂ catalyst under differential conditions, at 300°C, for three different partial pressures. As shown in Figure 19.III, the $1/r$ vs. $1/P$ plots rendered linear trends for all different reactants. The resulting adsorption and rate constants obtained by this method are summarized in Table. 6.III.

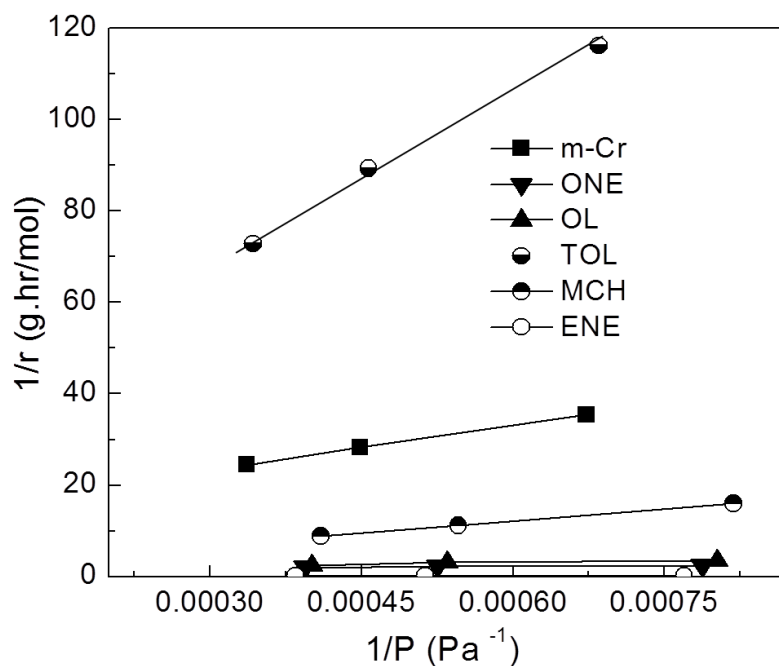


Figure 19.III. $1/r$ vs. $1/P$ plot for different reactants in differential reactor over Pt/SiO₂. Temperature = 300°C. Pressure = 1atm. $P_{m-Cr} = 1486$ Pa. MCH: methyl-cyclohexane; TOL: toluene; m-Cr: m-cresol; ONE: 3-methyl-cyclohexanone; OL: 3-methyl-cyclohexanol; ENE: 3-methyl-1-cyclohexene.

Reactant	Slope	Intercept	Adsorption Constant K x 1000 (Pa ⁻¹)	Rate Constant k x 10 (mol/(g·h·Pa))
m-Cr	32356	13.6	0.42	
ONE	863	1.7	1.96	
OL	2565	1.5	0.58	
TOL	125216	30.8	0.25	0.32
MCH	17416	1.7	0.10	5.8
ENE	24	0.35	0.15	

Table 6.III. Adsorption constants calculated from data in Figure 19. m-Cr: m-cresol; ONE: 3-methyl-cyclohexanone; OL: 3-methyl-cyclohexanol; TOL: toluene; MCH: methyl-cyclohexane; ENE: 3-methyl-1-cyclohexene.

To further validate this method, the kinetics and adsorption parameters obtained in the differential reactor for toluene and methyl-cyclohexane, were used to compare the data obtained in the integral reactor by using the full Langmuir-Hinshelwood rate expressions for toluene and methyl-cyclohexane conversions, respectively:

$$r_{TM} = \frac{k_{TM} \cdot K_{TOL} \cdot P_{TOL}}{1 + K_{TOL} \cdot P_{TOL} + K_{MCH} \cdot P_{MCH}} \quad (6)$$

$$r_{MT} = \frac{k_{MT} \cdot K_{MCH} \cdot P_{MCH}}{1 + K_{TOL} \cdot P_{TOL} + K_{MCH} \cdot P_{MCH}} \quad (7)$$

(where TM indicates toluene to methyl-cyclohexane and MT methyl-cyclohexane to toluene). The adsorption and rate constants for toluene (K_{TOL} and k_{TM}) as well as for methyl-cyclohexane (K_{MCH} , k_{MT}) from Table 3 (differential reactor) were directly used with the rate expressions (6) and (7) to model the integral reactor, resulting in excellent agreement over the entire W/F range, as shown in Figure 20.III.

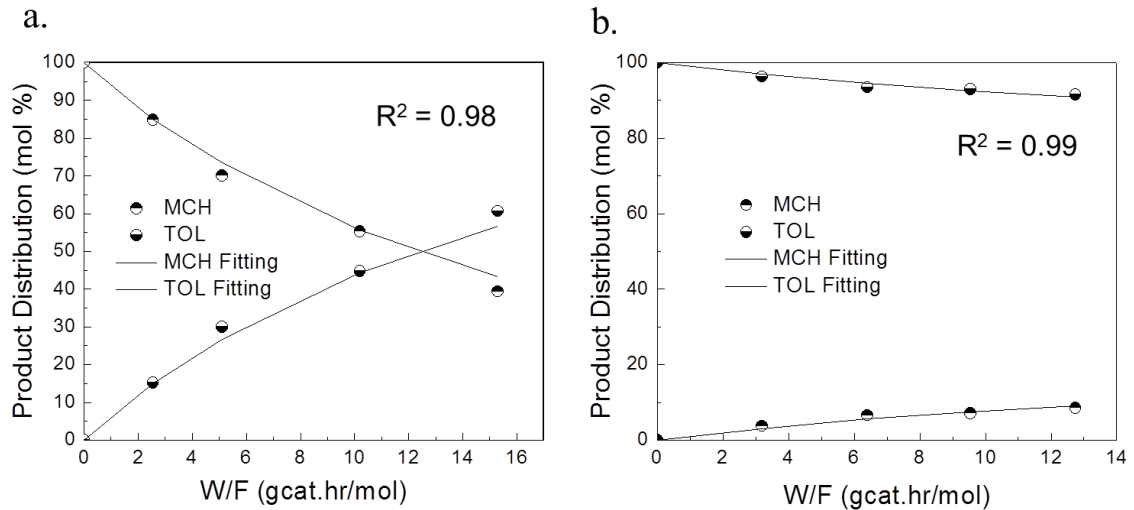


Figure 20.III. Product distribution from reaction of methyl-cyclohexane and toluene over Pt/SiO₂. (a) methyl-cyclohexane, (b) toluene. Temperature = 300°C. Pressure = 1atm. P_{MCH} (P_{TOL}) = 1486 Pa. MCH: methyl-cyclohexane; TOL: toluene. The points are experimental data and the lines are calculated from the kinetics model.

3.3.4. Goodness of the Fitting from the Integral Reactor

The adsorption constants obtained from the differential reactor (K_{TOL} , K_{MCH} as well as K_{Cr} , K_{ONE} , K_{OL} and K_{ENE}) were used unchanged in the kinetic fitting of the entire reaction pathway (Figure 16.III). Similarly, the rate constants k_{ET} and k_{EM} values obtained from feeding methylcyclohexene (Table 5.III) were also kept fixed. The rest of the rate constants, including k_{DOH} , k_{DW} , k_{CK} , k_{KC} , k_{KO} , k_{OK} , k_{OC} and k_{CO} were used as adjustable parameters to optimize the fitting. Figures 15.III (a, b, and c) illustrate the agreement between the experimental results of conversion data of m-cresol, 3-methyl-cyclohexanone (ONE), and 3-methyl-cyclohexanol (OL) and the simultaneous fitting using the same set of parameters. As mentioned above, the initial values for the adjustable parameters used in the fitting were chose from those obtained from the low conversion region in Figure 15.III. The final optimized values obtained were found to be within 20% of the initial inputs. As shown in Figure 15.III, the solid lines calculated from kinetic model fit the experimental data points very well. The rate constants resulting from the fitting are listed in Table 7.III.

Rate Constant	Parameter Value (mol/(g·h))
k_{DOH} (m-Cr → TOL)	0.024
k_{DW} (OL → ENE)	0.004
k_{CK} (m-Cr → ONE)	0.139
k_{KC} (ONE → m-Cr)	0.236
k_{KO} (ONE → OL)	0.055
k_{OK} (OL → ONE)	0.441
k_{OC} (OL → m-Cr)	0.244
k_{CO} (m-Cr → OL)	0.007
k_{ET} (ENE → TOL)	1.70
k_{EM} (ENE → MCH)	2.00
k_{TM} (TOL → MCH)	0.350

Table 7.III. Rate constant for different reaction steps. m-Cr: m-cresol; ONE: 3-methyl-cyclohexanone; OL: 3-methyl-cyclohexanol; TOL: toluene; MCH: methyl-cyclohexane; ENE: 3-methyl-1-cyclohexene.

The small rate constant obtained in the fitting for the 3-methyl-cyclohexanol dehydration ($k_{DW} = 0.004 \text{ mol}/(\text{g h})$) corresponds well with that directly measured over pure SiO_2 under the same reaction condition, ($k_{DW} = 0.005 \text{ mol}/(\text{g h})$) as shown in Table 5.III. This good agreement gives further support to the conclusion that the contribution of the HDO route to the deoxygenation of m-cresol on Pt/SiO_2 is very small. Also, as previously mentioned in a more qualitative way, the interconversion of m-cresol, 3-methyl-cyclohexanone (ONE), and 3-methyl-cyclohexanol (OL) is significantly faster than hydrodeoxygenation, as quantified by the relative values of the rate constants. For instance, k_{CK} (m-Cr \rightarrow ONE) and k_{KC} (ONE \rightarrow m-Cr) are 5-10 times larger than k_{DOH} (m-Cr \rightarrow TOL).

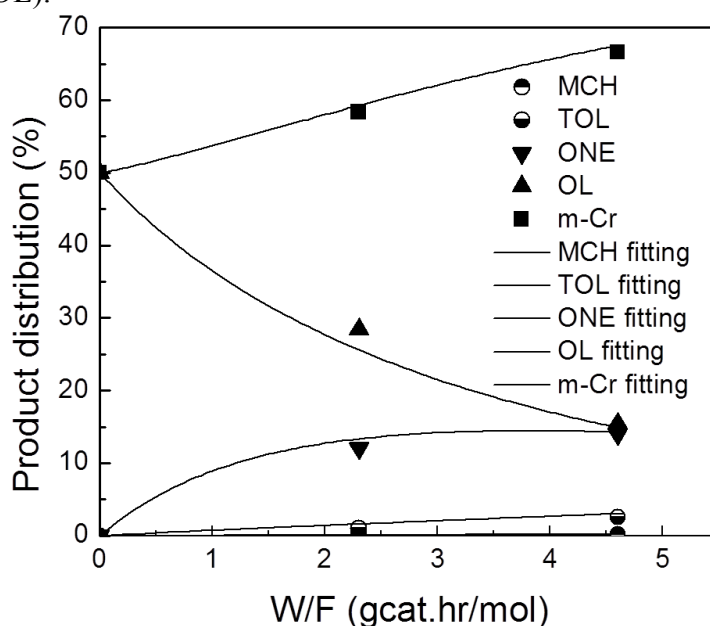


Figure 21.III. Product distribution from reaction of mixture of m-cresol and 3-methyl-cyclohexanol (1:1 molar ratio) over Pt/SiO_2 . Temperature = 300°C . Pressure = 1atm. MCH: methyl-cyclohexane; TOL: toluene; m-Cr: m-cresol; ONE: 3-methyl-cyclohexanone; OL: 3-methyl-cyclohexanol. The points are experimental data and the lines are calculated from the Langmuir-Hinshelwood kinetics model.

The validity and robustness of the kinetic model and fitting parameters was further tested by feeding a mixture of m-cresol and 3-methyl-cyclohexanol at a 1:1 molar ratio over Pt/SiO₂. Without changing any of the fitting parameters obtained in the original fitting, the experimental data were compared with the values predicted from the LH kinetic model. As shown in Figure 21.III, a very good agreement between the predicted values (solid lines) and the experimental data (symbols) was obtained in both additional runs.

The precise quantification of the reaction pathway shown in Figure 16 demonstrates that on the Pt/SiO₂ catalyst. The dominant path (i.e. higher rate constant k_{DOH}) is via the direct de-hydroxylation, while the other path, with a lower rate constant k_{DW} , is via hydrogenation of m-cresol to the corresponding alcohol followed by dehydration.

3.3.5. Analysis of the Toluene/Methylcyclohexane Product Ratio

A final and convincing corroboration against any important role of the hydrogenation/dehydration route on Pt/SiO₂ is obtained by analyzing the evolution of the toluene/methylcyclohexane product ratio as a function of conversion. Table 5.III shows the results of the conversion of 3-methyl-1-cyclohexene to toluene and m-cyclohexane over Pt/SiO₂ at 300°C. In the low conversion range (12.6% and 18.9%), the reaction is under kinetic control and the observed toluene/methylcyclohexane ratios are 0.87 and 1.2 respectively. Therefore, if during m-cresol deoxygenation toluene and methyl-cyclohexane would primarily arise from dehydration of 3-methyl-cyclohexanol to 3-methyl-1-cyclohexene, the subsequent dehydrogenation / hydrogenation would

produce toluene and methyl-cyclohexane at a ratio close to that obtained when feeding 3-methyl-1-cyclohexene alone (i.e., 0.87-1.2).

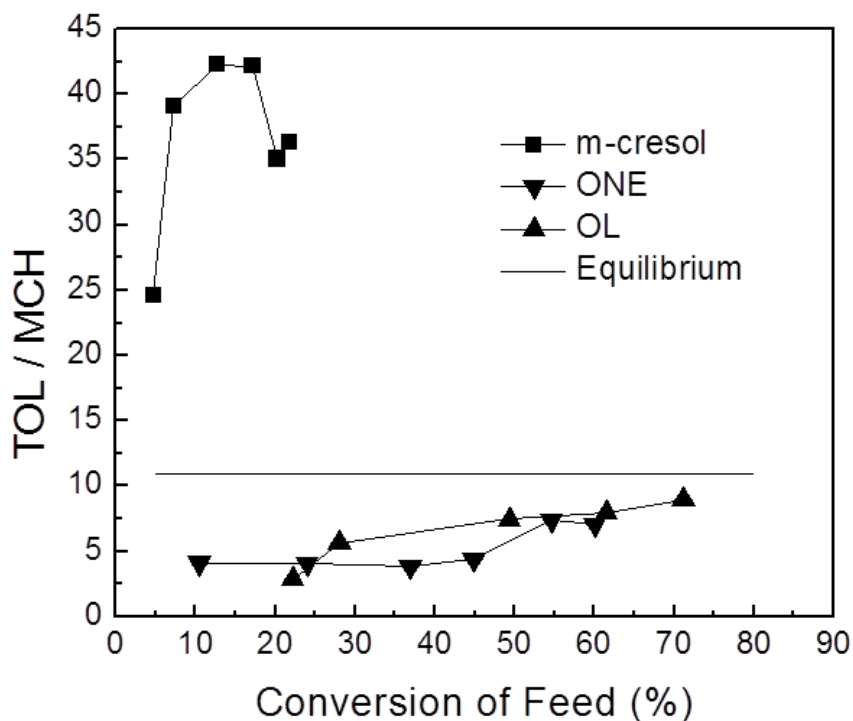


Figure 22.III. Product toluene to methyl-cyclohexane ratio as a function of conversion of different feeds over Pt/SiO₂ at 300°C. Pressure = 1atm. MCH: methyl-cyclohexane; TOL: toluene; m-Cr: m-cresol; ONE: 3-methyl-cyclohexanone; OL: 3-methyl-cyclohexanol.

However, as shown in Figure 22.III, the toluene/methyl-cyclohexane ratio obtained from m-cresol conversion is remarkably higher, i.e., more than 22. Moreover, it is suggestive that this value is far larger than the equilibrium ratio at this temperature, i.e. toluene/methyl-cyclohexane =11. In fact, as shown in the figure, one can see that when feeding any of the hydrogenated intermediates (3-methyl-cyclohexanone and 3-methyl-cyclohexanol) conversion, the toluene/methyl-cyclohexane ratio starts low and gradually approaches the equilibrium value of 11 as conversion increases. By contrast, when feeding m-cresol as a reactant, the approach to equilibrium starts at very high

ratios, which is a clear demonstration that a direct path to toluene, which does not include any of the hydrogenated intermediates, is operative.

3.3.6. Possible Direct Deoxygenation Pathways

As illustrated in Figure 23.III, different forms of direct deoxygenation have been previously considered in the literature: (a) direct dehydroxylation via hydrogenolysis of the Ar-OH bond, (b) partial hydrogenation of the aromatic ring followed by dehydration, or (c) tautomerization/CO hydrogenation/dehydration.

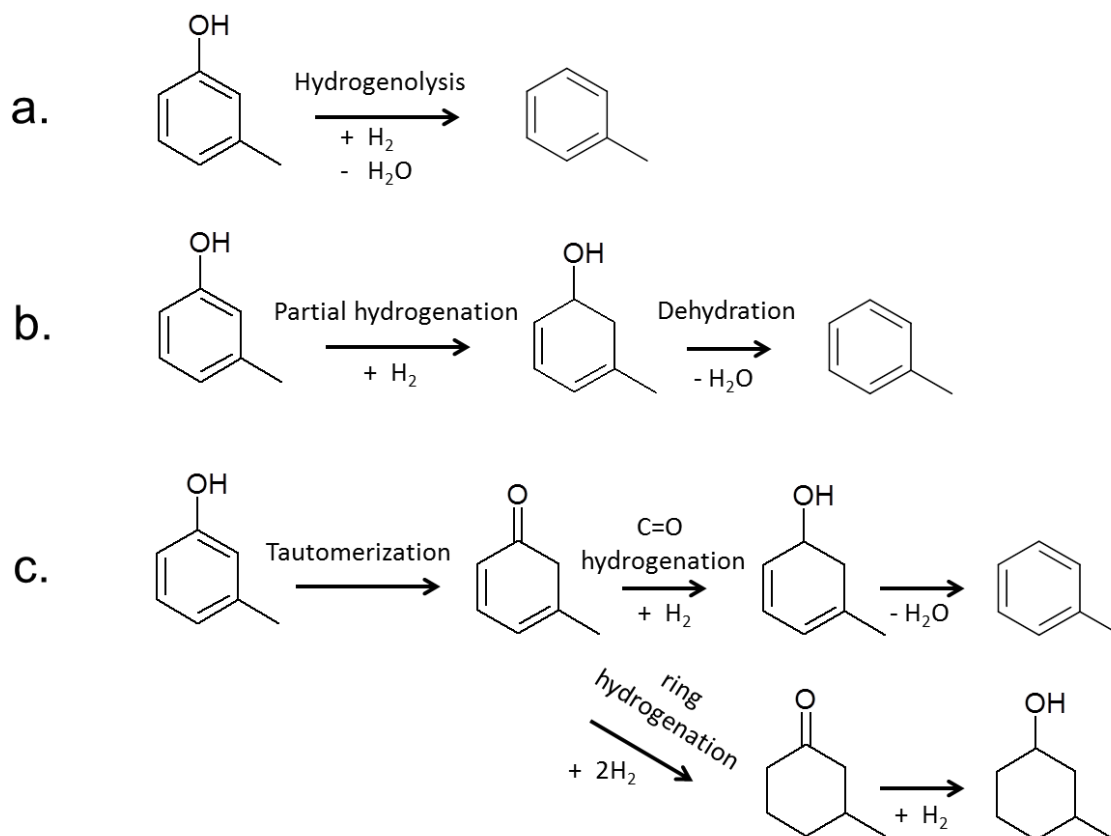


Figure 23.III. Deoxygenation reaction pathway: a. hydrogenolysis; b. partial hydrogenation with sequential dehydration; c. tautomerization route.

Bond Type	Bond Dissociation Energy (kJ/mol)
R-OH	~385
Ar-OH (Phenol)	469
Ar-NH ₂ (Aniline)	429
Ar-Cl (Chlorophenol)	406
Ar-SH (Benzenethiol)	361

Table 8.III. Bond dissociation energy [Ref:39].

The hydrogenolysis of the Ar-OH bond is a path energetically very unfavorable. It is well known that in the hydrodesulfurization reaction (HDS) reaction, analogous to hydrodeoxygenation (HDO), a possible path is the direct desulfurization by hydrogenolysis of a sulfur atom attached to an aromatic ring is well known and defined. However, as shown in Table 8.III that summarizes dissociation energies for various C-X bonds (X: O, N, S, Cl) [39], the bond energy for Ar-OH is around 100 kJ/mol higher than that of Ar-SH bond. Prins [22] has pointed out that direct cleavage of C-X bond as in C₆H₅-X is feasible for X = Cl and SH, but not for X= OH or NH₂ under normal hydrotreating conditions. The C-N and C-O bonds can only be broken when they are aliphatic. It is particularly important to note that the bond of the OH group to an aromatic carbon is 80 kJ/mol stronger than when attached to an aliphatic carbon. Therefore, it is suggestive that, as shown in Figure 15.III (c), methyl-cyclohexane is not produced from 3-methyl-cyclohexanol over Pt/SiO₂ under our reaction conditions. Clearly, C-O hydrogenolysis does not even occur for an aliphatic R-OH bond. So, from the point of view of bond energy alone, direct deoxygenation by Ar-OH should be ruled

out under. We have previously pointed out [32] that methyl-cyclohexane was not produced from 3-methyl-cyclohexanol over Ni-Fe/SiO₂, while toluene is readily produced from m-cresol.

Another possible deoxygenation pathway has been considered in recent publications [19,21]. It has been proposed that if the aromatic ring is partially hydrogenated, a reactive intermediate such as 3-methyl-3,5-cyclohexadienol, as in Fig. 8b, can be formed. Such an intermediate could be easily dehydrated since the aromaticity of the product makes this conversion favorable. However, this path leads to inconsistencies that make us rule it out. In the first place, as shown in Figure 15.III (a), methylcyclohexanone is a primary product and the partial hydrogenation mechanism does not contemplate the formation of this ketonic compound. Second, the partial hydrogenation of aromatics is an unlikely reaction. In fact, when an aromatic ring adsorbs flat on a metal surface in the presence of adsorbed H, breaking the methylcycloketone of the reactant is the most difficult step, while the olefinic intermediates most probably would not leave the surface without hydrogenating entirely to the saturated ring. For example, if one considers the hydrogenation of benzene [40-43], 1,3-cyclohexadiene is never observed as a reaction intermediate or even proposed as a reasonable transition state. In fact, a recent theoretical study [44] indicates that the hydrogenation of benzene takes place via sequential addition of H atoms in the meta-position of each other, with the addition of the fifth H atom as the rate-limiting step, not a sequential saturation of double bonds, as proposed above. A similar mechanism has

been proposed for the hydrogenation of toluene [43]. Therefore, the partial hydrogenation model is unlikely.

Finally, a third possible pathway has been recently proposed by our group [32] and is consistent with all the experimental data discussed above. This mechanism considers the formation of toluene via a fast (reversible) tautomerization of m-cresol to its keto form. This reactive keto intermediate can undergo two possible hydrogenation paths:

- a) Hydrogenation of the ring produces methylcycloketone, which is experimentally observed in large quantities, as a primary product. Being tautomerization such a fast reaction, it is expected that methylcycloketone appear as a primary product.
- b) Hydrogenation of the CO group instead of the ring produces 3-methyl-3,5-cyclohexadienol, which can be easily dehydrated to toluene. It must be noted that, contrary to the concept of partial ring hydrogenation, in this case, the formation of the unsaturated alcohol intermediate does not involve hydrogenation of the ring.

As we have recently proposed [32], the selectivity to each of these paths depends on the mode of adsorption of the m-cresol. When the molecule adsorbs with the ring flat on the surface, saturation of the ring is favored, leading to the formation of methylcycloketone. By contrast, on catalyst sites in which the adsorption mode is not parallel to the surface and with preferential attraction to the CO group, the first path is preferred leading to high selectivity to toluene. A catalyst that is remarkably selective for this second pathway is NiFe/SiO₂, on which flat ring adsorption is not preferred [32].

3.4 Support Effect

We have observed here that the selectivity of Pt catalyst to each of these paths can be controlled by the choice of support. As shown in Table 9.III, the product selectivities (measured at similar conversion levels) over different supported Pt catalysts greatly depend on the type of support used.

Catalyst	Conversion (%)	Selectivity (%)				
		TOL	ONE	OL	Benzene	MCH
1%Pt/ TiO ₂	17	88	3	0.0	1	8
1%Pt/ SiO ₂	17	28	57	14	0	1
1%Pt/ ZrO ₂	12	67	8	0.4	0.5	21

Table 9.III Product selectivity for m-cresol conversion over different support Pt catalysts at 300°C. Pressure = 1atm. MCH: methyl-cyclohexane; TOL: toluene; m-Cr: m-cresol; ONE: 3-methyl-cyclohexanone; OL: 3-methyl-cyclohexanol.

That is, when the support is TiO₂ or ZrO₂ the selectivity to toluene was greatly enhanced, compared to Pt/SiO₂, over which 3-methyl-cyclohexanone (ONE) was dominant. For the former, the main secondary product was methylcyclohexane while for the latter it was 3-methyl-cyclohexanol (OL). This difference can be ascribed to the chemoselective hydrogenation of the reaction intermediate 3-methyl-3,5-cyclohexadienone (i.e., the m-cresol tautomer). As mentioned above when the C=C double bonds of the keto-isomer is hydrogenated, the primary product is 3-methyl-cyclohexanone. By contrast, when the CO group of the ketone intermediate is hydrogenated, the product is 3-methyl-3,5-cyclohexadienone, which can be easily dehydrated to toluene as a deoxygenation product. As previously reported by Vannice et al [45] for the hydrogenation of crotonaldehyde, Pt/SiO₂ has a high preference for hydrogenating C=C double bonds. However Pt/TiO₂ results in higher selectivity for CO

hydrogenation, which is due to the strong interaction and stabilization of carbonyl group at interfacial Pt-TiO_x sites which are oxophilic. Thus, over Pt/TiO₂ as well as over Pt/ZrO₂, for a given conversion level, the toluene yield is much higher than on Pt/SiO₂.

3.5 *Conclusions*

Hydrodeoxygenation (HDO) of m-cresol, a model phenolic compound for fast pyrolysis bio-oil, over Pt/SiO₂ produces toluene as the major deoxygenation product. While the conversion of 3-methyl-cyclohexanone and 3-methyl-cyclohexanol respectively over the catalyst only produces minor toluene and methyl-cyclohexane. Fine Langmuir-Hinshelwood kinetic fitting with numerous parameters could be obtained by delicately combining a differential reactor and an integral reactor. The obtained kinetic parameters (rate constants) show that the hydrogenation/dehydrogenation between the reaction intermediates take place at a faster rate than deoxygenation. The adsorption of both the reactants and the products depress the reaction rates. Here over non-acidic Pt/SiO₂, under the reaction condition, the deoxygenation of m-cresol does not require a pre-hydrogenation of the aromatic ring. It is proved to mainly undergo via tautomerization route with minor HYD route (fully hydrogenation/dehydration/dehydrogenation). Moreover no hydrogenolysis of the Ar-OH bond exists. Using TiO₂ or ZrO₂ as the support instead of SiO₂ can greatly improve the hydrodeoxygenation selectivity. It is due to the chemoselective hydrogenation of the C=O bond in reaction intermediate 3-methyl-3,5-cyclohexadienone (i.e., the m-cresol tautomer).

References

- [1] Q. Bu, H. Lei, A.H. Zacher, L. Wang, S. Ren, J. Liang, Y. Wei, Y. Liu, J. Tang, Q. Zhang, R. Ruan, *Bioresource Technology* 124 (2012) 470-477.
- [2] J.P. Diebold, 'A review of the chemical and physical mechanisms of the storage stability of fast pyrolysis bio-oils' (2000) NREL/SR-570-27613.
- [3] D.M. Alonso, J.Q. Bond, J.A. Dumesic, *Green Chem.* 12 (2010) 1493-1513.
- [4] T. Pham, D. Shi, D.E. Resasco, *Appl. Catal. B* 145 (2014) 10-23.
- [5] A. Ausavasukhi, Y. Huang, A.T. To, T. Sooknoi, D.E. Resasco, *J. Catal.* 290 (2012) 90-100.
- [6] S. Boonyasuwat, T. Omotoso, D.E. Resasco, *Catal Lett.* 143(8) (2013) 783-791.
- [7] D.C. Elliott, *Energy Fuels* 21 (2007) 1792-1815.
- [8] D.C. Elliott, T.R. Hart, G.G. Neuenschwander, L.J. Rotness, M.V. Olarte, A.H. Zacher, Y. Solantausta, *Energy Fuels* 26 (2012) 3891-3896.
- [9] D.C Elliott, *WIREs Energy Environ.* 2 (2013) 525-533 doi: 10.1002/wene.74.
- [10] M.J. Girgis, B.C. Gates, *Ind. Eng. Chem. Res.* 30 (1991) 2021-2058.
- [11] A. Ausavasukhi, Y. Huang, A.T. To, T. Sooknoi, D.E. Resasco, *J. Catal.* 290 (2012) 90-100.
- [12] B. Feng, H. Kobayashi, H. Ohta, A. Fukuoka, *J. Mol. Catal. A: Chem.*(2013), <http://dx.doi.org/10.1016/j.molcata.2013.09.025>.
- [13] X. Zhu, L.L. Lobban, R.G. Mallinson, D.E. Resasco, *J. Catal.* 281 (2011) 21-29.
- [14] M. Saidi, F. Samimi, D. Karimipourfard, T. Nimmanwudipong, B.C. Gates, M.R. Rahimpour, *Energy Environ. Sci.* 7 (2014) 103.

-
- [15] D.C. Elliott, T.R. Hart, *Energy & Fuels* 23 (2009) 631-637.
- [16] C. Zhao, Y. Yu, A. Jentys, J.A. Lercher, *Applied Catalysis B* 132-133 (2013) 282-292.
- [17] C. Zhao, S. Kasakov, J. He, J.A. Lercher, *J. Catal.* 296 (2012) 12-23.
- [18] T. Nimmanwudipong, R.C Runnebaum, D.E. Block, B.C Gates, *Energy Fuels* 25(8) (2011) 3417-3427.
- [19] H. Wang, J. Male, Y. Wang, *ACS Catal.* 3 (2013) 1047-1070.
- [20] F.E. Massoth, J. Simons, *J. Phys. Chem. B* 110 (2006) 14283-14291.
- [21] A.J. Foster, P.T.M. Do, R.F. Lobo, *Top Catal* 55 (2012) 118-128.
- [22] R. Prins, *Handbook of Heterogenous Catalysis*, pp 2696-2718.
- [23] E.O. Odebunmi, D.F. Ollis, *J. Catal.* 80 (1983) 56-64.
- [24] E. Furimsky, *Apply Catal A: General* 199 (2000) 147-190.
- [25] B. Güvenatama, O. Kursun, E.H.J. Heeresb, E.A. Pidko, E.J.M. Hensen, *Catal. Today* (2013) , <http://dx.doi.org/10.1016/j.cattod.2013.12.011>.
- [26] J. He, C. Zhao, J.A. Lercher, *J. Catal* 309 (2014) 362-375.
- [27] B. Feng, H. Kobayashi, H. Ohta, A. Fukuoka, *J. Mol. Catal. A: Chem.* (2013), <http://dx.doi.org/10.1016/j.molcata.2013.09.025>.
- [28] P.M. Mortensen, J-D, Grunwaldt, P.A. Jensen, A.D. Jensen, *ACS Catal.* 3 (2013) 1774-1785.
- [29] B. Yoosuk, D. Tumnantong, P. Prasassarakich, *Chem. Eng. Sci* 79 (2012) 1-7.

-
- [30] M. Badawi, J.-F. Paul, E. Payen, Y. Romero, F. Richard, S. Brune, A. Popov, E. Kondratieva, J.-P. Gilson, L. Mariey, A. Travert, F. Maugé *Oil Gas Sci Technol.* 5 (2013) 829-840.
- [31] B.S. Gevert, J-E. Otterstedt, F.E. Massoth, *Appl. Catal* 31 (1987) 119-131.
- [32] L. Nie, P.M. de Souza, F.B. Noronha, W. An, T. Sooknoi, D.E. Resasco, J. *Mol. Catal. A: Chem.*(2013), <http://dx.doi.org/10.1016/j.molcata.2013.09.029>.
- [33] R.J. Madon, M. Boudart, *Ind. Eng. Chem. Fund.* 21 (1982) 438.
- [34] E.O. Odebunmi, D.F. Ollis, *J. Catal.* 80 (1983) 76-89.
- [35] S.Sitthisa, T. Sooknoi, Y. Ma, P.B. Balbuena, D.E. Resasco, *J. Catal.* 277 (2011) 1-13.
- [36] R.M. Watwe, R.D. Cortright, J.K. Norskov, J.A. Dumesic, *J. Phys. Chem. B.* 104 (2000) 2299-2310.
- [37] R.D. Cortright, J.A. Dumesic, *Adv Catal* 46 (2001) 161-264.
- [38] M.A. Vannice, *Kinetics of Catalytic Reactions.*
- [39] Y-R. Luo, *Comprehensive Handbook of Chemical Bond Energies.*
- [40] S.D. Lin, M.A. Vannice, *J. Catal* 143 (1993) 539-553.
- [41] P. Chou, M.A. Vannice, *J. Catal* 107 (1987) 140-153.
- [42] M. Saeys, M.-F. Reyniers, M. Neurock, G.B. Marin, *J. Phys. Chem. B* 109 (2005) 2064.
- [43] M. Saeys, M.-F. Reyniers, J.W. Thybaut, M. Neurock, G.B. Marin, *J. Catal* 236 (2005) 129-138.

-
- [44] M. Saeys, J.W. Thybaut, M. Neurock, G.B. Marin, *Mol Phys* 102(3) (2004) 267-272.
- [45] M.A. Vannice, B. Sen, *J. Catal.* 115 (1989) 65-78.

Chapter IV. Improving Carbon Retention in Biomass Conversion by Alkylation of Phenolics with Small Oxygenates

4.1 Introduction

Bio-oil produced by fast pyrolysis of lignocellulosic biomass has attracted considerable attention as an intermediate liquid product towards the production of fuels. However, its chemical instability, high viscosity, and corrosiveness limit their processability and storage [1-4]. Among several bio-oil upgrading approaches [5-7], hydroprocessing at high pressures over metal catalysts has been the most extensively investigated [8]. Severe hydrotreating may result in fungible fuel components, which are desirable. However, this process fails to retain small oxygenates such as acetic acid, acetol, and small aldehydes. Direct hydrodeoxygenation of these small oxygenates, which constitute a large carbon fraction of the whole bio-oil, results in production of light gases with significant losses in liquid yield. Therefore, to retain the carbon of the small oxygenates in the liquid is necessary to carry out C-C bond formation reactions to bring them to the fuel range before carrying out the hydrodeoxygenation. An attractive approach is to take advantage of the high reactivity of the oxygen functionalities before eliminating them. Based on this concept, we have investigated different catalytic strategies to enlarge the molecular weight of oxygenates, including ketonization / aldol condensation [9], transalkylation [10], and aromatization [7,11]. In this contribution, we will explore alkylation as an alternative path to incorporate C2-C3 oxygenates in phenolic compounds and form C8-C13 phenolics, which subsequently can be

deoxygenated to obtain drop-in fuel components, or stabilized feedstocks that can be further upgraded in a refinery.

Figure 4.I shows a simplified depiction of the process concept. Small aldehydes and ketones cannot be used directly to alkylate phenolic compounds. Therefore, as a first step we propose to hydrogenate the aldehydes or ketones to alcohols, which are known to be effective alkylating agents. Metal catalysts such as Ni, Ru, Pd, and Cu can be used to catalyze the hydrogenation of the short oxygenates [12,13], while acidic zeolites are highly effective for the alkylation step. Acidic catalysts such as H-Beta, HY, H-mordenite, HZSM-5 and MCM-41 have been previously used for alkylating phenol and cresol with small alcohols [14-16] and with olefins [17]. In general, larger-pore zeolites, such as H-Beta and HY zeolites are more effective in alkylation of cresol and other substituted phenolics than smaller-pore zeolites, such as HZSM-5 [14,17]. In this study, 1-propanol, 2-propanol, propanal, acetone and meta-cresol have been selected as model compounds to represent small oxygenates and phenolics, respectively.

4.2. Experimental

4.2.1 Catalyst Preparation

The SiO₂-supported metal catalysts (Cu, Ni, Ru, Pt, Pt-Fe) were prepared by incipient wetness impregnation (IWI) of precipitated silica (HiSil 210 from Pittsburg Plate Glass Co., BET surface area 135 m²/g), using aqueous solutions of Cu(NO₃)₂·2.5H₂O, Ni(NO₃)₂·6H₂O, Ru(NO)(NO₃)_x(OH)_y (x+y=3), H₂PtCl₆·6H₂O, and Fe(NO₃)₃·9H₂O (Sigma-Aldrich) as precursors. A liquid-to-solid ratio of 1.26 cc/g.cat. was used for the IWI method. After impregnation, the catalysts were dried overnight

and then calcined in air for 4 h at 400 °C. The metal loading was estimated from the amount of impregnated metal precursor used in the IWI preparation. Prior to each reaction, the catalysts were pretreated/reduced in situ under flowing H₂ at 400 °C for 1 h, and then cooled down to the reaction temperature. A commercial H-Beta zeolite (CP814C, Si/Al=19) from Zeolyst International was used as a catalyst for the alkylation step. Before reaction, the zeolite was calcined in dry air at 500 °C for 6 h to eliminate impurities.

4.2.2 Catalyst Characterization

The acid density of the H-Beta zeolite catalyst was measured by temperature programmed desorption of isopropylamine (IPA-TPD), using a 0.25 in. O.D. quartz reactor. Prior to each experiment, 50 mg of sample was pretreated for 0.5 h in He (30 cc/min) at 600 °C to remove any adsorbed water from the surface. Then, the probe molecule IPA was introduced in excess (4 µl/pulse, 10 pulses, 3 min/pulse) to saturate the surface at 100 °C. The weakly adsorbed IPA was removed by purging with He for 0.5 h. To conduct the TPD, the temperature was linearly increased to 650 °C with a heating ramp of 10 °C/min. The evolution of desorbed species was continuously monitored by a Cirrus mass spectrometer (MKS) recording the following signals $m/z = 17$ and 16 (NH₃), 18 (H₂O), 44 (IPA), and 41 (propylene). The density of acid sites was quantified by calibrating the MS signals with the average signal of ten 5-cc-pulses of 2% NH₃/He. The Brønsted acid density obtained from the IPA-TPD was 664 µmol/g, in good agreement with the Si/Al ratio = 24, measured by EDX, but somewhat lower than that calculated from the ratio specified by the manufacturer (Si/Al = 19). The good

agreement between the measured density of Brønsted sites and the total density of Al ions indicates that the majority of the Al ions in the zeolite are in the framework, forming Brønsted sites [10].

The average metal cluster size on the pre-reduced Cu catalyst was obtained from TEM observations conducted on a JEOL JEM-2000FX microscope. For this analysis, a suspension in ethanol was prepared by stirring the solid sample in an ultrasonic bath for 10 min. A few drops of the resulting suspension were deposited on a TEM grid and were subsequently dried and evacuated. The average diameter (d_{TEM}) [18] was estimated from the measurement of more than 100 particles, using the equation

$$d_{TEM} = \frac{\sum n_i \cdot d_i^3}{\sum n_i \cdot d_i^2}$$

where n_i is the number of particles with diameter d_i .

4.2.3 Catalytic Activity Testing

Catalytic activity measurements were carried out in a continuous flow system. 1-Propanol, 2-propanol, propylene, propanal, acetone and meta-cresol (ACS reagent, $\geq 99.5\%$ from Sigma-Aldrich) were used as feed in different experiments. The liquid feeds were introduced by a syringe pump to a heated line into a stream of H_2 that connected to a 20-in long 1/4 in o.d. quartz tube within an electric furnace. Catalyst loads of 10-200 mg were used with the appropriate flow rate to achieve the desired space time (W/F) for each run. Operating conditions were 120-300 °C and atmospheric pressure. All the lines were heated with heating tapes to keep the feed and products in the vapor phase. The same carrier gas, H_2 , was used during catalyst reduction and

reaction. Quantitative product analysis was made by online gas chromatography using a HP 6890A with a flame ionization detector. A Shimadzu GCMS-QP2010S was used for product identification.

For the experiments with the two-bed system, the two catalysts were located in series, inside the same reactor, with the supported metal catalyst in front of the acidic zeolite, separated by quartz wool at a fixed distance of 0.5 inch. The other operating conditions were kept the same as those described above.

4.3. Results and discussion

4.3.1 Alkylation of meta-Cresol with 2-Propanol

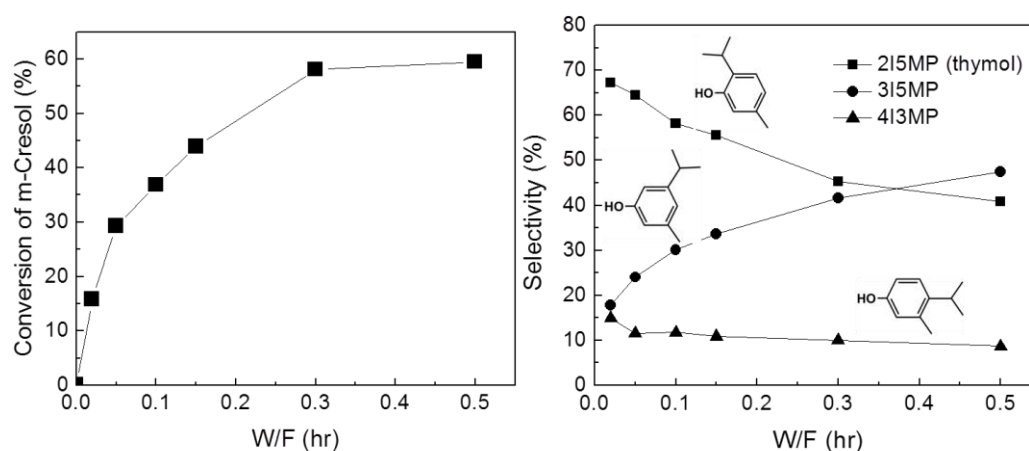


Figure 24. IV. Left: Conversion of m-Cresol; Right: Alkylate products selectivity as a function of W/F. Reaction conditions: 2-Propanol : m-Cresol = 2:1 (mole). Carrier gas H_2 60 ml/min. TOS = 15min. 200 °C. 215MP: 2-isopropyl-5-methylphenol; 315MP: 3-isopropyl-5-methylphenol; 413MP: 4-isopropyl-3-methylphenol.

Figure 24.IV shows the variation of meta-cresol conversion and alkylate product distribution as a function of W/F when co-feeding 2-propanol and meta-cresol (2:1 molar ratio) over the H-Beta zeolite catalyst at 200 °C. While 2-propanol was fed in

excess, it was completely converted to propylene in all runs, even operating at the lowest W/F, being consistent with 2-propanol fast dehydration over carbon acid catalysts [19]. By contrast, the rate of m-cresol alkylation was much lower, being the conversion of m-cresol much lower than that of 2-propanol at all space times. That is, it is clear that the alkylating agent is propylene rather than 2-propanol, which quickly disappears at this temperature.

As expected, 2-isopropyl-5-methylphenol (thymol), 3-isopropyl-5-methylphenol, 4-isopropyl-3-methylphenol were the observed products of the isopropylation of m-cresol [15]. For a shorter notation, we have labeled these products as 2I5MP, 3I5MP, and 4I3MP, respectively. While clearly 2I5MP is the dominant primary product, the selectivity to 4I3MP also seems to increase as conversion approaches zero. By contrast, the selectivity to meta-OH continuously increased with conversion at the expense of the other two products, particularly of 2I5MP. This is the expected trend since both OH and CH₃ are strong ortho/para directing groups. In 2I5MP the isopropyl group is in ortho and para positions with respect to the OH and CH₃-groups, respectively. Instead, in 4I3MP it is in ortho and para positions with respect to the CH₃ and OH-groups, respectively. That is, in both cases the alkylation is kinetically favored. By contrast, the 3I5MP is not kinetically favored but thermodynamically more stable.

Only trace amounts of dialkylation products (e.g., 2,4-diisopropyl-5-methylphenol) were observed. As previously discussed [15], the geometric constraints of the H-Beta pore inhibits the second alkylation step.

Figure 25.IV shows the evolution of products distribution with time on stream TOS at 200 °C and a rather low W/F. Under these conditions, all of the 2-propanol is

readily dehydrated to propylene while the alkylation is rather slow (yield ~ 17%). The relatively slow deactivation causes a decrease in the production of alkylates and a concomitant increase in the amount of propylene in the products, which is consumed to a lesser degree when the alkylation rate decreases.

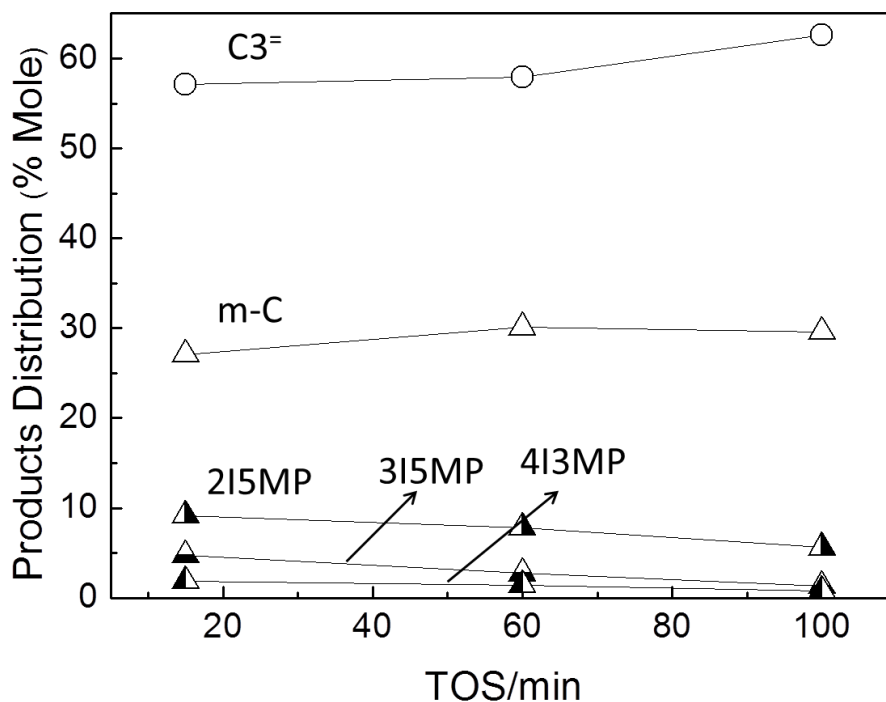


Figure 25.IV. Products Distribution as a function of TOS at 200 °C. W/F = 0.1hr. 2-Propanol : m-Cresol = 2:1 (mole). Carrier gas H₂ 60 ml/min.

4.3.2 Alkylation of meta-Cresol with different Alkylating Agents

Since the rate of 2-propanol dehydration to propylene is much faster than alkylation and propylene seems to be the actual alkylation agent, one would expect that the rate of alkylation with propylene in the feed instead of 2-propanol should be the same as that with 2-propanol. However, as shown below, that does not seem to be the case. In fact, as shown in Figure 26.IV, the rate of m-cresol alkylation significantly

varies when using either propylene, or 1-, or 2-propanol as alkylating agent. The observed alkylation activity follows the trend 2-propanol > propylene > 1-propanol.

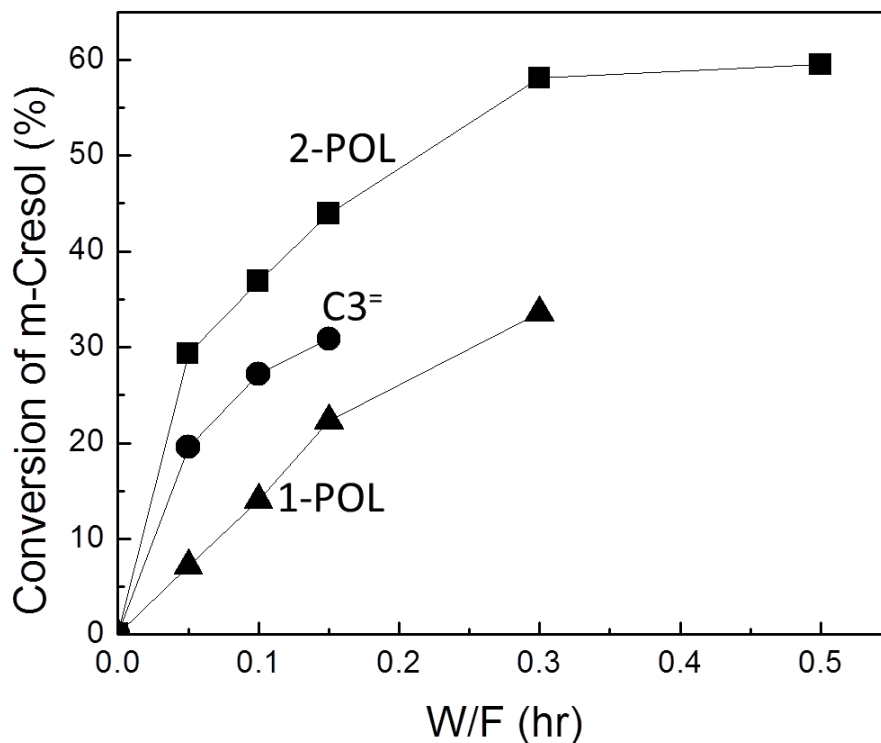


Figure 26.IV. Conversion of m-Cresol with different alkylating agent as a function of W/F. Alkylating agent : m-Cresol = 2:1 (mole). Carrier gas H₂ 60 ml/min. 200 °C. C3=: propylene; 2-POL: 2-propanol; 1-POL: 1-propanol.

Further analysis shows that the conclusion that propylene is the alkylating agent is still valid. However, a few points must be addressed to explain the observed differences in rate. First, the dehydration rate to propylene is fast and not rate limiting for the case of 2-propanol. By contrast, as shown in Figure 27.IV, when using 1-propanol in the feed, dehydration is not as fast and significant amounts of unconverted 1-propanol remain in the reactor. Not only the rate of alkylation decreases, but the presence of unconverted alcohol results in the production of dipropyl ether, which is the dominant product at low W/F and decreases with increasing W/F, while propylene

increases. Only then, the alkylation products become significant. That is, the rate of alkylation with 1-propanol is slow because dehydration of this alcohol is slow.

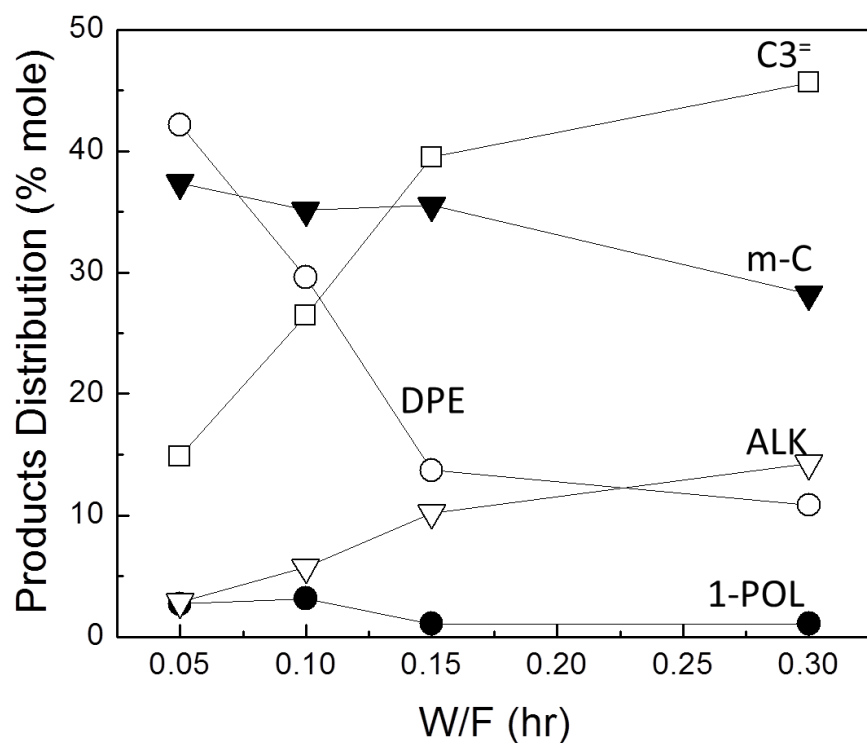


Figure 27.IV. Products Distribution as a function of W/F at 200 °C. 1-Propanol : m-Cresol = 2:1 (mole). TOS = 15min. Carrier gas H₂ 60 ml/min. C3⁼: propylene; m-C: m-cresol; DPE: dipropyl ether; ALK: alkylated products ; 1-POL: 1-propanol.

An interesting conclusion is inferred from the comparison of the rate of alkylation with 2-propanol and with propylene, with the former being higher than the later. In this case, we realize that when feeding 2-propanol, the fast dehydration to propylene produces stoichiometric amounts of water, which play an important role in inhibiting deactivation. In fact, as shown in Fig. 5, when cofeeding water at a water: propylene molar ratio of 2:1, the conversion of m-cresol as well as the products selectivity were essentially identical to those obtained when feeding 2-propanol. This indicates that propylene is indeed the alkylating agent, but water has a positive impact

on conversion. Comparing the data after different times on stream in Figure 28.IV we can see that when water is present, either by direct addition to the feed or as a product of 2-propanol dehydration, the activity of the catalyst is kept high for longer time than when the feed is dry propylene.

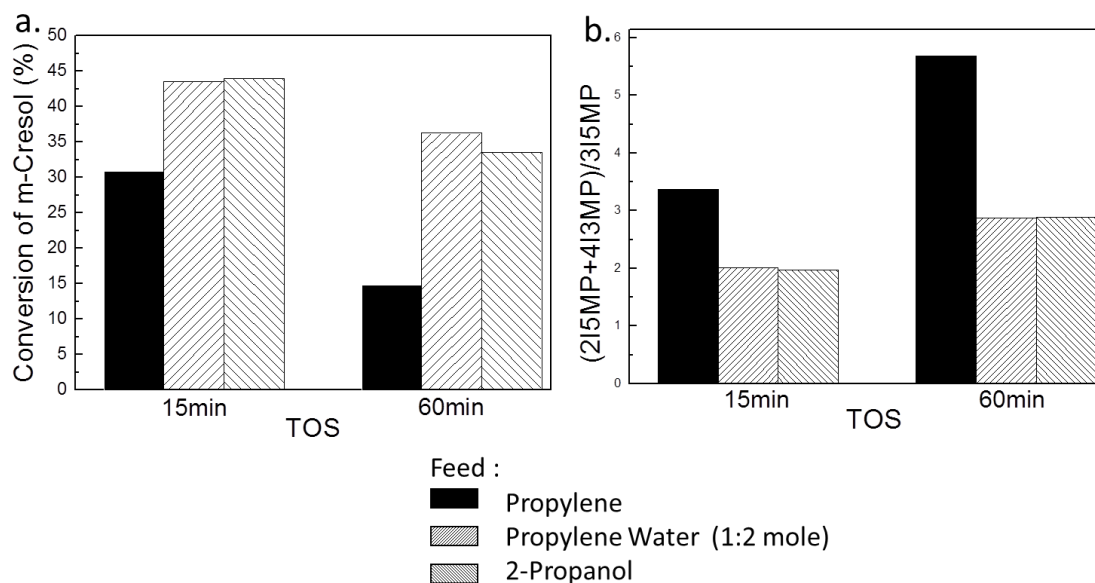


Figure 28.IV. a. Conversion of m-Cresol with different agents as a function of TOS; **b.** (ortho+para)/meta substitution ratio. Carrier gas H_2 60 ml/min. 200 °C. W/F = 0.15hr.

4.3.3 Catalyst Deactivation

The effect of the different reactants on the rate of deactivation is compared in Figure 29.IV. First, a standard run (curve a) was conducted at 200 °C, cofeeding propylene and m-cresol (2:1 molar ratio). In the next series of separate runs, the standard feed was stopped after 100 min on stream. At this time, water, m-cresol, or propylene was respectively fed for 1 h, before resuming the standard feed. In all cases, H_2 were used as carrier gas. It is clearly seen that feeding propylene alone caused a significant deactivation as propylene may oligomerize or even polymerize over the

acidic zeolite, causing the observed deactivation, as previously reported [20,21]. However, co-feeding controlled amounts of water actually helps recovering most of the original activity, perhaps by cleaning the carbon deposits from the zeolite surface [22]. It is also reported the presence of Lewis acid sites, associated with extra-framework Al species, might significantly increase olefin oligomerization and coke formation [23]. Proper amount of water would decrease the Lewis acid sites and favors the formation of new weak Brønsted sites [24]. Finally, the addition of m-cresol does not seem to cause neither enhanced deactivation nor activity recovery.

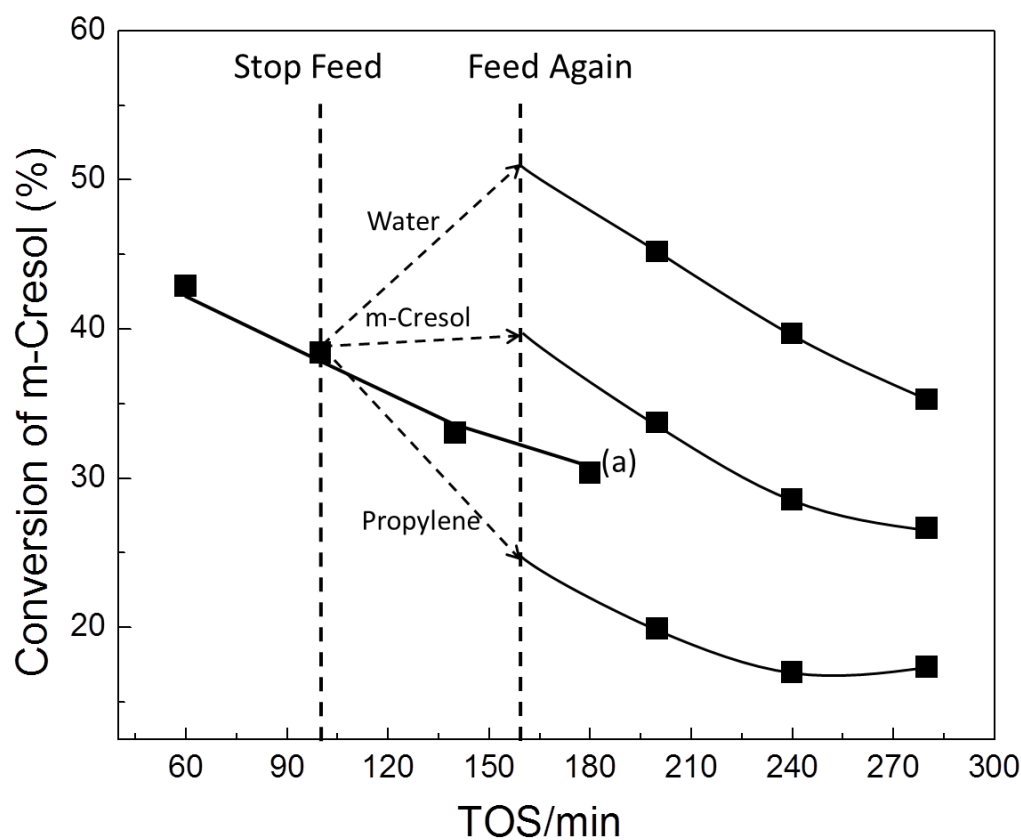


Figure 29.IV. Conversion of m-Cresol as a function of TOS. Propylene : m-Cresol = 2:1 (mole). Carrier gas H₂ 60 ml/min. W/F = 1hr. 200°C . (a): continuous feed.

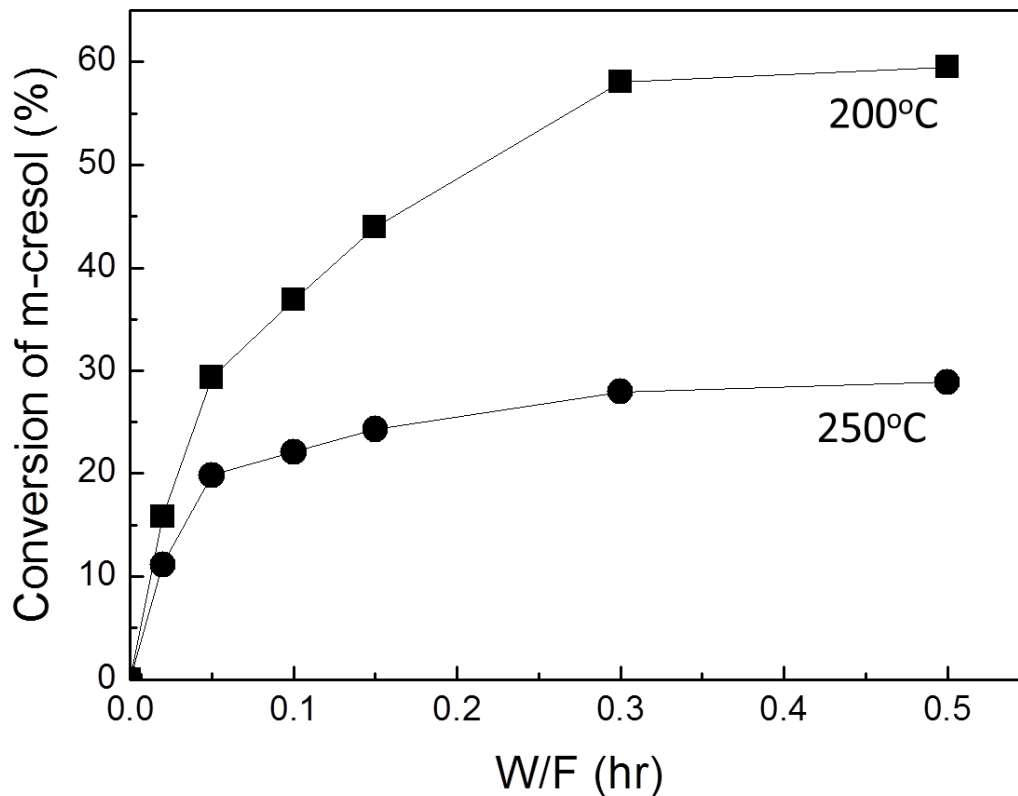


Figure 30.IV. Conversion of m-cresol over H-Beta at two temperatures as a function of W/F . 2-Propanol : m-Cresol = 2:1 (mole). Carrier gas H₂ 60 ml/min. TOS = 15min.

To study the effect of temperature on the rate of deactivation, the m-cresol/2-propanol reaction was conducted at 200 and 250 °C. Figure 30.IV shows the evolution of m-cresol conversion as a function of W/F at the two different temperatures. It is worth noting that the conversion at the lower temperature is higher in the overall W/F range. This difference is due to a combination of two factors. First, being alkylation an exothermic reaction, the equilibrium conversion decreases with increasing temperature (i.e. $x_{eq}(250\text{ °C}) = 25\%$, $x_{eq}(200\text{ °C}) = 60\%$, calculated by Pro II). Therefore, at high W/F equilibrium is responsible of the lower conversion observed at increasing temperature. Second, at low W/F, at conversions far from equilibrium, the reason for

the lower conversion observed at 250 °C than that observed at 200 °C should be ascribed to a faster rate of deactivation at the higher temperature. Figure 31.IV shows the conversion obtained as a function of temperature after 15 min on stream at a constant W/F= 0.3h. A maximum activity is observed at 200 C in accordance with the literature [15,17]. Here again, the drop in equilibrium conversion with temperature is combined with a faster deactivation as the temperature increased. In fact, as shown in the figure, after taking the measurement at 250°C, the reactor temperature was decreased to 200 C. The observed activity was not the initial $x = 57\%$, but rather near 25 %.

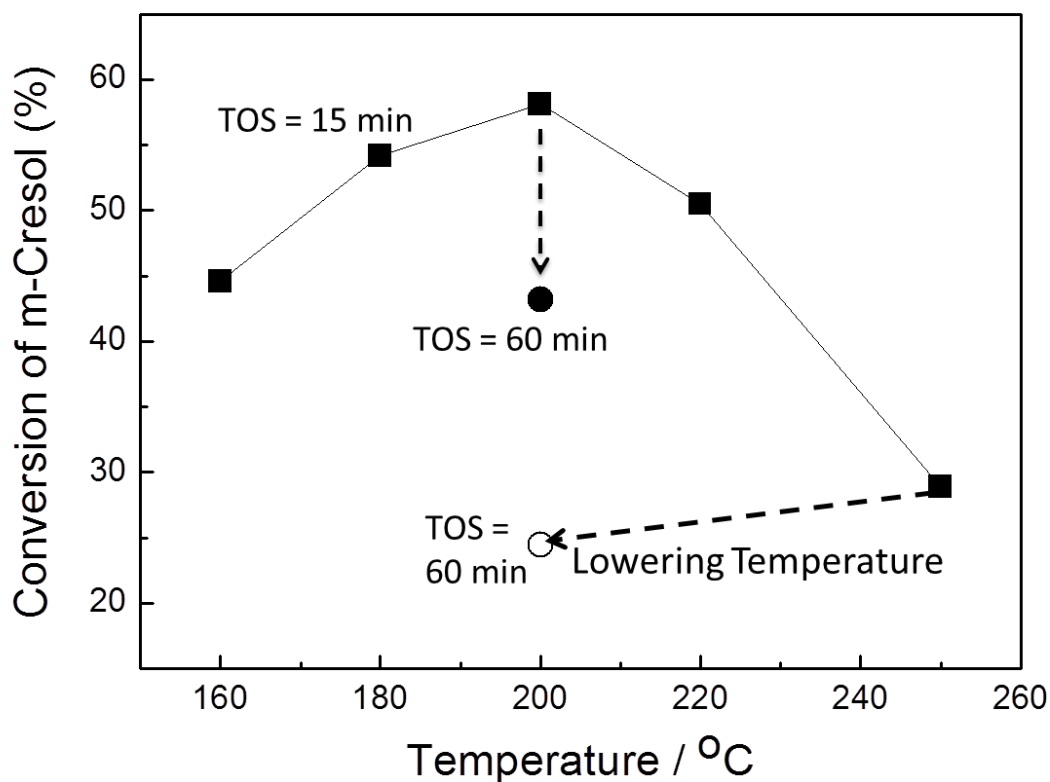


Figure 31. IV. Conversion of m-cresol as a function of temperature. 2-Propanol : m-Cresol = 2:1 (mole). TOS = 15min. Carrier gas H₂ 60 ml/min. W/F = 0.3h.

4.3.4 Hydrogenation of Propanal and Acetone

Aldehydes and ketones cannot directly alkylate aromatic compounds; hence it is necessary to hydrogenate them to alcohols that are rapidly dehydrated to olefins, which as pointed out above, are effective alkylating agents. That is, one can envision a bio-oil conversion strategy in which aldehydes and ketones are first hydrogenated to alcohols. However, if the small oxygenates are mixed in the feed with the phenolic compounds, a selective catalyst would be needed in this step to avoid hydrogenating the aromatic rings of the phenolic compounds, which would prevent the subsequent alkylation and result in unnecessary hydrogen consumption.

Catalyst	Propanal	m-Cresol
Ni(5wt%)/SiO ₂	71.5	29.0
Ni(25wt%)/SiO ₂	92.2	59.0
Ru(1wt%)/SiO ₂	10.3	4.0
Ru(3wt%)/SiO ₂	21.5	18.0
Cu(5wt%)/SiO ₂	57.0	0.0

NM = "not measured"

Table 10.IV. Yield of hydrogenation products of different metal catalysts. W/F = 0.5 h. Carrier gas H₂ 60 ml/min. 200 °C . TOS = 30min.

To illustrate this concept, we have conducted the selective hydrogenation of propanal and acetone in the presence of meta-cresol on several supported metal catalysts. As shown in Table 10.IV, while several metals are effective in hydrogenating propanal, Ni and Ru catalysts displayed a high, but undesirable, parallel activity for m-cresol hydrogenation. Previous studies suggest that Pt and Pd would be equally

unselective [25-28]. Unlike these Group VIII metal catalysts, we observed that a 5 wt% Cu/SiO₂ catalyst (Cu particle size 2.7 ± 0.5 nm by TEM [18]) was able to selectively hydrogenate propanal without converting m-cresol.

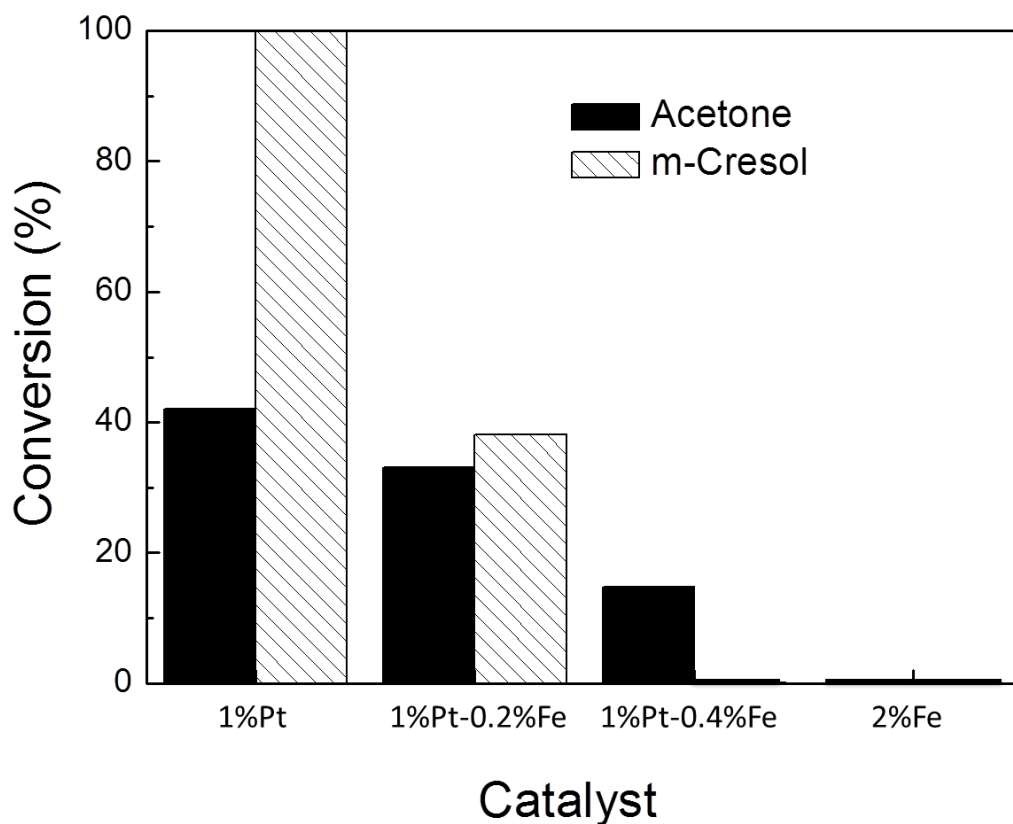


Figure 32.IV. Hydrogenation activity of metal/SiO₂ as a function of Iron loading . Acetone : m-Cresol = 4:1 (mole). TOS = 15min. Carrier gas H₂ 60 ml/min. W/F = 0.5hr. 200°C .

Hydrogenation of acetone, which is more representative of small oxygenates in bio-oil (arising from ketonization of acetic acid), was also investigated. This reaction proved to be more difficult than hydrogenation of propanal. For instance, while 5%Cu/SiO₂ was very effective for hydrogenating propanal, it was inactive for acetone at 200 °C. At the other extreme, 1%Pt/SiO₂ was able to hydrogenate acetone, but it was too active towards aromatic ring hydrogenation. Recent studies of our group [29] have

shown that adding Fe to Pd/SiO₂ catalysts results in an increase in selectivity towards hydrogenation of the carbonyl group, while leaving the aromatic ring unaffected. Thus, the same strategy was followed in this case and different amounts of Fe were loaded onto the Pt/SiO₂ catalyst to study the simultaneous hydrogenation of acetone and m-cresol, using a feed molar ratio of 4:1. The conversions of acetone and m-cresol in a 60 cc/min stream of H₂ at W/F = 0.5 hr and 200 °C are compared in Figure 32.IV for various Fe/Pt ratios. Only hydrogenation products (2-propanol and 3-methylcyclohexanol) were detected. While the conversion of both acetone and m-cresol decreased with increasing Fe/Pt ratio and pure Fe was inactive, the decrease in the conversion of the aromatic ring was much more pronounced than that of the acetone. For instance, while the 1%Pt-0.4%Fe/SiO₂ catalyst still kept a significant activity for acetone hydrogenation, it showed zero conversion of m-cresol.

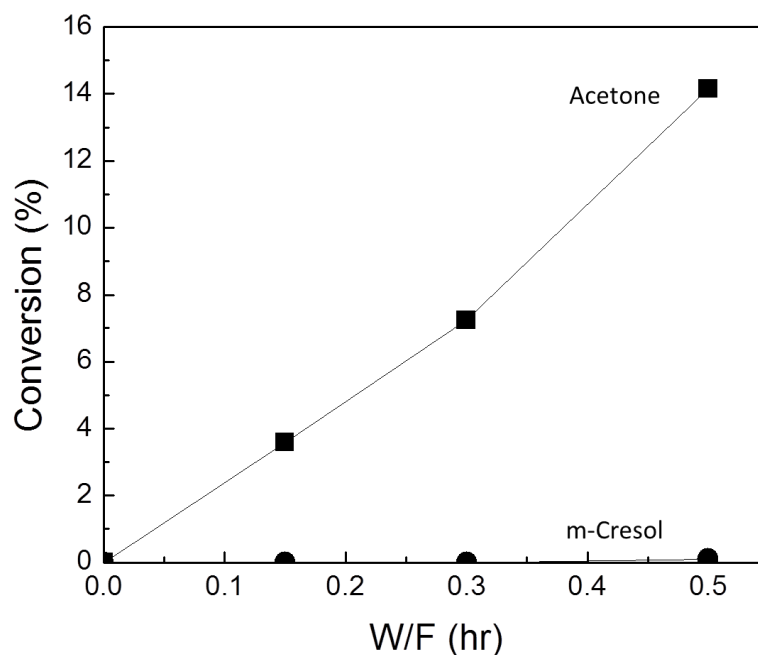


Figure 33.IV. Conversion as a function of W/F over 1%Pt-0.4%Fe/SiO₂. Acetone : m-Cresol = 4:1 (mole). TOS = 15 min. Carrier gas H₂ 60 ml/min. 200 °C.

Moreover, Figure 33.IV shows the conversion as a function of W/F over 1%Pt-0.4%Fe/SiO₂. Similar promoting effects of Fe on Pt have been observed in the selective hydrogenation of unsaturated aldehydes, such as cinnamaldehyde, in which the addition of Fe to Pt has resulted in enhanced hydrogenation of the carbonyl group compared to the double bond [30,31]. Possible explanations of this pronounced effect have been given in terms of modifications of the electronic structure, generation of bimetallic Pt-Fe sites, or the oxyphilicity of Fe [32, 33,34].

4.3.5. Combination of Hydrogenation and Alkylation

	Two Beds	One Bed
Catalyst	0.1g 5%Cu/SiO ₂ + HBeta	HBeta
Feed	Propanal : m-Cresol 4:1	Propanal :1-Propanol: m-Cresol 2:2:1
Propylene	5.6	5.1
Propanal	43.9	41.6
Dipropyl Ether	30.9	32.8
m-Cresol	18.5	19.1
Alklate	1.1	1.4
Conversion of m-cresol (%)	5.8	6.8

Table 11.IV. Products distribution for different feed and different catalysts. Carrier gas H₂ 60 ml/min. 200 °C. TOS =15min. HBeta 0.06g. Feed Rate 0.2ml/h.

To illustrate the concept proposed above, we have used a tandem of two catalyst beds to conduct simultaneously the hydrogenation and alkylation reaction starting with

a mixture of an aldehyde or a ketone and a phenolic compound. When using propanal and m-cresol as reactants, the first catalyst bed was a 5 wt% Cu/SiO₂ while the second was the acidic H-Beta zeolite. Table 11.IV shows the two-bed series catalytic reactions of combining hydrogenation and alkylation. The conversion of m-cresol is 5.8%. Propylene and dipropyl ether were detected at the outlet products. It can be deduced that propanal was first hydrogenated to 1-propanol on the Cu catalyst, and then on the H-Beta catalyst the corresponding alcohol was converted to dipropyl ether and propylene followed by alkylation with meta-cresol. As 1-propanol can be obtained from propanal hydrogenation over the copper catalyst, therefore we used 1-propanol, propanal and meta-cresol as model feed, which represent the outlet products from the first metal catalyst bed, and test the alkylation reaction over H-Beta. The products distribution of cofeeding propanal in the reactant stream is put in the right column.

Also sequential beds were used for alkylation reaction of acetone and cresol. The first bed was 1%Pt-0.4%Fe/SiO₂ whose amount was fixed to be 0.1 gram here while the second bed was H-Beta. Both catalyst beds were kept at 200 °C. As shown in the left column of Table 12.IV. The m-cresol was converted to thymol selectively with a conversion of 5.0% for 30mg zeolite H-Beta catalyst and 7.6% for 60mg H-Beta. Clearly here the existence of acetone in the stream had depressed the alkylation reaction by competition adsorption over the acid sites. Figure 34.IV illustrates the point that with acetone in the reactant the conversion of m-cresol was much lower. From this result, it is convincing that hydrogenating of the carbonyl compounds to alcohols is needed to retain the activity of alkylation reaction.

	Two Beds		One Bed
Catalyst	0.1g 1%Pt- 0.4%Fe/SiO ₂ + HBeta		HBeta
Feed	Acetone m-Cresol 4:1		Acetone:2-Propanol: m-Cresol 2:2:1
HBeta weight (mg)	30	60	60
Propylene	13.4	11.4	32.9
Acetone	65.4	62.4	39.1
m-Cresol	20.1	24.2	25.4
Alklate			
2I5MP (thymol)	1.07	2.01	1.82
3I5MP	-	-	0.31
4I3MP	-	-	0.39
Conversion of m-Cresol (%)	5.0	7.6	9.1

Table 12.IV. Products distribution for different feed and different catalysts. Carrier gas H₂ 60 ml/min. 200 °C. TOS =15min. Feed Rate 0.2ml/h.

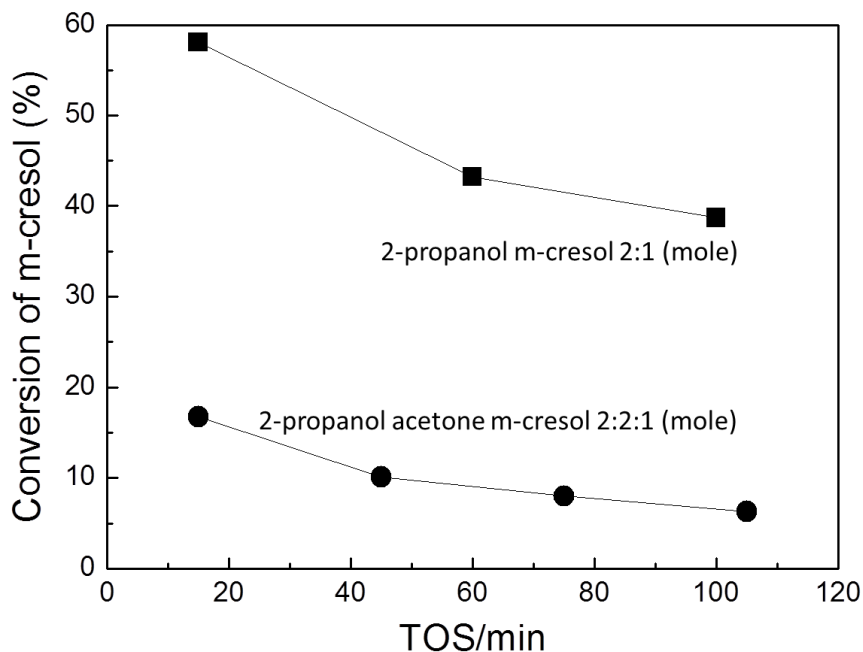


Figure 34.IV. Conversion of m-cresol with and without cofeeding acetone. W/F = 0.3 h. Carrier gas H₂ 60 ml/min.

In summary, the proposed process to implement in bio-oil refining is as follows: the carbonyl compounds are first selectively hydrogenated to alcohols on metal catalysts, and then the corresponding alcohols can alkylate the phenolic compounds on acidic zeolite resulting in coupled deoxygenation and alkylation simultaneously at relative low temperature 200 °C.

4.4. Conclusions

The main conclusions of this work can be summarized as follows:

- For isopropylation of m-cresol over HBeta, ortho- and para- substituted products (2I5MP and 4I3MP) are the primary products since they are kinetically favored. Meta- substituted product (3I5MP) is the secondary product coming from isomerization of 2I5MP and 4I3MP.
- Comparing with alkylation propanols dehydrate very fast over HBeta zeolite, while 2-propanol is faster than 1-propanol. Propylene, which is derived from corresponding alcohols, is the true alkylating agent. For 1-propanol, at low W/F dipropyl ether is a dominant product.
- The optimum reaction temperature for alkylation of 1-propanol and meta-cresol over H-Beta zeolite is 200 °C. A more severe deactivation of the catalyst is observed at a higher temperature. It is concluded that water plays a positive role in reducing the deactivation.
- Cu/SiO₂ and Pt-Fe/SiO₂ are able to selectively hydrogenate the C3 aldehyde and ketone respectively without changing the aromatic ring of m-cresol.

- Using two beds of catalysts is an efficient way of combining hydrogenation and alkylation reaction, that the carbonyl groups were first hydrogenated to hydroxyl group over the metal catalyst, and then alkylated meta-cresol over the H-Beta catalyst. This process has a potential application in upgrading bio-oil under mild conditions (200 °C) where the energy cost will be greatly reduced and also the deactivation of the catalyst.

Reference

- 1 S. Czernik, A.V. Bridgwater, *Energy & Fuels* 18 (2004) 590-598.
- 2 A Review of the Chemical and Physical Mechanisms of the Storage Stability of Fast Pyrolysis Bio-Oils, NREL/SR-570-27613.
- 3 D. Mohan, C.U.P. Pittman Jr., P.H. Steele, *Energy & Fuel* 20 (2006) 848-889.
- 4 A.G. Gayubo, B. Valle, A.T. Aguayo, M. Olazar, J. Bilbao, *J. Chem. Technol. Biotechnol* 85 (2010) 132-144.
- 5 C.A. Fisk, T. Morgan, Y. Ji, M. Crocker, C. Crofcheck, S.A. Lewis, *Appl. Catal. A* 358 (2009) 150–156.
- 6 X. Yang, S. Chatterjee, Z. Zhang, X. Zhu, C. U. Pittman Jr, *Ind. Eng. Chem. Res.* 49 (2010) 2003–2013.
- 7 T.Q. Hoang, X. Zhu, T. Sooknoi, D.E. Resasco, R.G. Mallinson, *J. Catal.* 271 (2010) 201-208.
- 8 D. C. Elliott, *Energy & Fuels* 21 (2007) 1792-1815.
- 9 A.Gangadharan, M. Shen, T. Sooknoi, D.E. Resasco, R.G. Mallinson, *Appl. Catal. A* 385 (2010) 80-91.
- 10 X. Zhu, L.L. Lobban, R.G. Mallinson, D.E. Resasco, *J. Catal.* 281 (2011) 21-29.
- 11 T.Q. Hoang, X. Zhu, L.L. Lobban, D.E. Resasco, R.G. Mallinson, *Catal Commun.* 11 (2010) 977-981.
- 12 F. Masaki, I. Hakuai, *Chem. Lett.* 6 (1987) 1205-8.
- 13 J. Bedia, R. Ruiz-Rosas, J. Rodríguez-Mirasol, T. Cordero, *J. Catal.* 271 (2010) 33–42.

-
- 14 A.V. Krishnan, K.Ojha, N.C. Pradhan, *Org. Proc. Res. Dev.* 6 (2002) 132–137.
- 15 M. Selvaraj, S. Kawi, *Micropor. Mesopor. Mater.* 109 (2008) 458–469.
- 16 M. Selvaraj, P.K. Sinha, *J. Mol. Catal. A* 264 (2007) 44–49.
- 17 C.T. O'Connor, G. Moon, W.Böhringer, J.C.Q. Fletcher, *Collect. Czech. Chem. Commun.* 68 (2003) 1949-1968.
- 18 T.T. Pham, L.L. Lobban, D.E. Resasco, R.G. Mallinson, *J. Catal.* 266 (2009) 9-14.
- 19 J. Bedia, R. Ruiz-Rosas, J. Rodriguez-Mirasol, T. Cordero, *J. Catal.* 271 (2010) 33-42.
- 20 G.C. Laredo, J. Castillo, H. Armendariz-Herrera, *Appl. Catal. A* 384 (2010) 115–121.
- 21 G. Girotti, F. Rivetti, S. Ramello, L. Carnelli, *J. Mol. Catal. A* 204–205 (2003) 571–579.
- 22 G. Kostrab, M. Lovic, I. Janotka, M. Bajus, D. Mravec, *Appl. Catal. A* 323 (2007) 210–218.
- 23 J. Cejka, N.Zilkova, Z. Tvaruzkova, B. Wichterlova, *Stud. Surf. Sci. Catal.* 97 (1995) 401-408.
- 24 C. Flego, G. Pazzuconi, C. Perego, *Stud. Surf. Sci. Catal.* 142 (2002) 1603-1610.
- 25 M. Higashijima, S. Nishimura, *Bull. Chem. Soc. Jpn.* 65 (1992) 824-830.
- 26 H. Hichri, A. Accary, J. Andrieu, *Chem. Eng. Process.* 30 (1991) 133-140.

-
- 27 W.K. Schumann, O.M. Kut, A. Baiker, *Ind. Eng. Chem. Res.* 28 (1989) 693-697.
- 28 Y. Takagi, *Inst. Phys. Chem. Res. Jpn.* 64 (1970) 39-61.
- 29 Surapas Sitthisa, University of Oklahoma Thesis (2012).
- 30 N. Mahata, F. Goncalves, M.F.R. Pereira, J.L. Figueiredo, *Appl. Catal. A* 339 (2008) 159-168.
- 31 P. Reyes, H. Rojas, *React. Kinet. Catal. Lett.* 88 (2006) 363-369.
- 32 A. Siani, O.S. Alexeev, G. Lafaye, M.D. Amiridis, *J. Catal.* 266 (2009) 26-38.
- 33 A. Siani, B. Captain, O.S. Alexeev, E. Stafyla, A.B. Hungria, P.A. Midgley, J.M. Thomas, R.D. Adams, M.D. Amiridis, *Langmuir*, 22 (2006) 5160–5167.
- 34 R. Hirschl, F. Delbecq, P. Sautet, J. Hafner, *J. Catal.* 217 (2003) 354-366.